ISSN 1881-7831 Online ISSN 1881-784X

DD&T

Drug Discoveries & Therapeutics

Volume 15, Number 4
August 2021

IRCA BSSA

IACMHR

www.ddtjournal.com

DD&T
Drug Discoveries & Therapeutics

ISSN: 1881-7831
Online ISSN: 1881-784X
CODEN: DDTRBX
Issues/Year: 6
Language: English
Publisher: IACMHR Co., Ltd.

Drug Discoveries & Therapeutics is one of a series of peer-reviewed journals of the International Research and Cooperation Association for Bio & Socio-Sciences Advancement (IRCA-BSSA) Group. It is published bimonthly by the International Advancement Center for Medicine & Health Research Co., Ltd. (IACMHR Co., Ltd.) and supported by the IRCA-BSSA.

Drug Discoveries & Therapeutics publishes contributions in all fields of pharmaceutical and therapeutic research such as medicinal chemistry, pharmacology, pharmaceutical analysis, pharmaceutics, pharmaceutical administration, and experimental and clinical studies of effects, mechanisms, or uses of various treatments. Studies in drug-related fields such as biology, biochemistry, physiology, microbiology, and immunology are also within the scope of this journal.

Drug Discoveries & Therapeutics publishes Original Articles, Brief Reports, Reviews, Policy Forum articles, Case Reports, Communications, Editorials, News, and Letters on all aspects of the field of pharmaceutical research. All contributions should seek to promote international collaboration in pharmaceutical science.

Editorial Board

Editorial and Head Office:

Pearl City Koishikawa 603,
2-4-5 Kasuga, Bunkyo-ku,
Tokyo 112-0003, Japan
E-mail: office@ddtjournal.com

Drug Discoveries & Therapeutics

Editorial and Head Office

Pearl City Koishikawa 603, 2-4-5 Kasuga, Bunkyo-ku,
Tokyo 112-0003, Japan

E-mail: office@ddtjournal.com
URL: www.ddtjournal.com

CONTENTS

Volume 15, Number 4, 2021

Review

Original Article

Brief Report

Case Report

Communication

Letter

Review

DOI: 10.5582/ddt.2021.01054

India and management of COVID-19: A case study on published guidelines

Rohit Kumar[1], Ankit Mittal[1], Shreya Das Adhikari[2], Eram Afroz[1], Nitin Gupta[3,*]

[1] Department of Medicine, All India Institute of Medical Sciences, New Delhi, India;
[2] Department of Anaesthesiology, Kasturba Medical College, Manipal Academy of Higher Education, Manipal, Karnataka, India;
[3] Department of Infectious Diseases, Kasturba Medical College, Manipal, Manipal Academy of Higher Education, Manipal, Karnataka, India.

SUMMARY In the face of the ongoing pandemic, the primary care physicians in India are dealing not only with an increased number of patients but are also facing difficulties in the management of complex critically ill patients. To guide the management plans of primary care physicians, several guidelines have been published by the central and state health bodies. In such a situation, an updated and unifying state, national and international guidelines based on critical analysis and appraisal of evolving data is the need of the hour. In this review, we critically analysed the current existing guidelines that have been formulated within India in light of recent evidence.

Keywords Coronavirus disease 2019, SARS-CoV-2, antiviral

1. Introduction

India's healthcare sector was on its knees during the second wave due to the high number of Coronavirus disease-2019 (COVID-19) cases. Besides the shortage of hospital beds, oxygen supply, and medications highlighted in the news reports, primary care physicians all over the country were dealing with increasingly complex and critically ill patients. With new research papers getting published every day, it is incredibly challenging for physicians to keep abreast with the latest evidence. As a result, most physicians resort to the clinical management guidelines published by competent authorities. The problem lies with the number of different guidelines (state, national, international) that differ on the critical aspects of management. For this commentary, the websites of the Infectious disease Society of America (IDSA), World Health Organisation (WHO), and health bodies of central/state governments of India were searched for the last available guidelines on the management of COVID-19 as of 31.05.2021. Apart from the national guidelines, the guidelines from various states were available. While most of the states endorsed the national management protocol; the states of Goa (GA), Jharkhand (JH), Karnataka (KA), Kerala (KL), Madhya Pradesh (MP), Maharashtra (MH), Meghalaya (MG), Tamil Nadu (TN), and West Bengal (WB) had their management guidelines. Last year, we published a comprehensive review pointing to the lack of congruency between these guidelines (*1*). Since then, the guidelines have been revised, but the lack of congruency continue to exist. This review aims to examine the existing guidelines for congruence and critically analyse them in light of current evidence.

The definitions for categorising the severity of COVID-19 varied with guidelines. For uniformity, the spectrum of COVID-19 has been categorised into mild, moderate and severe in this review. The multiple definitions for these categories used in the guidelines have been summarised in Table 1. The recommendations of the guidelines have been tabulated in Table 2. The current evidence on the utility of drugs and therapeutics of COVID-19 has been summarised in Table 3.

2. Hydroxychloroquine (HCQ)

HCQ was initially recommended based on small non-randomised studies, but later studies showed no effect of HCQ on mortality (*2,3*). However, it was evident from the results of the SOLIDARITY trial that the use of HCQ is not associated with any decrease in mortality, the requirement of ventilation and hospital stay (*4,5*). The drug was also suggested for post-exposure prophylaxis by some guidelines, but a randomised trial found that HCQ did not prevent illness when initiated within four days of exposure (*6*). HCQ also failed to show any reduction in symptom severity in patients of COVID-19 when given early in the course (*7*). Therefore, the WHO and IDSA have recommended

Table 1. Classification scheme of COVID-19 and definitions used by various guidelines

Guidelines	Mild	Moderate	Severe
WHO	Symptoms without evidence of viral pneumonia or hypoxia.	Pneumonia + no signs of severe pneumonia + SpO2 ≥ 90%	Pneumonia + RR > 30 per minute; severe respiratory distress; or SpO2 < 90%
IDSA	Non-severe illness - patient with SpO2 > 94%; not requiring supplemental oxygen		SpO2 ≤ 94%
India	No dyspnoea and Spo2 > 94%	Pneumonia + SpO2 90 to ≤ 93%, RR > 24 per minute	Pneumonia + RR >30 per minute, severe respiratory distress, SpO2 < 90%
Jharkhand	Non critically ill + hemodynamically stable	RR > 30 per minute, SpO2 < 90%, altered sensorium, oliguria, high lactate, bilateral radiograph opacities	
Kerala	No breathlessness or Hypoxia, RR < 24 per minute, SpO2 > 94%	RR - 24-29 per minute, SpO2 - 91-94%	RR > 30 per minute, SpO2 < 90 %
Madhya Pradesh	No dyspnoea, SpO2 > 94%, RR < 16/min	Pneumonia + SpO2 90 - 94%	Pneumonia + severe respiratory distress, SpO2 < 90%
Maharashtra	A - asymptomatic, B - Symptomatic without comorbidity, C - Symptomatic with comorbidity - obesity, age > 60 years, DM, hypertension/IHD, chronic lung disease, immunosuppressed, CKD	Pneumonia + SpO2: 90-94%, RR > 24 per minute.	Pneumonia + RR > 30 per minute, severe respiratory distress, SpO2 < 90%
Meghalaya	Category A - asymptomatic Category B - Symptomatic with no signs of severe pneumonia; RR - 16-24 per minute, Spo2 > 94%	Category C (Severe) - RR > 24 per minute, SpO2 < 94% Category D (Critical) - RR > 30 per minute, SpO2 < 90%	
Tamil Nadu	RR < 24 per minute, Spo2 > 94%	RR- 24-30 per minute, SpO2 - 90 - 94%	RR > 30 per minute, SpO2 < 90%
Goa	No dyspnoea, SpO2 > 93%	Pneumonia + SpO2 90 to ≤ 93%, RR > 24 per minute	Pneumonia + RR > 30 per minute, severe respiratory distress, SpO2 < 90%
West Bengal	Symptoms without shortness of breath	RR > 24 per minute; SpO2 < 94%; altered sensorium drowsiness/confusion/ stupor; infiltrates on Chest X-ray; altered liver and renal function tests	Moderate Disease + ARDS, sepsis, septic shock

Abbreviation: WHO, World Health Organisation; IDSA, Infectious disease Society of America; RR, respiratory rate; SpO2, oxygen saturation; DM, diabetes mellitus; IHD, ischaemic heart disease; CKD, chronic kidney disease; ARDS, acute respiratory distress syndrome.

against the use of HCQ in COVID-19 in their latest guidelines. While HCQ is no more recommended in national guidelines and state guidelines of KL, TN & WB, several state guidelines (JH, MG, MH, MP, KA) continue to recommend it.

3. Ivermectin

Ivermectin, an anti-parasitic drug, has also found a place in the treatment of COVID-19 since the start of the pandemic. A pilot randomised trial reported a reduction in self-reported symptoms using ivermectin within 72 hours of the onset of symptoms (*8*). Another study found reduced time to negativity with ivermectin (*9*). However, in two randomised, double-blind placebo-controlled trials, on mild (Lopez Medina *et al.*) and severe (Galan *et al.*) patients, there was no improvement in clinical outcomes with ivermectin (*10,11*). Ivermectin use has been incorporated in some guidelines based on a meta-analysis of 18 studies showing decreased mortality with ivermectin (*12*). However, most of these studies had a very high risk of bias and one of the study from the meta-analysis has been retracted. In the absence of new studies demonstrating absolute benefit, ivermectin has been removed from the national guidelines, but some states still recommend it (JH, KL, MH, TN, GA, WB).

4. Favipiravir

Favipiravir is a selective and potent inhibitor of influenza RNA polymerase. An initial, before-after, comparative study found a shorter median time to viral clearance and significant improvement in radiological findings (*13*). It was initially postulated that early administration of favipiravir might be more useful. Still, a study showed no difference in early *vs.* late administration of favipiravir in asymptomatic or mild COVID19 illness (*14*). In the open labelled trial from India, the viral clearance time was not significant, but the subjective clinical cure was faster in those who received favipiravir (*15*). However, subsequent studies by Dabbous *et al.*, Solaymani-Dodaran *et al.*, and Khamis *et al.* did not show any significant clinical benefit with favipiravir (*16-18*). The WHO and IDSA do not make any recommendation on the use of favipiravir in COVID-19. However, based on small studies showing limited benefit, favipiravir is recommended in some state guidelines (KL and MH).

Table 2. Comparison of recommendations by various guidelines on key drugs used in management of COVID-19

Items	Hydroxy-chloroquine	Ivermectin	Remdesivir	Favipiravir	Tocilizumab	Steroids	Inhaled steroids	Convalescent plasma	Anticoagulation
WHO	Recommends against use	Recommends against use	Recommends against use	No R	No R	Recommended in severe/ critical disease	No R	No R	Prophylactic doses in all hospitalized patients
IDSA	Recommends against use	Recommends against use	Recommended in severe disease	No R	Recommended in severe disease	Recommended if oxygen requirement	No R	Under research setting	Prophylactic doses in all hospitalized patients
National guidelines, India	Not R	Not R	Recommended in moderate-severe disease	No R	Recommended in severe disease	Recommended in moderate-severe disease	Recommended in mild illness	Not R	Prophylactic dose in moderate illness, intermediate dose in severe illness
Jharkhand	Recommended in all categories	Recommended in all categories	No R	No R	No R	Recommended in Moderate-severe disease	No R	No R	Prophylactic doses in critically ill
Kerala	Not R	Recommended in mild illness*	Recommended in moderate-severe disease	Recommended in mild illness*	Recommended in severe disease	Recommended in moderate-severe disease	Recommended in mild illness*	Early moderate disease (< 7 days from onset)	Prophylactic dose: moderate-severe disease; Therapeutic dose: confirmed VTE or high clinical suspicion
Madhya Pradesh	Recommended in moderate disease	No R	Recommended in moderate-severe disease	No R	Recommended in severe disease	Recommended in moderate-severe disease	No R	Under research settings	Therapeutic anticoagulation
Maharashtra	Recommended	Recommended in moderate disease	Recommended in mild disease*, moderate-severe disease	Recommended in mild illness* and moderate illness	Recommended in severe disease	Recommended in moderate-severe disease	No R	Moderate disease with no improvement	Prophylactic dose: Mild disease, Moderate and severe disease: therapeutic dose[#]
Meghalaya	Recommended in mild illness*, moderate-severe illness	No R	Recommended in Moderate-severe disease	No R	Recommended in severe disease	Recommended in moderate-severe disease	No R	Under research settings	Prophylactic dose anticoagulation if risk factors
Tamil Nadu	No R	Recommend	No R	No R	No R	Recommended in mild cases*, moderate and severe cases	No R	No R	Prophylactic doses in moderate-severe cases
Goa	Recommended in mild disease	Recommended in mild disease	Moderate-severe disease	No R	Recommended in severe disease	Recommended in moderate-severe disease	No R	No R	Prophylactic doses in moderate-severe disease
West Bengal	No R	Recommended in mild disease	Recommended in Moderate-severe disease	No R	Recommended in severe disease	Recommended in moderate-severe disease	No R	No R	Prophylactic dose in moderate-severe disease[#]

*mild disease with specific high-risk features, [#]moderate/severe disease with d-dimer cut-offs. Abbreviation: WHO, World Health Organisation; IDSA, Infectious disease Society of America; Not R, Not recommended; No R, No recommendation.

Table 3. Summary of studies of pharmaceuticals used for the treatment of COVID-19

Study	N	Type of study	Severity	Study arms	Results	*Ref.*
Hydroxychloroquine (HCQ) with/without azithromycin (A)						
Geleris *et al.*	1376	Retrospective	All severity	HCQ-59% No HCQ-41%	No association between HCQ use and decrease in intubation or death	(*2*)
Rosenberg *et al.*	1438	Retrospective	All severity	HCQ-51% HCQ+A-19% A-15% Neither-15%	Treatment with either drug not associated with improvement in mortality	(*3*)
RECOVERY	11,197	Open RCT	Hospitalised patients	HCQ-1561 Usual care-3155	Treatment with HCQS was not associated with a reduction in mortality	(*4*)
SOLIDARITY	1860	Open RCT	Hospitalised adults (All severity)	HCQ-954 No HCQ-906	No decrease in mortality, a requirement of ventilation and hospital stay	(*5*)
Boulware *et al.*	821	Double blind placebo RCT	Exposure to case within four days	HCQ-50% Placebo-50%	HCQ did not prevent infection when used as a post-exposure prophylaxis	(*6*)
Skipper *et al.*	491	Double blind placebo RCT	Symptomatic non-hospitalised	HCQ-50% Pacebo-50%	HCQ did not reduce symptom severity	(*7*)
Ivermectin (IVM)						
Chaccour *et al.*	24	Double blind placebo RCT	Mild	IVM-12 Placebo-12	No difference in Day 7 viral load	(*8*)
Babalola et al	62	Double blind placebo RCT	Mild	IVM-6mg-21 IVM-12 mg-21 LPV/r-20	Time to negativity was lesser in IVM (dose-dependant)	(*9*)
Galan *et al.*	168	Double blind RCT	Severe	HCQ-54 CQ-61 IVM-53	No difference in requirement of ICU admission or mortality	(*10*)
Lopez Medina *et al.*	400	Double blind placebo RCT	Mild, less than seven days	IVM-200 Placebo-200	No significant improvement in resolution of symptoms	(*11*)
Favipiravir CT						
Cai *et al.*	80	Open non-RCT	Mild	FPV-35 LPV/r-45	Shorter time to viral clearance with FPV. Significant improvement in radiology more common with FPV.	(*13*)
Doi *et al.*	89	Open RCT	Mild	Early FPV (D1)-44 Late FPV (D6)-45	No significant difference in viral clearance in early *vs* late	(*14*)
Udwadia *et al.*	150	Open RCT	Mild	FPV-75 SOC-75	Time to cessation of viral shedding- not significantly different but faster clinical cure	(*15*)
Dabbous *et al.*	100	Open RCT	Mild and Moderate	FPV-50 HCQ-50	Time to defervescence and time to negativity not different	(*16*)
Solaymani-dodaram *et al.*	380	Open RCT	Moderate/severe	FPV-193 LPV/r-187	Mortality, requirement of intubation, ICU admission, Duration of stay not different	(*17*)
Khamis *et al.*	89	Open RCT	Moderate/severe	FPV-44 HCQ-45	No significant difference in clinical outcomes	(*18*)
Remdesivir (RDV)						
Wang *et al.*	237	Double blind placebo RCT	Moderate/Severe	RDV-67% Placebo-33%	RDV not associated with significant clinical improvement	(*19*)
Beigel *et al.* (ACTT1)	1059	Double blind placebo RCT	Pneumonia	RDV-51% Placebo-49%	RDV shortened the time to recovery	(*20*)
SOLIDARITY	5451	Open RCT	Hospitalised (All severity)	RDV-2743 No RDV-2708	No decrease in mortality, requirement of ventilation and hospital stay	(*5*)

Abbreviation: SOC, standard of care; ICU, Intensive Care Unit; Dexa, dexamethasone; MPS, methylprednisolone; hydrocort, hydrocortisone; ECMO, extracorporeal membrane oxygenation; RCT, randomised controlled trial; Open, Open-labelled, placebo- placebo controlled.

5. Remdesivir

Remdesivir is a nucleoside analogue, which acts by inhibiting the ribonucleic acid (RNA) dependent RNA polymerase. In a multi-centric placebo-controlled trial from China, remdesivir use was not associated with a difference in time to clinical improvement (*19*). Two of the most significant studies on the use of remdesivir showed contradictory results. In the ACTT-1 trial, remdesivir showed a faster time to recovery in patients with lung involvement (*20*). However, the results of the SOLIDARITY trial showed no significant benefit

Table 3. Summary of studies of pharmaceuticals used for the treatment of COVID-19 (continued)

Study	N	Type of study	Severity	Study arms	Results	*Ref.*
Steroids						
RECOVERY	6,425	Open RCT	Hospitalised	Dexa-33% SOC-67%	Reduced mortality in those receiving oxygen therapy or mechanical ventilation	(*21*)
Edalatifard *et al.*	68	Single arm	Severe, hospitalised patients	MPS pulse-34 SOC-34	Significant improvement in survival time	(*22*)
Tomazini *et al.*	299	Open RCT	Moderate-severe ARDS	Dexa-151 SOC-148	Significant increase in ventilator-free days	(*23*)
REMAP-CAP trial	384	Open RCT	Severe	Hydrocort-283 SOC-101	No signifcant difference	(*24*)
Tang *et al.*	86	Single-blind, RCT	Hospitalised	MPS-43 Control-43	No significant difference	(*25*)
Gudino *et al.*	64	Open RCT	Moderate-severe disease	MPS-35 SOC-26	No significant difference	(*26*)
Tocilizumab (Tcz)						
Guaraldi *et al.*	544	Retrospective	Severe	SOC-67% Tcz-33%	Tcz associated with reduced mortality and mechanical ventilation	(*30*)
Biran *et al.*	764	Retrospective	ICU patients	SOC-73% Tcz-27%	Tcz was associated with decreased mortality	(*31*)
Salama *et al.*	389	Double blind placebo RCT	Moderate/severe	Tcz-249 Placebo-128	Reduced likelihood of getting mechanically ventilated; no benefit in overall survival	(*32*)
Soin *et al.*	180	Open RCT	Moderate to severe COVID19	Tcz-90 SOC-90	tocilizumab did not provide additional benefit	(*33*)
RECOVERY	1,350	Open RCT	Moderate/severe CRP > 75 mg/L	Tcz-621 SOC-729	Improved survival and other clinical outcomes with tcz	(*34*)
Convalescent Plasma (CP)						
Xia *et al.*	1,568	Retrospective	Severe/critical	CP-9% No CP-91%	Reduction in mortality and improvement of clinical symptoms	(*35*)
Abolghasemi *et al.*	189	Open non-RCT	Moderate/severe	CP-61% No CP-39%	Decreased hospital stay and mortality	(*36*)
Li *et al.*	103	Open RCT	Severe/life-threatening	CP-50% No CP-50%	No significant improvement in time to clinical improvement	(*37*)
PLACID trial	464	Open RCT	Moderate	CP-235 SOC-229	CP not associated with a reduction in progression or reduction of mortality	(*38*)
Libster *et al.*	160	Double blind placebo RCT	Older adults within 72 hours of mild disease	CP with high titre-80 Placebo-80	Early administration of high titre CP reduced disease progression	(*39*)
Abani *et al.* (RECOVERY)	11,558	Open RCT	Hospitalised	CP-5795 SOC-5763	CP does not decrease mortality	(*40*)
Inhaled Steroids						
STOIC trial	146	Open RCT	Mild within 7 days	Budesonide-73 SOC-73	Early administration reduced the requirement of urgent care	(*41*)
PRINCIPLE trial	1,779	Open RCT	Mild within < 14 days	Budesonide-751 SOC-1028	Time to clinical recovery shorter	(*42*)
Anti-coagulation						
INSPIRATION trial	600	Open RCT	ICU patients	Intermediate-276 Standard- 286	No significant difference in the composite outcome of thrombosis, treatment with ECMO, or mortality	(*43*)
ATTACC	1,074	Open RCT	Severe	Therapeutic dose- 529 Standard prophylaxis-545	No significant difference in organ-support free days and survival	(*44*)
ATTACC	2,245	Open RCT	Hospitalized but not critically ill	Therapeutic dose- 1190 Standard prophylaxis-1055	Improved survival with therapeutic dose	(*45*)

Abbreviation: SOC, standard of care; ICU, Intensive Care Unit; Dexa, dexamethasone; MPS, methylprednisolone; hydrocort, hydrocortisone; ECMO, extracorporeal membrane oxygenation; RCT, randomised controlled trial; Open, Open-labelled, placebo- placebo controlled.

with remdesivir (*5*). Based on available data, the WHO gave a conditional recommendation against remdesivir, but the IDSA recommends its use in severe COVID-19 cases. The national and state guidelines (KL, MH, MG and WB) recommend its use in hospitalised, moderate to severe COVID-19 cases. Several parts of the country reported a shortage of remdesivir in the second wave. In addition, there were reports of patient attendants paying an excessive amount of money to procure this drug. It must be therefore emphasised that the drug has limited impact on improvement in mortality outcomes.

6. Systemic steroids (oral/intravenous)

In the RECOVERY trial, dexamethasone was found to help decrease 28-day mortality in patients requiring oxygen (*21*). Other large studies echoed the findings of the RECOVERY trial (*22-24*). The RECOVERY trial showed that the benefit of steroids was in patients who had > 7 days of illness. Early use (< 7 days) of steroids was associated with worse outcomes. A study by Tang *et al.* showed that early use of steroids might prolong viral shedding (*25*). Despite the lack of evidence, national guidelines allow steroids in those without oxygen requirements but with illness (fever and cough) beyond seven days. TN state has also recommended the use of steroids in a sub-category of patients with mild illness. Overall, although the national and state guidelines are consistent with their recommendation on steroid use in moderate-severe cases, there is a lot of heterogeneity in dosing schedules. While some guidelines (IDSA, WHO, MG, MP) mention fixed-dose steroids, others recommend weight-based dosing. MP guidelines recommend the use of 500 mg methylprednisolone pulse therapy in severe disease, which any other guideline has not endorsed. Except for a few studies with small sample size, steroids use in patients requiring oxygen is generally associated with improved outcomes (*26*). Increasing immunosuppression without forethought can be detrimental by increasing secondary infections and sepsis (*27*). This becomes more important as we see an unprecedented rise in COVID-19 associated mucormycosis cases. Steroids not only suppresses the immune system but also causes deranged blood sugar levels, both of which are important risk factors for the development of mucormycosis (*28,29*).

7. Tocilizumab

Tocilizumab, an interleukin (IL)-6 receptor inhibitor, is an approved treatment for chimeric antigen receptor (CAR) T-cell therapy-related cytokine release syndrome. In severe COVID19, tocilizumab was postulated to decrease the cytokine surge and associated hyper-inflammation, in severe illness, by blocking the site of IL-6. In a case-control study, including 544 patients of severe COVID19 pneumonia (RR > 30/min, Spo2 < 93% on room air) (*30*), the use of tocilizumab was associated with statistically significant benefit in reducing the need for ventilation or death. In another retrospective cohort study of 764 patients, tocilizumab in 210 patients was associated with reduced mortality (*31*). The first prospective data came from a multi-national, multi-centric study of 389 patients, randomised in a 2:1 manner in tocilizumab and placebo groups, respectively (*32*). The use of tocilizumab in 249 patients reduced the likelihood of getting mechanically ventilated, but no benefit in overall survival was noted. In a trial from India including 180 patients (1:1 manner) in tocilizumab and standard of care groups, tocilizumab did not provide additional benefit (*33*). The results of the RECOVERY trial showed improved survival in those with saturation less than 93% and C-reactive protein > 75 mg/L (*34*). Whereas WHO has made no recommendation on its use, IDSA, Indian national guidelines, and certain states (KL, MH, MG and WB) have recommended its use in a select few cases.

8. Convalescent plasma

Convalescent plasma (CP) was postulated to act as a source of neutralising antibodies that can inhibit the replication of the virus. The data from retrospective, observational studies, showing benefit, provided the basis for prospective studies (*35,36*). However, randomised control trials failed to show any benefit with convalescent plasma (*37,38*). Libster *et al.* showed that early use of high-titre CP (within 72 hours) might halt the disease progression in elderly individuals (*39*). However, the use of CP within three days of onset in a high burden resource-limited setting is highly impractical. Besides, the results of the RECOVERY trial show that even high titre CP does not decrease mortality (*40*). Therefore, in accordance with the WHO and IDSA, the national guidelines have changed their stance on 17.05.21 and do not recommend CP in COVID-19. While most states recommend CP only in a trial setting, KL and MH continue to recommend CP as a part of clinical care in COVID-19.

9. Inhaled steroids

Owing to the remarkable success of systemic steroids, it was hypothesised that inhaled steroids might play a role in preventing progression when given early in course in patients with persistent symptoms. The two published, STOIC trial and PRINCIPLE trial showed a reduced time to recovery and reduced need for emergency care (*41,42*). The WHO and IDSA do not make any recommendations on inhaled steroid use in COVID-19. However, inhalational budesonide has been recommended in mild illness with persistent symptoms by the national guidelines and KL state guidelines.

10. Anticoagulation

Anticoagulation has been one of the critical pillars in moderate-severe disease management. Although their use in moderate to severe diseases is uniformly recommended, there is a lack of clarity on the dosing schedule (low-dose *vs*. intermediate/high-dose prophylaxis or therapeutic anticoagulation). INSPIRATION trial in critically ill patients with COVID-19 showed no difference between standard *vs*. intermediate prophylactic dose of anticoagulation in terms of the composite outcome of thrombosis, treatment with extracorporeal membrane oxygenation, or mortality within 30 days (*43*). While the WHO and IDSA recommend using low dose anticoagulation for thromboprophylaxis, national and state guidelines have mentioned variable doses. Pooled analysis from three trials (REMAP-CAP, ACTIV-4a and ATTAC trials) show that although the incidence of thrombotic events is lesser in the therapeutic anticoagulation group, there was no difference in major thrombotic events and mortality (*44*). In another analysis, therapeutic doses of anticoagulation decreased the need for oxygen support in non-critically ill hospitalised patients (*45*). Only MP state guidelines mention therapeutic doses of anticoagulation but do not distinguish between critically and non-critically ill patients.

In summary, despite the lack of evidence, some guidelines continue to recommend HCQ, ivermectin, favipiravir and convalescent plasma. With regards to indication, dose and duration of steroids and anti-coagulants, there was wide variability amongst the various guidelines. Many of the recommendations in the guidelines were only expert-based and sometimes even contradictory to the best available evidence. In addition to the massive spurt of cases in the second wave that hampered the access to quality care, the lack of concordance in guidelines might have added to the confusion. Therefore, there is a need to develop a unified living guideline for COVID management that is evidence-informed and beneficial in curbing the proportion of inappropriate prescriptions.

Funding: The views in this article are of the author's personal opinions and do not necessarily indicate the views of their institution.

Conflict of Interest: The authors have no conflicts of interest to disclose.

References

1. Kumar R, Vinod KS, Mittal A, Adhikari SD, Gupta N. Review of current clinical management guidelines for COVID-19 with special reference to India. Drug Discov Ther. 2020;14:171-176.
2. Geleris J, Sun Y, Platt J, Zucker J, Baldwin M, Hripcsak G, Labella A, Manson DK, Kubin C, BArr RG, Sobieszczyk ME, Schluger NW. Observational study of hydroxychloroquine in hospitalised patients with Covid-19. N Engl J Med. 2020; 382:2411-2418.
3. Rosenberg ES, Dufort EM, Udo T, Wilberschied LA, Kumar J, Tesoriero J, Weinberg P, Kirkwood J, Muse A, DeHovitz J, Blog DS, Hutton B, Holtgrave DR, Zucker HA. Association of treatment with hydroxychloroquine or azithromycin with in-hospital mortality in patients with COVID-19 in New York state. JAMA. 2020; 323:2493-2502.
4. RECOVERY Collaborative Group, Horby P, Mafham M, *et al.* Effect of hydroxychloroquine in hospitalised patients with Covid-19. N Engl J Med. 2020; 383:2030-2040.
5. WHO Solidarity Trial Consortium, Pan H, Peto R, *et al.* Repurposed antiviral drugs for Covid-19 - Interim WHO Solidarity trial results. N Engl J Med. 2021; 384:497-511.
6. Boulware DR, Pullen MF, Bangdiwala AS, *et al.* A randomised trial of hydroxychloroquine as postexposure prophylaxis for Covid-19. N Engl J Med. 2020; 383:517-525.
7. Skipper CP, Pastick KA, Engen NW, *et al.* Hydroxychloroquine in nonhospitalised adults with early COVID-19: A randomised trial. Ann Intern Med. 2020; 173:623-631.
8. Chaccour C, Casellas A, Blanco-Di Matteo A, *et al.* The effect of early treatment with ivermectin on viral load, symptoms and humoral response in patients with non-severe COVID-19: A pilot, double-blind, placebo-controlled, randomised clinical trial. EClinicalMedicine. 2021; 32:100720.
9. Babalola OE, Bode CO, Ajayi AA, Alakaloko FM, Akase IE, Otrofanowei E, Salu OB, Adeyemo WL, Ademuyiwa AO, Omilabu S. Ivermectin shows clinical benefits in mild to moderate COVID19: A randomised controlled double-blind, dose-response study in Lagos. QJM. 2021; hcab035.
10. Galan LEB, Santos NMD, Asato MS, *et al.* Phase 2 randomised study on chloroquine, hydroxychloroquine or ivermectin in hospitalised patients with severe manifestations of SARS-CoV-2 infection. Pathog Glob Health. 2021; 115:235-242.
11. López-Medina E, López P, Hurtado IC, *et al.* Effect of ivermectin on time to resolution of symptoms among adults with mild COVID-19: A randomised clinical trial. JAMA. 2021; 325:1426-1435.
12. Hill A, Abdulamir A, Ahmed S, Asghar A, Babalola OE, Basri R, Chaccour C, Chachar AZ, Chowdhury AT, Elgazzar A, Ellis L. Meta-analysis of randomised trials of ivermectin to treat SARS-CoV-2 infection. Open Forum Infect Dis. 2021; ofab358.
13. Cai Q, Yang M, Liu D, *et al.* Experimental treatment with favipiravir for COVID-19: An open-label control study. Engineering (Beijing). 2020; 6:1192-1198.
14. Doi Y, Hibino M, Hase R, *et al.* A prospective, randomized, open-label trial of early versus late favipiravir therapy in hospitalised patients with COVID-19. Antimicrob Agents Chemother. 2020; 64:e01897-20.
15. Udwadia ZF, Singh P, Barkate H, Patil S, Rangwala S, Pendse A, Kadam J, Wu W, Caracta CF, Tandon M. Efficacy and safety of favipiravir, an oral RNA-dependent RNA polymerase inhibitor, in mild-to-moderate COVID-19: A randomised, comparative, open-label, multicenter, phase 3 clinical trial. Int J Infect Dis. 2021;

103:62-71.
16. Dabbous HM, El-Sayed MH, El Assal G, Elghazaly H, Ebeid FFS, Sherief AF, Elgaafary M, Fawzy E, Hassani SM, Riad AR, TagelDin MA. Safety and efficacy of favipiravir versus hydroxychloroquine in management of COVID-19: A randomised controlled trial. Sci Rep. 2021; 11:7282.
17. Solaymani-Dodaran M, Ghanei M, Bagheri M, *et al.* Safety and efficacy of favipiravir in moderate to severe SARS-CoV-2 pneumonia. Int Immunopharmacol. 2021; 95:107522.
18. Khamis F, Al Naabi H, Al Lawati A, Ambusaidi Z, Al Sharji M, Al Barwani U, Pandak N, Al Balushi Z, Al Behrani M, Al Salmi I, Al-Zakwani I. Randomized controlled open label trial on the use of favipiravir combined with inhaled interferon beta-1b in hospitalised patients with moderate to severe COVID-19 pneumonia. Int J Infect Dis. 2021; 102:538-543.
19. Wang Y, Zhang D, Du G, *et al.* Remdesivir in adults with severe COVID-19: a randomised, double-blind, placebo-controlled, multicentre trial. Lancet. 2020; 395:1569-1578. Erratum in: Lancet. 2020; 395:1694.
20. Beigel JH, Tomashek KM, Dodd LE, *et al.* Remdesivir for the treatment of Covid-19 - final report. N Engl J Med. 2020; 383:1813-1826.
21. RECOVERY Collaborative Group, Horby P, Lim WS, Emberson JR, Mafham M, Bell JL, *et al.* Dexamethasone in hospitalised patients with Covid-19. N Engl J Med. 2021; 384:693-704.
22. Edalatifard M, Akhtari M, Salehi M, *et al.* Intravenous methylprednisolone pulse as a treatment for hospitalised severe COVID-19 patients: results from a randomised controlled clinical trial. Eur Respir J. 2020; 56:2002808.
23. Tomazini BM, Maia IS, Cavalcanti AB, *et al.* Effect of dexamethasone on days alive and ventilator-free in patients with moderate or severe acute respiratory distress syndrome and COVID-19: The CoDEX randomized clinical trial. JAMA. 2020; 324:1307-1316.
24. Angus DC, Derde L, Al-Beidh F, *et al.* Effect of hydrocortisone on mortality and organ support in patients with severe COVID-19: The REMAP-CAP COVID-19 corticosteroid domain randomized clinical trial. JAMA. 2020; 324:1317-1329.
25. Tang X, Feng YM, Ni JX, *et al.* Early use of corticosteroid may prolong SARS-CoV-2 shedding in non-intensive care unit patients with COVID-19 pneumonia: A multicenter, single-blind, randomized control trial. Respir Int Rev Thorac Dis. 2021; 100:116-126.
26. Corral-Gudino L, Bahamonde A, Arnaiz-Revillas F, *et al.* Methylprednisolone in adults hospitalised with COVID-19 pneumonia : An open-label randomised trial (GLUCOCOVID). Wien Klin Wochenschr. 2021; 133:303-311.
27. Yang Z, Liu J, Zhou Y, Zhao X, Zhao Q, Liu J. The effect of corticosteroid treatment on patients with coronavirus infection: a systematic review and meta-analysis. J Infect. 2020; 81:e13-20.
28. Stone N, Gupta N, Schwartz I. Mucormycosis: time to address this deadly fungal infection. Lancet Microbe 2021. *https://www. thelancet.com/journals/lanmic/article/PIIS26665247(21)00148-8/fulltext* (17 June 2021, date last accessed).
29. Singh AK, Singh R, Joshi SR, Misra A. Mucormycosis in COVID-19: A systematic review of cases reported worldwide and in India. Diabetes Metab Syndr. 2021; 15:102146.
30. Guaraldi G, Meschiari M, Cozzi-Lepri A, *et al.* Tocilizumab in patients with severe COVID-19: a retrospective cohort study. Lancet Rheumatol. 2020; 2:e474-e484.
31. Biran N, Ip A, Ahn J, *et al.* Tocilizumab among patients with COVID-19 in the intensive care unit: a multicentre observational study. Lancet Rheumatol. 2020; 2:e603-612.
32. Salama C, Han J, Yau L, *et al.* Tocilizumab in patients hospitalised with Covid-19 pneumonia. N Engl J Med. 2021; 384:20-30.
33. Soin AS, Kumar K, Choudhary NS, *et al.* Tocilizumab plus standard care versus standard care in patients in India with moderate to severe COVID-19-associated cytokine release syndrome (COVINTOC): an open-label, multicentre, randomised, controlled, phase 3 trial. Lancet Respir Med. 2021; 9:511-521.
34. RECOVERY Collaborative Group. Tocilizumab in patients admitted to hospital with COVID-19 (RECOVERY): a randomised, controlled, open-label, platform trial. Lancet Lond Engl. 2021; 397:1637-1645.
35. Xia X, Li K, Wu L, *et al.* Improved clinical symptoms and mortality among patients with severe or critical COVID-19 after convalescent plasma transfusion. Blood. 2020; 136:755-759.
36. Abolghasemi H, Eshghi P, Cheraghali AM, *et al.* Clinical efficacy of convalescent plasma for treatment of COVID-19 infections: Results of a multicenter clinical study. Transfus Apher Sci. 2020; 59:102875.
37. Li L, Zhang W, Hu Y, *et al.* Effect of convalescent plasma therapy on time to clinical improvement in patients with severe and life-threatening COVID-19: A randomised clinical trial. JAMA. 2020; 324:460-470.
38. Agarwal A, Mukherjee A, Kumar G, Chatterjee P, Bhatnagar T, Malhotra P; PLACID Trial Collaborators. Convalescent plasma in the management of moderate covid-19 in adults in India: open label phase II multicentre randomised controlled trial (PLACID trial). BMJ. 2020; 371:m3939.
39. Libster R, Marc GP, Wappner D, *et al.* Early high-titer plasma therapy to prevent severe Covid-19 in older adults. N Engl J Med. 2021; 384:610-618.
40. Abani O, Abbas A, Abbas F, *et al.* Convalescent plasma in patients admitted to hospital with COVID-19 (RECOVERY): a randomised controlled, open-label, platform trial. Lancet. 2021; 397:2049-2059.
41. Ramakrishnan S, Nicolau DV, Langford B, *et al.* Inhaled budesonide in the treatment of early COVID-19 (STOIC): a phase 2, open-label, randomised controlled trial. Lancet Respir Med. 2021; 9:763-772.
42. Yu LM, Bafadhel M, Dorward J, *et al.* Inhaled budesonide for COVID-19 in people at high risk of complications in the community in the UK (PRINCIPLE): a randomised, controlled, open-label, adaptive platform trial. Lancet. 2021; S0140-6736(21)01744-X.
43. INSPIRATION Investigators, Sadeghipour P, Talasaz AH, *et al.* Effect of intermediate-dose vs standard-dose prophylactic anticoagulation on thrombotic events, extracorporeal membrane oxygenation treatment, or mortality among patients with COVID-19 admitted to the intensive care unit: The INSPIRATION randomized clinical trial. JAMA. 2021; 325:1620.
44. Remap-Cap T, ACTIV-4a, Investigators A, Zarychanski R. Therapeutic anticoagulation in critically ill patients

with Covid-19 – Preliminary report. medRxiv. 2021; 2021.03.10.21252749.
45. The ATTACC A-4a, Lawler PR, Goligher EC, *et al.* Therapeutic anticoagulation in non-critically ill patients with Covid-19. medRxiv. 2021; 2021.05.13.21256846.

Received June 21, 2021; Revised August 16, 2021; Accepted August 22, 2021

**Address correspondence to:*
Nitin Gupta, Department of Infectious Diseases, Kasturba Medical College, Manipal, Manipal Academy of Higher Education, Manipal, Karnataka-576104, India.
E-mail: nityanitingupta@gmail.com

Released online in J-STAGE as advance publication August 26, 2021.

Original Article

DOI: 10.5582/ddt.2021.01059

Inhibitory effect of traditional herbal (kampo) medicines on the replication of human parainfluenza virus type 2 *in vitro*

Jun Uematsu[1,*,§], Hidetaka Yamamoto[2,§], Sahoko Kihira[3,a,§], Kae Sakai-Sugino[3,b,§], Yuhko Ishiyama[3], Misaki Chindoh[3], Aya Baba[3], Rina Kazuta[3], Tomomi Hasegawa[3], Keiko Fujimoto[3], Aya Funauchi[3], Ai Itoh[3], Ayumi Ookohchi[3], Saemi Satoh[3], Yurie Maeda[3], Mitsuo Kawano[4], Masato Tsurudome[4], Miwako Nishio[4], Kazuyuki Hirai[2], Myles O'Brien[5], Hiroshi Komada[1,c]

[1] Microbiology and Immunology Section, Department of Clinical Nutrition, Graduate School of Health Science, Suzuka University of Medical Science, Suzuka, Mie, Japan;
[2] Faculty of Pharmaceutical Sciences, Suzuka University of Medical Science, Suzuka, Mie, Japan;
[3] Department of Clinical Nutrition, Faculty of Health Science, Suzuka University of Medical Science, Suzuka, Mie, Japan;
[4] Department of Microbiology, Mie University Graduate School of Medicine, Tsu, Mie, Japan;
[5] Graduate School of Mie Prefectural College of Nursing, Tsu, Mie, Japan.

SUMMARY Thirteen herbal medicines, Kakkonto (TJ-001), Kakkontokasenkyushin'i (TJ-002), Hangekobokuto (TJ-016), Shoseiryuto (TJ-019), Maoto (TJ-027), Bakumondoto (TJ-029), Hochuekkito (TJ-041), Goshakusan (TJ-063), Kososan (TJ-070), Chikujountanto (TJ-091), Gokoto (TJ-095), Saibokuto (TJ-096), and Ryokankyomishingeninto (TJ-119) were tested for human parainfluenza virus type 2 (hPIV-2) replication. Eight (TJ-001, TJ-002, TJ-019, TJ-029, TJ-041, TJ-063, TJ-095 and TJ-119) out of the thirteen medicines had virus growth inhibitory activity. TJ-001 and TJ-002 inhibited virus release, and largely inhibited genome, mRNA and protein syntheses. TJ-019 slightly inhibited virus release, inhibited gene and mRNA syntheses, and largely inhibited protein synthesis. TJ-029 slightly inhibited virus release, largely inhibited protein synthesis, but gene and mRNA syntheses were unaffected. TJ-041 only slightly inhibited virus release, the gene and mRNA syntheses, but largely inhibited protein synthesis. TJ-091 largely inhibited gene, mRNA and protein syntheses. TJ-095 largely inhibited gene synthesis, but NP and HN mRNAs were slightly detected, and protein syntheses were observed. TJ-119 inhibited gene, mRNA and protein syntheses. TJ-001, TJ-002, TJ-091, TJ-095 and TJ-119 inhibited multinucleated giant cell formation derived from cell-to-cell spreading of virus. However, in TJ-019, TJ-029 and TJ-041 treated infected cells, only small sized fused cells with some nuclei were found. TJ-019 and TJ-041 slightly disrupted actin microfilaments, and TJ-001 and TJ-002 destroyed them. TJ-041 slightly disrupted microtubules, and TJ-001 and TJ-002 disrupted them. In general, the medicines effective on common cold and bronchitis inhibited hPIV-2 replication.

Keywords virus replication, recombinant green fluorescence protein-expressing hPIV-2 without matrix protein, negative-strand RNA virus

1. Introduction

Human parainfluenza virus type 2 (hPIV-2) is one of the major human respiratory tract pathogens of infants and children. hPIV-2 is a member of the genus *Rubulavirus* in the family *Paramyxoviridae*, and it possesses a single-stranded, non-segmented, negative stranded RNA genome of 15,654 nucleotides (*1*). hPIV-2 has seven structural proteins, nucleoprotein (NP), the fifth (V), phospho (P), matrix (M), fusion (F), hemagglutinin-neuraminidase (HN) and large (L) proteins. The gene order of hPIV-2 is 3'-(leader)-NP-V/P-M-F-HN-L-(trailer)-5'. All genes of hPIV-2 were sequenced by our group (*2-7*). Monoclonal antibodies (mAbs) were made, and antigenic diversity of clinical isolates was investigated, by Tsurudome (*8*). The infectious hPIV-2 from cDNA clone was constructed by Kawano, and it was shown that its growth property was the same as that of control natural hPIV-2 (*9*).

Traditional herbal medicines have had an important role in Far East countries, especially in China, Korea and Japan for many years. Shoseiryuto inhibited mouse

adapted influenza A/G/(H3N2) or B virus replication in nasal cavity and lung of ~6 month-old BALB/c mice after oral administration from 7 days to 4 days after infection, suggesting that it is useful for influenza virus infection in aged persons and protects against both subtypes A and B (*10*). Maoto has clinical and virological efficacy for influenza virus by inhibiting uncoating of influenza virus A (*11*). Hochuekkito also has protective effects against influenza virus, and it stimulates the upper respiratory mucosal immune system (*12*). However, there are no reports on the effect of traditional herbal medicines on human parainfluenza viruses. We here report the effects of traditional herbal medicines on the replication of hPIV-2.

In the present investigation, thirteen herbal medicines were tested for hPIV-2 growth, and it was found that eight had inhibitory effects on hPIV-2. To investigate the effects of the medicines on viral genome synthesis, virus RNA was prepared and analyzed by PCR and real-time PCR. To elucidate the effects of the eight drugs on mRNA synthesis, cDNA was synthesized using oligo(dT) primer and PCR was carried out. Virus protein expression was observed by indirect immunofluorescence study using mAbs against NP, F and HN proteins of hPIV-2 (*8*). The inhibitory effects of the drugs on cell-to-cell spreading of hPIV-2 were analyzed using a recombinant green fluorescence protein (GFP)-expressing hPIV-2 without matrix protein (rhPIV-2ΔM-GFP) (*9,13,14*). The number of viruses released from infected cells was determined. Cytoskeleton was reported to have an important role in paramyxovirus replication. Actin microfilaments are important in the hPIV-3 life cycle, specifically at the level of viral transport and replication (*15*). Tubulin also acts as a positive transcription factor for *in vitro* RNA synthesis by Sendai virus (*16*). The effects of the drugs on actin microfilaments and microtubules were analyzed using rhodamine phalloidin and anti-tubulin α mAb, respectively.

2. Materials and Methods

2.1. Herbal medicines

Thirteen herbal medicines were chosen because they are effective on common cold and respiratory tract disease. Kakkonto (TJ-001: mainly effective on common cold, fever, headache), Kakkontokasenkyushin'i (TJ-002: sniffle, nasal inflammation), Hangekobokuto (TJ-016: neurosis), Shoseiryuto (TJ-019: nasal inflammation, common cold), Maoto (TJ-027: common cold, rheumatoid arthritis), Bakumondoto (TJ-029: cough, bronchitis), Hochuekkito (TJ-041: tuberculosis, bad appetite, common cold), Goshakusan (TJ-063: gastroenteritis, headache, common cold), Kososan (TJ-070: an early stage of common cold with poor digestion), Chikujountanto (TJ-091: sleeplessness in the convalescent stage of influenza or cold), Gokoto (TJ-095: cough, asthma), Saibokuto (TJ-096: asthma, bronchitis), Ryokankyomishingeninto (TJ-119: bronchitis, asthma) were tested for hPIV-2 growth inhibition. The medicines were kind gifts of Tsumura & Co. (Tokyo, Japan) and Akatsuka Pharmacy and Minami Kampo Pharmacy in Tsu City, Mie, Japan.

They were suspended in phosphate-buffered saline (PBS) (100 mg/mL), autoclaved for 15 min, centrifuged at 2,000 rpm for 5 min, and the supernatants were added to the cell culture. The supernatant was stored at -80°C until use.

2.2. Virus and recombinant virus

The virus and the recombinant virus were approved by the relevant biosafety committees of Suzuka University of Medical Science. hPIV-2 (Toshiba strain) was used. rhPIV-2ΔM-GFP was constructed according to the method described previously (*9,13,14*), and it was shown that it did not produce infectious virus particles without addition of M protein gene *in trans* (data not shown). The virus titer was determined using Vero cells and the titer was about 1×10^5 $TCID_{50}$/mL.

2.3. Cell line and cultivation of cells

$LLCMK_2$ cells (rhesus monkey kidney cell line) were cultured in a flat-bottomed 24-well plate in 1 mL culture medium. Minimum essential medium α (MEMα: FUJIFILM Wako Pure Chemical, Osaka, Japan), supplemented with 2% fetal calf serum (FCS) and 0.1 mg/mL kanamycin (Nacalai Tesque, Kyoto, Japan), was used. The cells were cultured at 37°C in a humidified atmosphere with 5% CO_2. After three days, when the cells became confluent (5×10^5 cells), the medium was changed to MEMα with 0.5% FCS and 0.1 mg/mL kanamycin. The medicines were added to the cells, and the cells were infected with hPIV-2 (3×10^2 $TCID_{50}$).

2.4. Cytopathogenic assay

Cell fusion was observed at four days post infection under a cell culture microscope.

2.5. RNA preparation, cDNA synthesis, real-time PCR and PCR

RNA was extracted from the cells (2×10^6 cells) cultured in a flat-bottomed 6-well plate using TRIZOL reagent (Thermo Fisher Scientific, Waltham, MA, USA) according to the manufacturer's method. cDNA was synthesized with 1 μg RNA using Reverse Tra Ace qPCR RT Master Mix (TOYOBO, Osaka, Japan) and NP gene specific primer (nucleotide number 1661-1679: 5'-CAACATTCAATGAATCAGT-3'). Real-time PCR was performed on the ABI PRISM 7700 Sequence Detection System (Thermo Fisher Scientific, Waltham,

MA, USA) using TaqMan Probe (1932-1956: 5'-FAM-AAGCACCGGATTTCTAACCCGTCCG-TAMRA-3'), forward primer (1851-1875: 5'-ACACACTCATCCAG ACAAATCAAAC-3'), and reverse primer (1958-1980: 5'-TGTGGAGGTTATCTGATCACGAA-3').

cDNA was synthesized with 1 μg RNA using forward primers for NP (nucleotide number 1,081-1,100: 5'-CATGGCCAAGTACATGGCTC-3'), F (5,821-5,840: 5'-CCCTATCCCTGAATCACAAT-3') and HN (7,741-7,760: 5'-ATTTCCTGTATATGGTGGTC-3') and superscript II reverse transcriptase (Thermo Fisher Scientific, Waltham, MA, USA), and PCR was carried out with forward primers for NP (nucleotide number 1,081-1,100), F (5,821-5,840) and HN (7,741-7,760), and reverse primers for NP (1,466-1,489: 5'-CCTCC GAGTATCGATTGGATTGAA-3'), F (6,661-6,681: 5'-TGTCACGAGACGTTACGGACA-3') and HN (8,481-8,500: 5'-GAACTCCCCTAAAAGAGATG-3') genes and Ex Taq (Takara BIO, Kusatsu, Shiga, Japan).

2.6. Detection of messenger RNA (mRNA)

cDNA was synthesized with 1 μg RNA using oligo(dT) primer and superscript II reverse transcriptase, and PCR was carried out with forward primers for NP (nucleotide number 1,081-1,100: 5'-CATGGCCAAGTACATGGCTC-3'), F (5,821-5,840: 5'-CCCTATCCCTGAATCACAAT-3') and HN (7,741-7,760: 5'-ATTTCCTGTATATGGTGGTC-3') genes of hPIV-2, and reverse primers for NP (1,466-1,489: 5'-CC TCCGAGTATCGATTGGATTGAA-3'), F (6,661-6,681): 5'-TGTCACGAGACGTTACGGACA-3') and HN (8,481-8,500: 5'-GAACTCCCCTAAAAGAGATG-3') genes and Ex Taq.

2.7. Immunofluorescence study

To detect virus proteins in the infected cells, the cells were fixed with 3.7% formaldehyde solution in PBS at room temperature for 15 min. The cells were further incubated with 0.05% Tween-20 in PBS at room temperature for 15 min to detect NP protein that exists mainly in the cytoplasm, or 3 min to detect F and HN proteins that are both in the cytoplasm and in the cell membrane, washed with PBS, and incubated with mouse mAbs against NP, F and HN proteins of hPIV-2 at room temperature for 30 min. After washing with PBS, the cells were incubated with Alexa 488 conjugated secondary antibody to mouse IgGs (Thermo Fisher Scientific, Waltham, MA, USA) at room temperature for 30 min, and observed under a fluorescence microscope (Olympus, Tokyo, Japan).

Actin was detected using rhodamine phalloidin (Thermo Fisher Scientific, Waltham, MA, USA) and microtubules were observed using anti-tubulin α mAb against sea urchin tubulin α (clone B-5-1-2, Sigma-Aldrich, St Louis, MO, USA) at four days of cultivation. The cells were fixed with 3.7% formaldehyde solution in PBS at 37°C for 15 min, washed with PBS, and the cells were further incubated with 0.05% tween20 in PBS at 37°C for 3 min to detect actin and for 15 min to detect microtubules.

2.8. Cell-to-cell spreading of hPIV-2

The drugs were added to the cells, and immediately after the addition, the cells were infected with rhPIV-2ΔM-GFP (1×10^4 $TCID_{50}$), and cultured for four days. They were then fixed with 1.2% formaldehyde solution in PBS at room temperature for 15 min and observed under a fluorescence microscope.

3. Results

3.1. Inhibitory effects of the herbal medicines

Different doses of the supernatants of the thirteen medicines were added to the cell culture, and the cells were infected with hPIV-2, and the cell fusion was observed and a hemadsorption test was carried out at four days post infection. Eight exhibited dose-dependent inhibitory effects and three caused cell toxicity, while two had no inhibitory effect. Table 1 shows the amount (μL) of supernatants of the herbal medicines that had an inhibitory effect on hPIV-2 replication. TJ-001, TJ-002, TJ-019, TJ-029, TJ-041, TJ-091, TJ-095 and TJ-119 had an inhibitory effect on hPIV-2 induced cell fusion and hemadsorption. TJ-027 and TJ-70 had no inhibitory effect. TJ-016, TJ-063 and TJ-096 showed cell toxicity at low concentration. Mainly the medicines which are effective on common cold and bronchitis inhibited hPIV-2 replication. The eight medicines were used in the following experiments.

3.2. Effect of the eight medicines on the release of hPIV-2

The supernatants of virus-infected cells with the medicines were harvested at four days of virus infection; they were diluted, infected to the cells, and the virus titer was determined by the observation of cell fusion and hemadsorption test at four days of culture. Figure 1 shows the titers (averages ± s.e.m. from five independent experiments) of the medicines. TJ-001, TJ-002 and TJ-119 completely inhibited the release of the virus (below 1/10,000). However, TJ-019, TJ-029, TJ-041, TJ-091 and TJ-095 only partially inhibited the release (1/100 to 1/1,000), though they showed both cell fusion inhibition and hemadsorption inhibition.

3.3. Effect of eight herbal medicines on viral genome RNA and mRNA syntheses

RNA was prepared from the infected cells at four days

Table 1. Inhibitory effect of herbal medicines and the amounts needed to inhibit virus induced cell fusion and hemadsorption

Product number	Herbal medicine	Inhibitory effect	Concentration
TJ-001	Kakkonto	+	140 μL/mL
TJ-002	Kakkontokasenkyushin'i	+	80 μL/mL
TJ-016	Hangekobokuto	-	a
TJ-019	Shoseiryuto	+	100 μL/mL
TJ-027	Maoto	-	b
TJ-029	Bakumondoto	+	160 μL/mL
TJ-041	Hochuekkito	+	100 μL/mL
TJ-063	Goshakusan	-	a
TJ-070	Kososan	-	b
TJ-091	Chikujountanto	+	80 μL/mL
TJ-095	Gokoto	+	80 μL/mL
TJ-096	Saibokuto	-	a
TJ-119	Ryokankyomishingeninto	+	120 μL/mL

a: cell toxicity; b: no inhibitory effect.

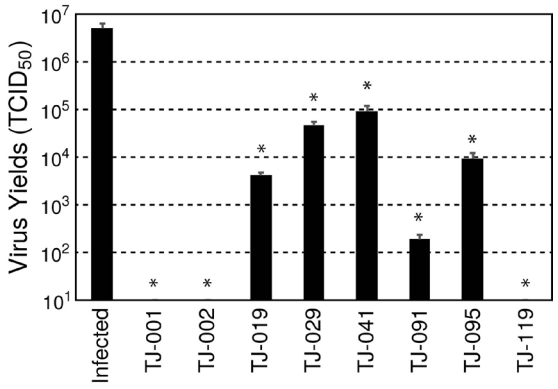

Figure 1. Effect of the medicines on hPIV-2 release from the cells. The supernatants were harvested at four days post infection and the virus titers were determined. Results are means ± s.e.m. from five independent experiments. Significant differences from the control infected cells are indicated by $^{*}(p < 0.01)$. TJ-001, TJ-002 and TJ-119 completely inhibited the release of the virus (below 1/10,000). TJ-019, TJ-029, TJ-041, TJ-091 and TJ-095 only partially inhibited the release (1/100 to 1/1,000).

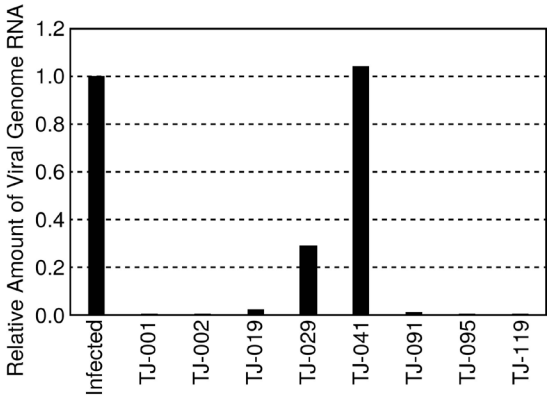

Figure 2. Effect of the medicines on viral genome RNA synthesis analyzed by quantitative real-time PCR. The medicines were added to the cell culture, infected with hPIV-2 and cultured for four days. RNA was extracted and viral genome RNA was analyzed by real-time PCR. The positive control infected cells are shown as 1. TJ-001, TJ-002, TJ-091, TJ-095 and TJ-119 almost completely inhibited viral genome RNA synthesis. TJ-019 and TJ-29 largely inhibited. TJ-041 did not inhibit.

post infection, and viral genome RNA was analyzed by real-time PCR and PCR. Viral mRNA was analyzed by PCR.

Figure 2 shows that TJ-001, TJ-002, TJ-019, TJ-091, TJ-095 and TJ-119 almost completely inhibited viral genome RNA syntheses. TJ-029 reduced the amount of viral genome RNA to about one-third of the control infected cells, but TJ-041 did not inhibit viral genome RNA synthesis.

Similar results were obtained by PCR (Figure 3). In Figure 3, NP, F and HN protein genes were detected in TJ-041 treated infected cells and they were seen as faint bands in TJ-029 treated cells. The other medicines almost completely inhibited NP, F and HN gene syntheses. These results are similar to those of real-time PCR.

Figure 4 shows the seven medicines also inhibited viral mRNA syntheses. NP, HN and F mRNAs were seen in TJ-029 and TJ-041 treated infected cells. In TJ-095 treated cells, NP and HN mRNAs were detected as faint bands. In TJ-019 and TJ-091 treated cells, only NP mRNA was faintly detected.

These results indicated that six out of eight medicines had inhibitory effects on viral genome and mRNA syntheses.

3.4. Effect on protein syntheses

Indirect immunofluorescence study was carried out using mAbs against NP, HN and F proteins to examine the effects of eight medicines on viral protein syntheses at four days post infection (Figure 5). Negative control non-infected cells had no immunofluorescence (data not shown). In Figure 5, A, B and C show the NP, F and HN protein expression in hPIV-2 infected cells, respectively. In hPIV-2 infected cells, NP, F and HN proteins were observed in almost all the cells: NP protein was observed in many strong fluorescent dots mainly in the cytoplasm, while F and HN proteins were in small dots

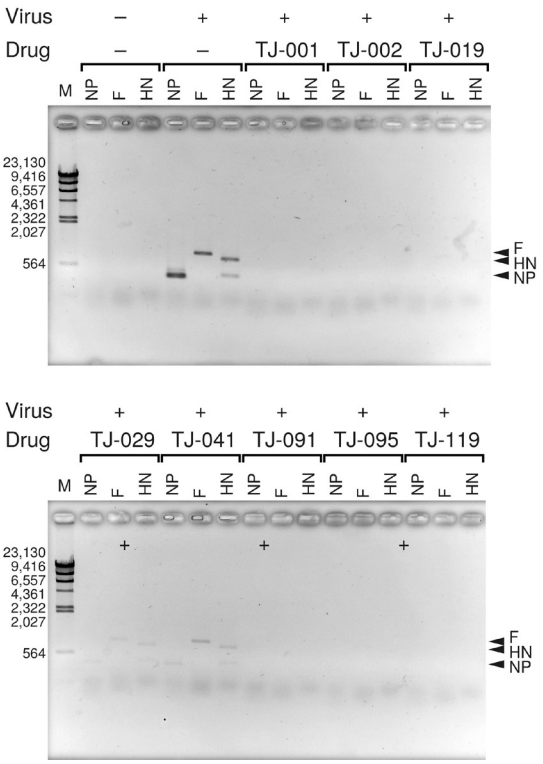

Figure 3. Effect of the medicines on viral genome RNA synthesis analyzed by PCR. NP, F and HN genes were detected using specific primers. TJ-001, TJ-002, TJ019, TJ-091, TJ-095 and TJ-119 inhibited viral genome RNA synthesis. TJ-029 and TJ-041did not inhibit it. M: size marker.

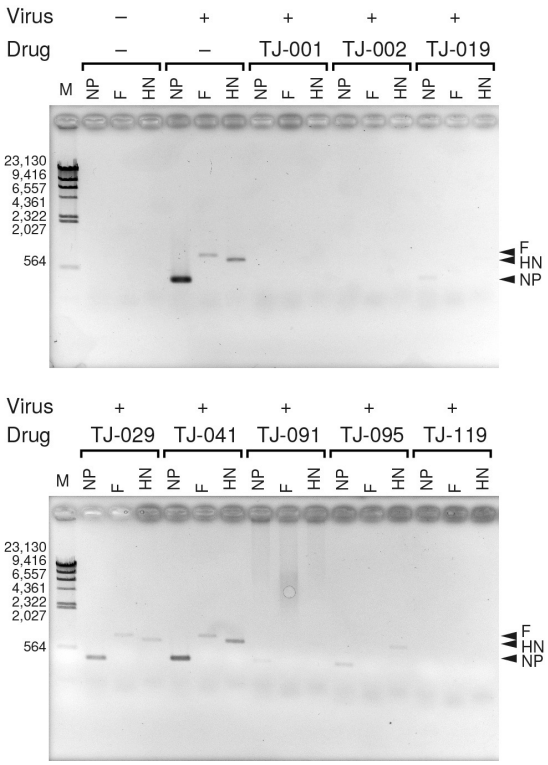

Figure 4. Effect of the medicines on viral mRNA synthesis analyzed by PCR. RNA was extracted and cDNA was synthesized by oligo(dT) primer. NP, F and HN mRNA were detected using specific primers. TJ-029 and TJ-041 did not inhibit mRNA synthesis. In TJ-095 treated infected cells, NP and HN mRNA were slightly observed, and in TJ-019 and TJ-091, only NP mRNA was faintly detected. M: size marker.

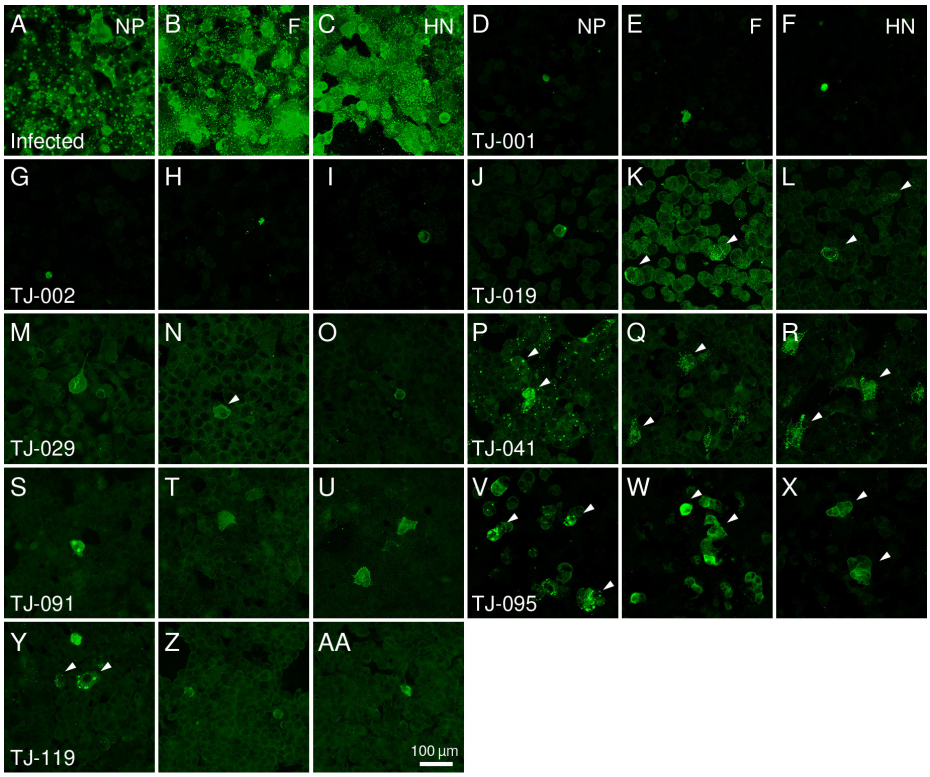

Figure 5. Effect of the medicines on viral protein synthesis. TJ-001 (D-F), TJ-002 (G-I), TJ-029 (M-O) and TJ-091 (S-U) largely inhibited protein synthesis. TJ-119 inhibited F and HN protein synthesis (Z and AA, respectively). In TJ-019 (J-L), TJ-041 (P-R) and TJ-119 (Y) treated infected cells, some positive cells were observed, however, there were no fused giant cells. Arrowheads indicate positive cells. Bar: 100 µm.

in the cytoplasm and on the cell surface. TJ-001 almost completely inhibited the protein syntheses: only a small number of cells were positive in NP, F and HN proteins of infected cells cultured withTJ-001 (Figure 5: D, E and F, respectively). TJ-002 also almost completely inhibited NP, F and HN protein syntheses just the same as TJ-001 treated cells (Figure 5: G, H and I, respectively). TJ-019 also largely inhibited the protein synthesis, but there are some positive cells (arrowheads) especially in F protein (Figure 5: J, K and L: NP, F and HN, respectively). TJ-029 also largely inhibited the protein syntheses (Figure 5: M, N and O: NP, F and HN, respectively). The arrowheads show positive cells. TJ-041 partially inhibited protein syntheses: some positive cells (arrowheads) can be seen (Figure 5: P, Q and R: NP, F, HN, respectively). TJ-091 also largely inhibited protein syntheses (Figure 5: S, T and U: NP, F and HN, respectively). TJ-095 partially inhibited protein syntheses: some positive cells are seen (arrowheads) (Figure 5: V, W and X, respectively). TJ-119 largely inhibited protein syntheses. However, a small number of cells were NP positive (arrowheads in Figure 5Y). Almost no cells were positive on F and HN proteins (Figure 5: Z and AA, F and HN, respectively).

3.5. Effect on the multinucleated giant cell formation

The cells were added with the medicines and immediately after that the cells were infected with rhPIV-2ΔM-GFP and cultured for four days. The cells were fixed with 1.2% formaldehyde and observed with the fluorescence microscope. Figure 6A is a positive control. There are many multinucleated giant cells with strong fluorescence. TJ-001 (Figure 6B) and TJ-002 (Figure 6C) inhibited the giant cell formation: there was a small number of single cells, but no giant cells. TJ-001 and TJ-002 also inhibited the virus release (Figure 1) and virus genome syntheses (Figure 2). TJ-019 (Figure 6D), TJ-029 (Figure 6E) and TJ-041 (Figure 6F) partially inhibited the giant cell formation: there were small sized fused cells with strong fluorescence. TJ-019, TJ-029 and TJ-041 partially inhibited virus release from the cells (Figure 1). TJ-091 also inhibited the giant cell formation (Figure 6G), but a small number of viruses were released (Figure 1). TJ-095 (Figure 6H) inhibited the giant cell formation, but there were some small fused cells (arrowheads in Figure 6H). TJ-095 only partially inhibited the number of released viruses (Figure 1). TJ-119 (Figure 6I) inhibited the giant cell formation: there are some small sized fused cells with weak fluorescence (arrowhead in Figure 6I). TJ-119 inhibited the number of released viruses (Figure 1). The multinucleated giant cell formation, the number of released viruses from the cells, and genome RNA syntheses were in good accordance.

3.6. Effect on actin microfilaments

The medicines were added to the cell culture without virus infection and cultured for four days. F-actin was stained with rhodamine phalloidin. Figure 7A is the positive control: bundles of actin microfilaments were clearly seen. TJ-001 (Figure 7B), TJ-002 (Figure 7C), TJ-019 (Figure 7D) and TJ-095 (Figure 7H) destroyed actin microfilaments. TJ-041 (Figure 7F) partially destroyed them. TJ-029 (Figure 7E), TJ-091 (Figure 7G) and TJ-119 (Figure 7I) had almost no effect on them. There are some discrepancies among virus titer, genome RNA

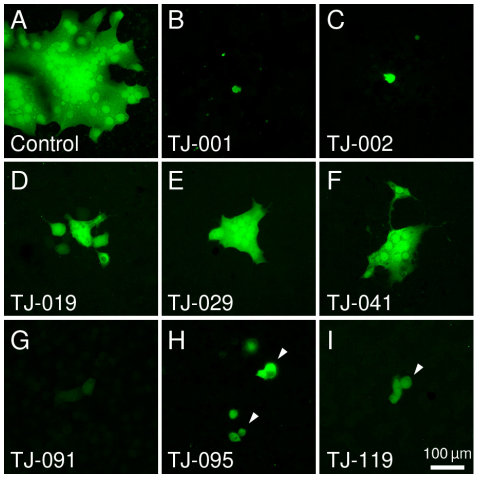

Figure 6. Effect of the medicines on multinucleated giant cell formation. The cells were added with the medicines and infected with rhPIV-2ΔM-GFP. Immunofluorescence study was carried out at four days post infection. In positive control cells, many multinucleated giant cells with strong fluorescence were observed **(A)**. TJ-001 **(B)**, TJ-002 **(C)**, TJ-091 **(G)**, TJ-095 **(H)** and TJ-119 **(I)** largely inhibited giant cell formation. TJ-019 **(D)**, TJ-029 **(E)**, and TJ-041 **(F)** did not inhibit cell fusion, but the size is small compared with positive control. Bar: 100 µm.

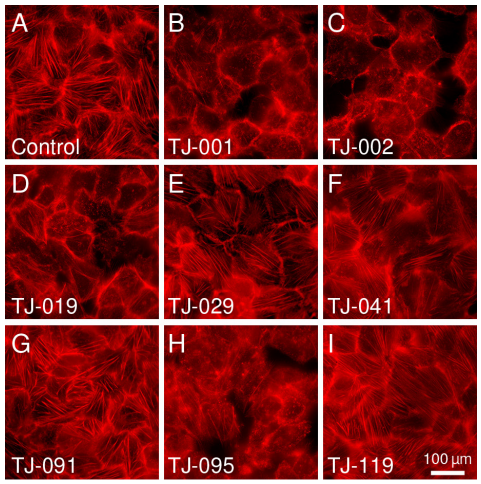

Figure 7. Effect of the medicines on actin microfilaments. The medicines were added to the cell culture without virus infection, and cultured for four days. The cells were stained with rhodamine phalloidin. In non-treated cells **(A)**, actin microfilaments were clearly seen. TJ-001 **(B)**, TJ-002 **(C)**, TJ-019 **(D)** and TJ-095 **(H)** almost completely destroyed the filaments. TJ-041 **(F)** caused partial damage. TJ-029 **(E)**, TJ-091 **(G)** and TJ-119 **(I)** showed almost no damage. Bar: 100 µm.

syntheses, and actin filaments, especially in TJ-041. We cannot explain the discrepancy. It was shown that the damage to actin microfilaments caused some inhibitory effects on the release of virus from the cells to culture medium.

3.7. Effect on microtubules

The cells were added with the medicines without virus infection, and cultured for four days. Microtubules were stained with anti-tubulin mAb. Figure 8A is the positive control: microtubule net was seen in the cytoplasm. TJ-001 (Figure 8B) and TJ-002 (Figure 8C) disrupted microtubules. TJ-019 (Figure 8D), TJ-041 (Figure 8F), TJ-095 (Figure 8H), and TJ-119 (Figure 8I) caused a little damage in microtubules. TJ-029 (Figure 8E) and TJ-091 (Figure 8G) had almost no effect on microtubules. Microtubules are also important for virus replication, so one of the causes of virus replication inhibition had some relation with the disruption of microtubules.

4. Discussion

Thirteen herbal medicines, which are effective on common cold and respiratory diseases, were tested against hPIV-2 replication *in vitro*. Eight out of thirteen medicines had inhibitory effects on hPIV-2 replication. The effects on genome RNA synthesis, viral mRNA synthesis, protein expression, multi-nucleated giant cell formation and cytoskeleton (actin microfilaments and microtubules) were analyzed.

Kakkonto (TJ-001), Kakkontokasenkyushin'i (TJ-002) and Ryokankyomishingeninto (TJ-119) had strong inhibitory effects on hPIV-2 replication. They inhibited virus genome RNA synthesis, virus mRNA synthesis, virus-induced multinucleated giant cell formation and virus protein synthesis, though in TJ-119 treated infected cells, a small number of cells were NP positive. TJ-001, TJ-002 almost completely inhibited virus induced multinucleated giant cell formation. In Shoseiryuto (TJ-019), Bakumondoto (TJ-029) and Hochuekkito (TJ-041) treated infected cells, small sized giant cells were observed, indicating that these three medicines could not fully inhibit the transmission of virus to the nascent cells. Chikujountanto (TJ-091), Gokoto (TJ-095) and TJ-119 inhibited giant cell formation, but some non-fused fluorescent cells were observed. In TJ-019, TJ-029 and TJ-041 treated infected cells, F protein expression was not fully inhibited. This may be one of the reasons for the appearance of small sized fused cells. In TJ-095 added infected cells, though the expression of NP, F and HN proteins were observed, there were almost no fused cells. In TJ-019, TJ-029 and TJ-041 treated infected cells, F protein was expressed as small dots on the cell surface. However, in TJ-095 treated infected cells, F protein was expressed mainly in the cytoplasm, not in the cell membrane, resulting in the inhibition of cell fusion. TJ-001 and TJ-002 caused damage to actin microfilaments and microtubules, but TJ-119 did not cause damage in actin microfilaments or microtubules. One of the reasons for inhibition by TJ-001 and TJ-002 was damage to actin microfilaments and microtubules, suggesting that the inhibitory mechanisms by TJ-119 may be different from those of TJ-001 and TJ-002.

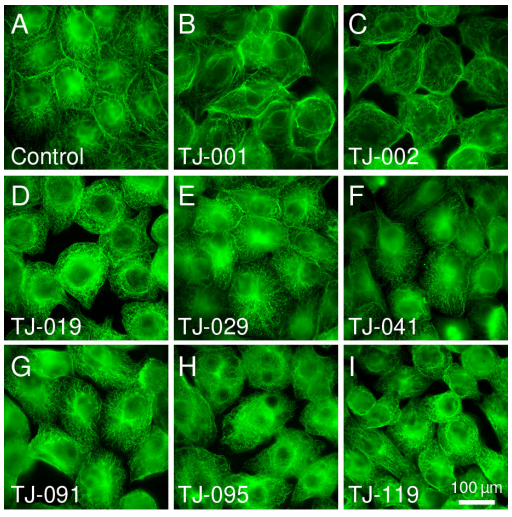

Figure 8. Effect of the medicines on microtubules. The cells were added to the cell culture without virus infection, and cultured for four days. The cells were stained with anti-tubulin α mAb against sea urchin tubulin α. In non-treated cells **(A)**, microtubules were clearly seen in the cytoplasm. TJ-001 **(B)** and TJ-002 **(C)** destroyed microtubules. TJ-041 **(F)** partially destroyed microtubules. TJ-019 **(D)**, TJ-029 **(E)**, TJ-091 **(G)**, TJ-095 **(H)** and TJ-119 **(I)** had almost no effect on microtubules. Bar: 100 µm.

Many investigations show that the medicines tested in this study inhibit various virus replications by different mechanisms. For instance, Kakkonto inhibits human respiratory syncytial virus infection by preventing viral attachment and internalization to the host cells (*17*). Kakkonto also possesses inhibitory activity against influenza viral polymerase acidic protein endonuclease (*18*). Hochuekkito binds to influenza virus particles and forms complexes and can obstruct the entry of the virus into cells (*12*). Hochuekkito also inhibits rhinovirus infection *in vitro*, partly by inhibiting the expression of its receptor, ICAM-1 (*19*). Shoseiryuto inhibits human cytomegalovirus replication *in vitro* by inhibiting viral DNA replication (*20*). Shoseiryuto is also effective against human respiratory syncytial virus infection on airway epithelia by preventing viral attachment and internalization to the host cells and by stimulating interferon secretion (*21*). Maoto has clinical efficacy for seasonal influenza, and it has equivalent clinical and virological efficacy to oseltamivir and zanamivir (*22*). It inhibits uncoating of influenza virus by inhibiting acidification and blocks influenza virus entry to cytoplasm (*11*).

One of the questions is which components of the medicines are effective on virus replication.

Table 2. Crude drugs contained in herbal medicines

TJ-001 Kakkonto	TJ-002 Kakkontokasenkyushin'i	TJ-027 Maoto	TJ-119 Ryokankyomishingeninto
Puerariae radix	*Puerariae radix*	*Ephedrae herba*	*Poria sclerotium*
Ziziphi fructus	*Ziziphi fructus*	*Cinnamomi cortex*	*Glycyrrhizae radix*
Ephedrae herba	*Ephedrae herba*	*Armeniacae semen*	*Pinelliae tuber*
Glycyrrhizae radix	*Glycyrrhizae radix*	*Glycyrrhizae radix*	*Zingiberis rhizoma processum*
Cinnamomi cortex	*Cinnamomi cortex*		*Armeniacae semen*
Paeoniae radix	*Paeoniae radix*		*Schisandrae fructus*
Zingiberis rhizoma	*Magnoliae flos*		*Asiasari radix*
	Ligustici chuanxiong rhizoma		
	Zingiberis rhizoma		

Glycyrrhizin is the effective component of *Glycyrrhizae radix*, and has an inhibitory efficacy for various virus replications *in vitro*, such as H5N1 influenza A virus (*23*), cytomegalovirus (*20*), rhinovirus (*19*) and human respiratory syncytial virus (*24*). Most herbal medicines which are effective on common cold and respiratory diseases contain extract of *Glycyrrhizae radix*. The medicines tested in this study contain *Glycyrrhizae radix* as an ingredient, except for Hangekobokuto (TJ-016). Glycyrrhizin also inhibits hPIV-2 replication *in vitro* (*25*), but effective concentration is much higher than that in these medicines and there is a significant difference in inhibitory efficacy between the medicines (Table 1). Therefore, glycyrrhizin may have only a small contribution to inhibit hPIV-2 replication in the medicines.

Both Kakkonto (*18*) and Maoto (*11*) have inhibitory effects on influenza virus replication. Maoto has inhibitory efficacy in influenza virus replication and its efficacy is partly derived from *Glycyrrhizae radix* (*26*). Kakkonto (TJ-001) and Kakkontokasenkyushin'i (TJ-002) showed strong inhibitory effects on hPIV-2 replication (Figure 1), although Maoto (TJ-027) did not (Table 1). Three crude drugs, *Ephedrae herba*, *Cinnamomi cortex* and *Glycyrrhizae radix*, are common ingredients to these three medicines (Table 2). Therefore, the inhibitory mechanism for hPIV-2 replication by herbal medicines may be different from that for influenza virus. Four crude drugs, *Puerariae radix*, *Ziziphi Fructus*, *Paeoniae radix* and *Zingiberis rhizoma*, are contained in Kakkonto and Kakkontokasenkyushin'i, but not in Maoto (Table 2). The results in this study suggest that one of the four crude drugs, or combination of two, three or all of them, is effective to inhibit hPIV-2 replication.

Ryokankyomishingeninto (TJ-119) also showed a strong inhibitory effect on hPIV-2 replication (Figure 1). It contains *Glycyrrhizae radix* as an ingredient, but not *Puerariae radix*, *Ziziphi fructus*, *Paeoniae radix* or *Zingiberis rhizoma* (Table 2), which are contained in Kakkonto and Kakkontokasenkyushin'i. Therefore, the inhibitory mechanism on hPIV-2 replication by Ryokankyomishingeninto may be different from that of Kakkonto and Kakkontokasenkyushin'i.

The inhibitory mechanism for hPIV-2 replication by herbal medicines may be multiple. The medicines have many components, and some can inhibit virus genome synthesis, mRNA synthesis and/or protein synthesis, and at the same time, destroy actin microfilaments and/or microtubules. In the present study, the medicines were suspended in PBS, autoclaved, and the supernatant was added to the cell culture, so some insoluble materials and heat unstable substances that may have inhibitory effects might be missing.

The next aim is to analyze and to extract the compounds that can inhibit not only parainfluenza virus but also respiratory syncytial virus, measles virus, mumps virus and metapneumovirus.

Funding: None.

Conflict of Interest: The authors have no conflicts of interest to disclose.

References

1. Lamb RA, Parks GP. Paramyxoviridae: The viruses and their Replication. In: Fields Virology, 5th edn. (Kniep DM, Howley PM, eds.). Lippincott Williams and Wilkins, Philadelphia, USA, 2008; pp. 1449-1496.
2. Yuasa T, Bando H, Kawano M, Tsurudome M, Nishio M, Kondo K, Komada H, Ito Y. Sequence analysis of the 3' genome end and NP gene of human parainfluenza type 2 virus: sequence variation of the gene-starting signal and the conserved 3' end. Virology. 1990; 179:777-784.
3. Ohgimoto S, Bando H, Kawano M, Okamoto K, Kondo K, Tsurudome M, Nishio M, Ito Y. Sequence analysis of P gene of human parainfluenza type 2 virus; P and cystein-rich proteins are translated by two mRNAs that differ by two non-templated G residues. Virology. 1990; 177:116-123.
4. Kawano M, Bando H, Ohgimoto S, Okamoto K, Kondo K, Tsurudome M, Nishio M, Ito Y. Complete nucleotide sequence of the matrix gene of human parainfluenza type 2 virus and expression of the M protein in bacteria. Virology. 1990; 179:857-861.
5. Kawano M, Bando H, Ohgimoto S, Okamoto K, Kondo K, Tsurudome M, Nishio M, Ito Y. Sequence of the fusion protein gene of human parainfluenza type 2 virus and its 3' intergenic region: lack of small hydrophobic (SH) gene. Virology. 1990; 178:289-292.
6. Kawano M, Bando H, Yuasa T, Kondo K, Tsurudome

M, Komada H, Nishio M, Ito Y. Sequence determination of the hemagglutinin-neuraminidase (HN) gene of human parainfluenza type 2 virus and the construction of a phylogenetic tree for HN proteins of all the paramyxoviruses that are infectious to humans. Virology. 1990; 174:308-313.
7. Kawano M, Okamoto K, Bando H, Kondo K, Tsurudome M, Komada H, Nishio M, Ito Y. Characterizations of the human parainfluenza type 2 virus gene encoding the L protein and the intergenic sequences. Nucleic Acids Res. 1991; 19:2739-2746.
8. Tsurudome M, Nishio M, Komada H, Bando H, Ito Y. Extensive antigenic diversity among human parainfluenza type 2 virus isolates and immunological relationships among paramxoviruses revealed by monoclonal antibodies. Virology. 1989; 171:38-48.
9. Kawano M, Kaito M, Kozuka Y, Komada H, Noda N, Namba K, Tsurudome M, Ito M, Nishio M, Ito Y. Recovery of infectious human parainfluenza type 2 virus from cDNA clones and properties of the defective virus without V-specific cysteine-rich domain. Virology. 2001; 284:99-112.
10. Nagai T, Urata T, Yamada H. *In vivo* anti-influenza virus activity of kampo (Japanese herbal) medicine "Sho-seiryu-to" – effects on aged mice, against subutypes of a viruses and B virus, and therapeutic effect. Immunophamacol Immunotoxicol. 1996; 18:193-208.
11. Masui S, Nabeshima S, Ajisaka K, Yamauchi K, Itoh R, Ishii K, Soejima T, Hiromatsu K. Maoto, a traditional Japanese herbal medicine, inhibits uncoating of influenza virus. Evid Based Complement Alternat Med. 2017; 2017:1062065.
12. Dan K, Takanashi K, Akiyoshi H, Munakata K, Hasegawa H, Ogawa K, Watanabe K. Mechanism of action of the anti-influenza virus active kampo (traditional Japanese herbal) medicine, Hochuekkito. Pharmacology. 2018; 101:148-155.
13. Uematsu J, Koyama A, Takano S, Ura Y, Tanemura M, Kihira S, Yamamoto H, Kawano M, Tsurudome M, O'Brien M, Komada H. Legume lectins inhibit human parainfluenza virus type 2 infection by interfering with the entry. Viruses. 2012; 4:1104-1115.
14. Kitagawa H, Kawano M, Yamanaka K, Kakeda M, Tsuda K, Inada H, Yoneda M, Sakaguchi T, Nigi A, Nishimura K, Komada H, Tsurudome M, Yasutomi Y, Nosaka T, Mizutani H. Intranasally administered antigen 85B gene vaccine in non-replicating human parainfluenza type 2 virus vector ameliorates mouse atopic dermatitis. Plos One. 2013; 8:e66614.
15. De BP, Banerjee AK. Involvement of actin microfilaments in the transcription/replication of human parainfluenza virus type 3: possible role of actin in other viruses. Microsc Res Teck. 1999; 47:114-123.
16. Moyer SA, Baker SC, Lessard JL. Tubulin: a factor necessary for the synthesis of both Sendai virus and vesicular stomatitis virus RNAs. Proc Natl Acad Sci U S A. 1986; 83:5405-5409.
17. Chang JS, Wang KC, Shieh DE, Hsu FF, Chiang LC. Ge-Gen-Tang has anti-viral activity against human respiratory syncytial virus in human respiratory tract cell lines. J Ethnopharmacol. 2012; 139:305-310.
18. Shirayama R, Shoji M, Sriwilaijaroen N, Hiramatsu H, Suzuki Y, Kuzuhara T. Inhibition of PA endonuclease activity of influenza virus RNA polymerase by Kampo medicines. Drug Discov Ther. 2016; 10:109-113.
19. Yamada M, Sasaki T, Yasuda H, Inoue D, Suzuki T, Asada M, Yoshida M, Seki T, Iwasaki K, Nishimura H, Nakayama K. Hochu-ekki-to inhibits rhinovirus infection in human tracheal epithelial cells. Br J Pharmacol. 2007; 150:702-710.
20. Murayama T, Yamaguchi N, Matsuno H, Eizuru Y. *In vitro* anti-cytomegalovirus activity of kampo (Japanese herbal) medicine. Evid Based Complement Alternat Med. 2004; 1:285-289.
21. Chang JS, Yeh CF, Wang KC, Shieh DE, Yen MH, Chiang LC. Xiao-Qing-Long-Tang (Sho-seiryu-to) inhibited cytopathic effect of human respiratory syncytial virus in cell lines of human respiratory tract. J Ethnopharmacol. 2013; 147:481-487.
22. Nabeshima S, Kashiwagi K, Ajisaka K, Masui S, Takeoka H, Ikematsu H, Kashiwagi S. A randomized, controlled trial comparing traditional herbal medicine and neuraminidase inhibitors in the treatment of seasonal influenza. J Infect Chemother. 2012; 18:534-543.
23. Michaelis M, Geiler J, Naczk P, Sithisarn P, Leutz A, Doerr HW, Cinatl J Jr. Glycyrrhizin exerts antioxidative effects in H5N1 influenza A virus-infected cells and inhibits virus replication and pro-inflammatory gene expression. Plos One. 2011; 6:e19705.
24. Yeh CF, Wang KC, Chiang LC, Shieh DE, Yen MH, Chang JS. Water extract of licorice had anti-viral activity against human respiratory syncytial virus in human respiratory tract cell lines. J Ethnopharmacol. 2013; 148:466-473.
25. Sakai-Sugino K, Uematsu J, Kamada M, Taniguchi H, Suzuki S, Yoshimi Y, Kihira S, Yamamoto H, Kawano M, Tsurudome M, O'Brien M, Itoh M, Komada H. Glycyrrhizin inhibits human parainfluenza virus type 2 replication by the inhibition of genome RNA, mRNA and protein syntheses. Drug Discov Ther. 2017; 11:246-252.
26. Nomura T, Fukushi M, Oda K, Higashiura A, Irie T, Sakaguchi T. Effects of traditional kampo drugs and their constituent crude drugs on influenza virus replication *in vitro*: Suppression of viral protein synthesis by *glycyrrhizae radix*. Evid Based Complement Alternat Med. 2019; 2019:3230906.

Received June 26, 2021; Revised August 16, 2021; Accepted August 17, 2021

[§]These authors contributed equally to this work.
**Address correspondence to:*
Jun Uematsu, Microbiology and Immunology Section, Department of Clinical Nutrition, Graduate School of Health Science, Suzuka University of Medical Science, 1001-1 Kishioka, Suzuka, Mie 510-0293, Japan.
E-mail: uematsu@suzuka-u.ac.jp

Present Address:
[a] Department of Life Vista, Nara Saho College, Nara, Japan;
[b] Department of Life and Environmental Science, Tsu City College, Tsu, Mie, Japan;
[c] Department of Microbiology, Mie University Graduate School of Medicine, Tsu, Mie, Japan.

Released online in J-STAGE as advance publication August 26, 2021.

Original Article

DOI: 10.5582/ddt.2021.01069

Ectopic expression of Id1 or Id3 inhibits transcription of the *GATA-4* gene in P19CL6 cells under differentiation condition

Yumei Yokura-Yamada[1], Makoto Araki[2], Masatomo Maeda[1,*]

[1] Graduate School of Pharmaceutical Sciences, Osaka University, Suita, Osaka, Japan;
[2] Meiji Pharmaceutical University, Tokyo, Japan.

SUMMARY Inhibitor of DNA binding (Id) is a dominant negative form of the E-box binding basic-helix-loop-helix (bHLH) transcription factor since it is devoid of the basic region required for DNA binding and forms an inactive hetero dimer with bHLH proteins. The E-box sequence located in the promoter region of the GATA-binding protein 4 (*GATA-4*) gene is essential for transcriptional activation in P19CL6 cells. These cells differentiate into cardiomyocytes and start to express GATA-4, which further triggers cardiac-specific gene expression. In this study, expression plasmids for Ids tagged with human influenza hemagglutinin (HA)-FLAG were constructed and introduced into P19CL6 cells. The stable clones expressing the recombinant Id proteins (Id1 or Id3) were isolated. The *GATA-4* gene expression in these clones under differentiation condition in the presence of 1% dimethyl sulfoxide (DMSO) was repressed, with concomitant abolishment of the transcription of α-myosin heavy chain (α-MHC), which is a component of cardiac myofibrils. Thus, the increased expression of Id protein could affect *GATA-4* gene expression and negatively regulate the differentiation of P19CL6 cells.

Keywords Inhibitor of DNA binding, GATA transcription factor, cardiomyocyte differentiation, transcription

1. Introduction

It is well known that many gene products participate spatio-temporally in a complex manner in the developmental process (*1*). In mouse heart formation, transcription factor GATA-binding protein 4 (GATA-4) together with NK2 homeobox 5 (Nkx2.5) and T-box factor 5 (Tbx5), and chromatin remodeling protein SMARCD3 (BAF60c) are key upstream regulators of cardiomyocyte differentiation in the cardiogenic splanchnic mesoderm (*2*). Expression of GATA-4 in the extraembryonic endoderm in the embryo is required for folding morphogenesis to form a primitive heart tube and foregut (*3*). Consistent with the expression of GATA-4 in cardiomyocytes at all stages of cardiac development in mouse (*4*), it is reported that mutations of the *GATA-4* gene lead to variable phenotypes of human congenital heart diseases (*5*).

To study cardiomyocyte differentiation at the cellular level, P19 mouse embryonic carcinoma cells and their derivative P19CL6 cells have been used because they easily start differentiating into beating cardiomyocytes upon the addition of dimethyl sulfoxide (DMSO) (*6*). It was further demonstrated that expression of the *GATA-4* gene is required for the differentiation of cardiomyocytes (*7*). As for transcriptional regulation, the *GATA-4* gene is transcribed from two alternative 5' untranslated exons (E1a and E1b) (*8,9*), and the level of the E1a transcript of mouse heart is 20-times higher than that of E1b (*8*). Analyses of the promoter for E1a demonstrated that the conserved E-box sequence (CACGTG) is essential for transcription from the E1a exon (*10,11*), suggesting that the basic-helix-loop-helix (bHLH) transcription factor(s) may play a role in transcription of the *GATA-4* gene (*9,12*). It is also reported that more euchromatic state of the further upstream region of the cluster of GC-boxes and E-box activates the *GATA-4* promoter (*13*).

The inhibitor of DNA binding (Id) proteins (Id1-Id4) which do not have the amino-terminal basic region of bHLH transcription factor function as a dominant negative form of bHLH proteins, and their functions seem to be redundant or compensatory although Ids are required for heart development (*14*). Ids are also suggested to play a role in keeping precursor cells immature and expanding the cell population size during development (*15*). Id1 and Id3, although the latter is less active, are essential for specification of mesendosomal progenitors into cardiac progenitors in the first heart field (*16*). Biochemical studies further demonstrated that Id1, Id2 and Id3 bind GATA-4 and Nkx2.5 proteins and

inhibit their synergistic transcriptional activation due to inhibition of DNA binding and/or mutual interaction (*17*). Stable expression of Id3 ectopically in P19 cells inhibited the differentiation concomitant decrease of GATA-4 expression (*17*). In this study we constructed expression plasmids for tagged-Id1, Id2 and Id3, and tried to express these tagged proteins stably in P19CL6 cells to determine whether their differentiation into cardiomyocytes is inhibited or not.

2. Materials and Methods

2.1. Cell culture

P19CL6 cells (RIKEN Cell Bank, Tsukuba, Ibaraki, Japan) were cultured at 37°C in α-Eagle's minimal essential medium (MEM) (Sigma, St. Louis, MO, USA) containing 10% (v/v) fetal bovine serum (FBS) (GIBCO BRL, Gaithersburg, MD, USA) and antibiotics [2.5 μg/ml fungizon (GIBCO BRL), 100 units/mL benzylpenicillin (Wako, Osaka, Japan), and 100 μg/mL streptomycin sulfate (Wako)]. Cells (1×10^5 cells in Φ 10 cm dish) were allowed to differentiate in the presence of 1% (v/v) DMSO (Wako) (*10*). The medium was changed 4 days after inoculation and then every 2 days.

2.2. Analysis of RNA

Total cellular RNA was extracted with Isogen (Nippon Gene, Toyama, Japan) from a Φ 10 cm dish according to the manufacturer's protocol, and an aliquot (5 μg) was reverse transcribed with Moloney Murine Leukemia Virus (M-MLV) Reverse Transcriptase (TaKaRa, Kusatsu, Shiga, Japan) and the oligo$(dT)_{15}$ primer in a volume of 20 μL. After RNase H (TaKaRa) treatment, cDNA (0.3 μL) was subjected to semi-quantitative PCR analysis (*18*) with *GoTaq*® DNA polymerase (Promega, Madison, WI, USA). The unsaturated conditions for polymerase chain reaction (PCR) comprised preheating (94°C, 3 min), followed by 17-27 cycles of denaturation (94°C, 0.5 min), annealing (55-61°C, 0.5 min), and extension (72°C, 0.5 min), and then post-incubation (72°C, 5 min): typically, GATA-4 (27 cycles, 55°C), α-myosin heavy chain (α-MHC) (24 cycles, 60°C), Id1 (21 cycles, 61°C), Id2 (21 cycles, 60°C), Id3 (21 cycles, 60°C), and β-actin (17 cycles, 60°C). The primer pairs used for PCR are shown in Table 1A. The PCR products were size-separated by 2% (w/v) agarose gel-electrophoresis, and DNA bands were visualized with ethidium bromide. Images were recorded with a FAS-III UV-imaging system (Toyobo, Osaka, Japan).

2.3. Cloning of cDNAs for mouse Id1, Id2 and Id3

P19CL6 cells were cultured for 12 days in the presence of 1% (v/v) DMSO. cDNA was synthesized from total cellular RNA as prepared in *2.2*., and was subjected to PCR using a primer pair [YY001/YY002 to amplify cDNA for the coding region of Id1 cDNA, YY003/YY002 for Id2, or YY005/YY006 for Id3 (Table 1B)] and *GoTaq*® DNA polymerase. The PCR conditions were [preheating (94°C, 3 min), followed by 30 cycles of denaturation (94°C, 0.5 min), annealing (60°C for Id1, 51°C for Id2 and 63°C for Id3, 30 sec), and extension (72°C, 0.5 min), and then post-incubation

Table 1. Sequences of oligonucleotides used in this study

(A)	GATA-4	SSPN031	5'-gta ggc ctc tcc tgt g-3'
		SSPN033	5'-cgc tga tta cgc ggt gat-3'
	α-MHC	MHC S	5'-gga aga gtg agc ggc gca tca agg-3'
		MHC A	5'-ctg ctg gag agg tta ttc ctc g-3'
	Id1	Id1f	5'-tgg acg agc agc agg tga acg-3'
		Id1r	5'-gca ctg atc tcg ccg ttc agg-3'
	Id2	Id2f	5'-agc ctt cag tcc ggt gag gtc c-3'
		Id2r	5'-tca gat gcc tgc aag gac agg-3'
	Id3	Id3f-2	5'-ctc tac tct cca aca tga agg cg-3'
		Id3r	5'-agt gag ctc agc tgt ctg gat-3'
	β-actin	YSactin S	5'-gca gga gat ggc cac tgc cgc-3'
		YSactin A	5'-tct cct tct gca tcc tgt cag c-3'
(B)	Id1	YY001	5'-tt cat ATG AAG GTC GCC AGT GG-3'
		YY002	5'-cc TCA GCG ACA CAA GAT GCG-3'
	Id2	YY003	5'-tt cat ATG AAA GCC TTC AGT C-3'
		YY004	5'-at TTA GCC ACA GAG TAC-3'
	Id3	YY005	5'-tt cat ATG AAG GCG CTG AGC CCG-3'
		YY006	5'-gg TCA GTG GCA AAA GCT CCT CTT-3'
(C)	M13F		5'-gta aaa cga cgg cca gt-3'
	M13R		5'-gga aac agc tat gac cat g-3'
	T7 primer		5'-taa tac gac tca cta tag-3'

In (B), an *Nde*I site (underlined) was introduced at the initiation codon in the sense primer (the primer S in Figure 1). The primer A in Figure 1 showed the antisense primer. Capital letters in (B) indicate the nucleotide residues identical to those in the coding region, while lower case letters indicate unrelated residues introduced.

(72°C, 5 min)]. The products were size-separated by 2% (w/v) agarose gel-electrophoresis, and the amplified cDNA bands (454, 412 and 367 bp for Id1, Id2 and Id3, respectively) visualized with ethidium bromide were extracted with a GENECLEAN® III Kit (BIO101, Vista, CA, USA). The cDNAs were ligated into the pGEM T-easy vector (Promega) and then introduced into *Escherichia coli* TOP-10F'. The sequence of the cloned DNA was determined by the dideoxy chain-termination method (*19*) with a sequence primer (M13F or M13R) (Table 1C) and a BigDye™ Terminator v3.1 Cycle Sequencing Kit (Applied Biosystems, Waltham, MA, USA), using an ABI PRISM TM 310 Genetic Analyzer.

2.4. Construction of expression plasmids for Ids tagged with human influenza hemagglutinin (HA) and FLAG

The cDNA moiety of the Ids in the pGEM T-easy vector was excised with *Apa*I (Id1) or *Nsi*I (Id2 and Id3), followed by Klenow treatment and then *Nde*I digestion. The fragment was inserted into pHA/FLAG(AS)-7 (*20*), which had been digested with *Sph*I followed by Klenow treatment, and then digested with *Nde*I. The DNA sequence of the resulting plasmid, "Id in pHA/FLAG", was verified as described in *2.3*. with a sequence primer (T7 primer or M13R) (Table 1C). The *Not*I - *Hin*dIII fragment derived from "Id in pHA/FLAG" was further cloned into pDsRed2-N1 (CLONETECH, Mountain View, CA, USA). This expression plasmid was named pneo-HA/FLAG-Id. We further replaced the neomycin-resistance gene with that of hygromycin. The pGL4.14[*luc*2/Hygro] vector (Promega) containing the hygromycin-resistance gene was treated with *Bgl*II and *Bam*HI, and the large fragment was self-ligated, resulting in deletion of the luciferase gene moiety. Into the *Eco*RV site of the multi-cloning site of the self-ligation product (phyg), the HA-FLAG-Id portion together with promoter from pneo-HA/FLAG-Id were inserted; the fragment being obtained on *Nsi*I digestion followed by Klenow treatment and *Ssp*I digestion. The procedure is schematically shown in Figure 1. The molecular biological methods for DNA manipulations were based on standard procedures (*21*).

2.5. Transfection of expression plasmids for Ids tagged with HA and FLAG

We first expressed the tagged Id proteins (HA/FLAG-Ids) transiently by means of the diethylaminoethyl (DEAE)-dextran method (*22*) to verify the expression of tagged Ids derived from the plasmid constructs; Cos-1 cells (ATCC, Manassas, VA, USA) were grown in Dulbecco's modified Eagle medium (DMEM) (GIBCO BRL) supplemented with 7% (v/v) FBS. Cells (5×10^5 cells) in 5 mL medium were plated onto a *Φ* 6 cm dish. Into each dish the plasmid construct was introduced at a concentration of 2.5 μg/dish. Cells were

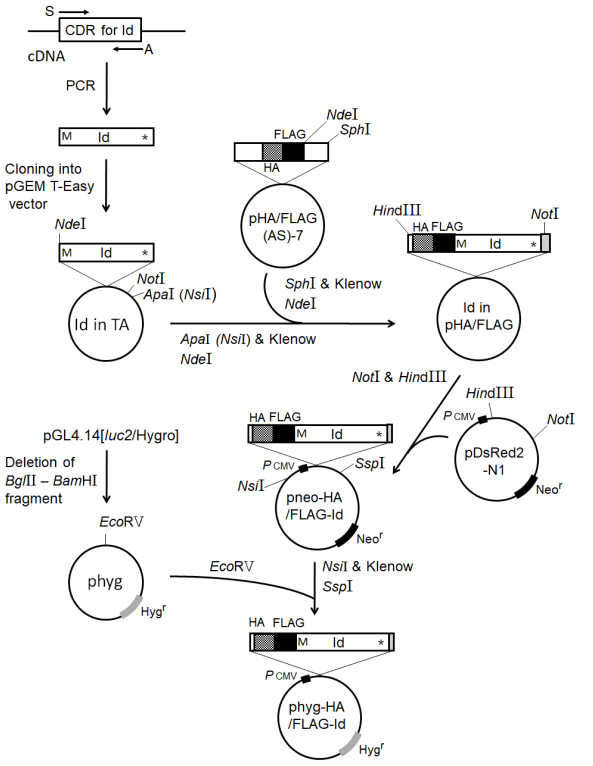

Figure 1. Construction of expression plasmids for Id1, Id2 and Id3 with an amino-terminal tandem HA/FLAG-tag. The coding regions (CDRs) for Id1, Id2 and Id3 were cloned from cDNAs prepared from differentiated P19CL6 cells, and inserted into pGEM T-Easy vector (Id in TA). The primer pairs listed in Table 1B were designed from the registered cDNA sequences; NM_010495 (Id1), NM_010496 (Id2), and NM_008321 (Id3), respectively. The expression plasmids for Ids with an amino-terminal HA/FLAG-tag (pneo-HA/FLAG-Id) were constructed as described under Materials and Methods. The neomycin-resistance gene (Neo^r) was further substituted with the hygromycin-resistance gene (Hyg^r) to produce phyg-HA/FLAG-Id. The initiation and termination codons for Id are indicated by "M" and "*", respectively. The coding regions for the HA (YPYDVPDYA) and and FLAG (DYKDDDDK) peptide moieties are schematically shown by mesh and black shading, respectively. HA/FLAG-Id was transcribed under the cytomegalovirus (CMV) promoter (P_{CMV}).

treated with chloroquine followed by glycerol, and then further cultured for 2 days. The whole cell extract for immunoprecipitation was prepared from duplicate samples. Protein concentrations were determined with a BioRad Protein Assay Kit (Hercules, CA, USA) using bovine serum albumin (Fraction V) (Sigma) as a standard (*23*).

We further isolated P19CL6 clones that express tagged Ids stably by the calcium-phosphate method (*21*); briefly, cells (5×10^5 cells) were plated onto a *Φ* 6 cm dish. On the next day, the DNA solution was poured onto the culture medium and left for 4 hr. The medium was removed and washed with phosphate-buffered saline [10 mM phosphate buffer (pH7.2), 137 mM NaCl, 3 mM KCl] (PBS). Cells were further cultured in fresh medium for 24 hr, and then neomycin (G418) (100 μg/mL) (Nacalai, Kyoto, Japan) or hygromycin (300 μg/mL) (Wako) was added. On the following day, cells were plated onto 2 dishes (*Φ* 10 cm) containing the

antibiotic. After ~12 days, single colonies were isolated. A whole cell extract was prepared from a confluent culture of undifferentiated clones grown in two Φ 6 cm dishes.

2.6. Preparation of a whole cell extract and immunoprecipitation

After washing with ice-cold PBS three times, cells were suspended in 1 mL 20 mM tris(hydroxymethyl) aminomethane (Tris)-HCl (pH 7.5), 150 mM NaCl, 2 mM ethylenediaminetetraacetic acid containing 10 μg/mL leupeptin, 10 μg pepstatin A and 1% (v/v) NP-40 [TNE (+)] and kept on ice for 30 min. All the following procedures were carried out at 4°C. The cell suspension was sheered through a 25G needle 10 times, and then centrifuged (12,000× g, 30 min). The supernatant was used as the whole cell extract.

The Protein G Sepharose beads (GE Healthcare, Chicago, IL, USA) was pre-washed twice with TNE (+) and then centrifuged (2,000× g, 5 min). The whole cell extract was incubated for 1 hr in a Mini Disk Rotor BC-710 (BIO CRAFT, Tokyo, Japan) with a 30 μL bed volume of pre-washed Protein G Sepharose beads. The supernatant was incubated on a Rotor for 1 hr with 5 μL of Monoclonal anti-HA (HA-7) (Sigma), and then further incubated in a Rotor with a 50 μL bed volume of pre-washed Protein G Sepharose beads for 1hr. The beads were precipitated (2,000× g, 5 min) and then washed five times (three times by rotation and then twice without rotation) with 500 μL 20 mM Tris-HCl (pH 7.5), 150 mM NaCl, 2 mM ethylenediaminetetraacetic acid (TNE). The recovered immuno-complex was heated at 95°C for 5 min together with 15-20 μL of 2 × sample buffer for sodium dodecyl sulfate (SDS)-polyacrylamide gel-electrophoresis (*24*).

2.7. SDS-polyacrylamide gel-electrophoresis and Western blotting

All the solubilized protein was subjected to SDS-polyacrylamide gel-electrophoresis [mini-gel (10 cm × 10 cm), 1 mm thickness, consisting 3% (w/v) stacking gel (60 V) and 18% (w/v) separation gel (100 V)] (*24*), and then electro-blotted [200 mA, 90 min.; ATTO Model-AE6675 (ATTO, Tokyo, Japan)] onto an Immobilon™-P membrane [Millipore (Billerica, MA, USA) polyvinylidene difluoride (PVDF) membrane (0.45 μm), IPVH00010] (*25*). The filter was washed with PBS and then blocked 1hr at 4°C with PBS plus 0.1 % (v/v) Tween 20 (PBS-T) containing 5% (w/v) skim-milk (BD, Franklin Lakes, NJ, USA). The filter was washed with PBS-T and then reacted for 2 hr at room temperature with ANTI-FLAG M2® monoclonal antibody-peroxidase conjugate (Sigma) (× 1,500 diluted). Chemiluminescence was detected with an ECL Western blotting kit (GE Healthcare) using Scientific Imaging Film (KODAK, Rochester, NY, USA).

2.8. Chemicals

Restriction enzymes were obtained from New England Biolabs (Ipswich, MA, USA) and Toyobo. The Klenow enzyme, T4 DNA ligase (Ligation Kit Ver2.1), and Agarose-LE Classic Type were provided by TaKaRa. Tween 20 and chloroquine diphosphate were obtained from Nacalai. DEAE-dextran, NP-40, leupeptin and pepstatin A were from Sigma. Oligonucleotides were purchased from Gene Design Inc. (Ibaraki, Osaka, Japan). All other chemicals used were of the highest grade commercially available.

3. Results

3.1. Construction of expression plasmids for Ids

The cDNAs for mouse Ids (Id1, Id2 and Id3) were cloned from P19CL6 cells by means of reverse transcription PCR (RT-PCR) and then inserted into a mammalian expression plasmid pDsRed2-N1. To detect ectopic expression, we introduced a HA/FLAG-tag at the amino terminus of each Id. The neomycin-resistance marker was also replaced with that of hygromycin (Figure 1). Plasmids were introduced into Cos-1 cells, and the Id proteins transiently expressed were detected by Western blotting to verify their molecular sizes. Since we sometimes experienced difficulty in detecting the tagged Id proteins in a whole cell extract, an immunoprecipitation method was developed, as shown under Materials and Methods. The HA/FLAG-Id in the whole cell extract was first immunoprecipitated with anti-HA antibody and then detected by means of Western blotting with anti-FLAG antibody. As shown in Figure 2, the calculated molecular size of the tagged-Id (see legend to Figure 2) was not significantly different from its molecular size on the gel.

3.2. Stable expression of Ids in P19CL6 cells

The expression plasmids for tagged Ids were introduced into P19CL6 cells and neomycin-resistance colonies were isolated. However, most of the resistant clones did not express HA/FLAG-Id in spite of several trials of transfection. Typical results are shown in Figures 3A and 3B; two clones for tagged Id1 ($Id1_{A5}$ and $Id1_{B7}$) and one for tagged Id3 ($Id3_{A3}$) were obtained in two separate transfection experiments. However, clones for tagged Id2 could not be obtained. We also did not obtain a clone from hygromycin-resistant colonies.

3.3. Transcription level of GATA-4 under differentiation condition for P19CL6 cells

As already reported, many preceding studies involving

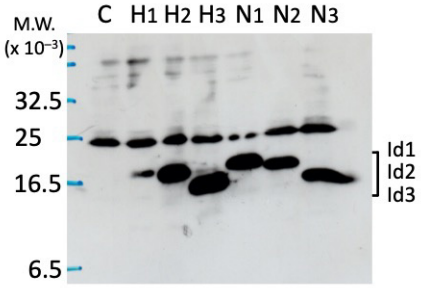

Figure 2. Transient expression of Id1, Id2, or Id3 tagged with a HA/FLAG peptide in Cos-1 cells. Cos-1 cells were transfected with the expression plasmid for either tagged Id1, Id2 or Id3 by means of the DEAE-dextran method [H_1 (phyg-HA/FLAG-Id1), H_2 (phyg-HA/FLAG-Id2), H_3 (phyg-HA/FLAG-Id3), N_1 (pneo-HA/FLAG-Id1), N_2 (pneo-HA/FLAG-Id2), N_3 (pneo-HA/FLAG-Id3), and C (without plasmid)]. Cells were grown for 2 days, and then the transiently expressed HA/FLAG-Id protein in the whole cell extract was immunoprecipitated with anti-HA antibody. HA/FLAG-Id protein was detected by Western blotting with peroxidase conjugated anti-FLAG antibody after SDS-polyacrylamide gel-electrophoresis as described under Materials and Methods. Chemiluminescence was detected after 15 min exposure. The average molecular mass of the tagged Id protein was calculated with GENETYX-MAC GENETIC INFORMATION PROCESSING SOFTWARE (GENETYX Corporation, Tokyo, Japan); HA/FLAG-Id1, 19.1 kDa; HA/FLAG-Id2, 18.5 kDa; and HA/FLAG-Id3, 16.7 kDa. The values were the sums of the amino acid residues of the native Id (148, 134 and 119 residues for Id1, Id2 and Id3, respectively) and HA/FLAG peptide (31 residues) (*20*). The Id1 used in this study was a smaller isoform produced by removing a coding intron (*49*).

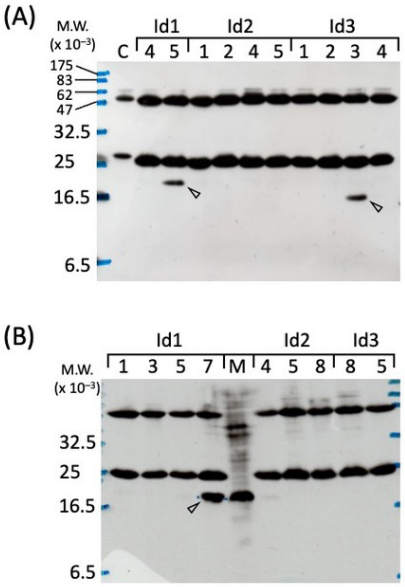

Figure 3. Detection of Ids tagged with a HA/FLAG peptide stably expressed in P19CL6 cells. (A) P19CL6 cells were transfected with the expression plasmid for either tagged Id1, Id2 or Id3 by means of the calcium-phosphate method [Id1 (pneo-HA/FLAG-Id1), Id2 (pneo-HA/FLAG-Id2), Id3 (pneo-HA/FLAG-Id3), and C (P19CL6 cells without transfection)] as described under Materials and Methods. Six colonies resistant to neomycin were isolated from each transfection. The whole cell extract of each clone was treated with anti-HA antibody, and the immune-precipitated HA/FLAG-Id was detected by means of Western blotting with anti-FLAG antibody after SDS-polyacrylamide gel-electrophoresis. Chemiluminescence was detected after 1 hr exposure. The numbers of clones from each expression plasmid are indicated above. **(B)** P19CL6 cells were transfected similarly to as described in (A), and eight colonies resistant to neomycin were isolated from each transfection. M, whole cell extract (20 μg protein) prepared from Cos-1 cells transiently expressing the Id1 expression plasmid (pneo-HA/FLAG-Id1). Open triangles in (A) and (B) indicated the tagged Id proteins (HA/FLAG-Id1 and HA/FLAG-Id3). The positive clones are denoted as clone $Id1_{A5}$, clone $Id1_{B7}$ and clone $Id3_{A3}$, respectively, in the text. Id proteins could not be detected in the rest of the clones not indicated in the figure (not shown).

P19 and P19CL6 cells revealed that the transcription of *GATA-4* gene starts at around 4 days under differentiation conditions, that of the genes for the components of cardiac muscle following later (*7,26-28*). Figure 4 (left) shows that GATA-4 mRNA was actually detected within 4 days after DMSO addition and that of α-MHC appeared at 8 days weakly and at 12 days clearly. However, transcription of the *GATA-4* gene did not occur in $Id1_{A5}$ and $Id3_{A3}$ cells even in the presence of DMSO, ectopically HA/FLAG-Id1 and HA/FLAG-Id3 being expressed, respectively (Figure 4, middle and right). As the transcription of cardiac muscle genes such as *α-MHC*, *β-MHC*, cardiac troponin C (*cTpC*), atrial myosin light-chain 1 ($MLC\text{-}1_A$) and ventricular MLC-1 ($MLC\text{-}1_V$) is positively regulated by GATA-4 (*29*), the expression of α-MHC was not induced in $Id1_{A5}$ and $Id3_{A3}$ cells without GATA-4 expression (Figure 4). It must be further noted that the *GATA-4* and *α-MHC* genes were also repressed in $Id1_{B7}$ cells, similar to in Figure 4 (middle) under differentiation condition (not shown), which may suggest that ectopic Id1 reproducibly inhibits *GATA-4* gene transcription under our experimental condition.

The Ids were transcribed even in an undifferentiated state, as shown at Day 0 in Figure 4, as the Ids were usually detected in the control samples without DMSO (*17,28,30*). Regarding the behavior of the expression pattern in our study, the mRNA level of Id2 was clearly increased in a later stage of culture in the presence of DMSO independently of the forced expression of Id1 and Id3 (Days 8 and 12 in Figure 4). The mRNA levels of Id1 and Id3 seemed to increase or to be maintained during culture, although those of the transcripts for Ids in $Id1_{A5}$ cells decreased immediately after differentiation.

4. Discussion

Transcription of the *GATA-4* gene in heart could be activated by ubiquitous E-box binding proteins (*9*) and heart-specific upstream enhancer (G2), which is a direct target of Forkhead box (Fox) and GATA transcription factors (*31*). Ids are known to directly inhibit ubiquitous E-box binding bHLH transcription factors such as Transcription factor 3 (Tcf3 known as E2A) (*16*) and UCF2 (*32*), and indirectly Foxa2 (*16*). Furthermore, Id proteins bind to GATA-4 and inhibit its DNA binding to the GATA motif (*17*). These observations suggest that

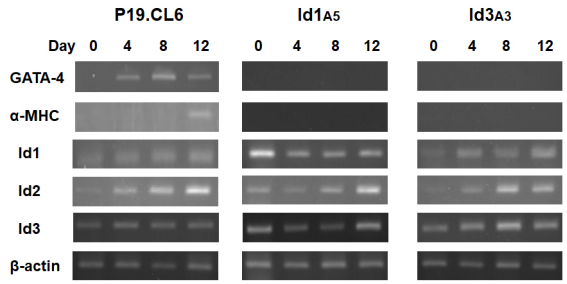

Figure 4. Inhibition of *GATA-4* gene transcription under differentiation condition in the P19CL6 cells with overexpressed Id1 and Id3 tagged with a HA/FLAG peptide. P19CL6 cells and clones $Id1_{A5}$ and $Id3_{A3}$ were cultured in the presence of 1% DMSO. Total RNA was prepared on the indicated days after the addition of DMSO. The mRNA levels (GATA-4, α-MHC, Id1, Id2, Id3 and β-actin) were determined by means of RT-PCR under semi-quantitative conditions using the primer pairs shown in Table 1A. The products (537, 302, 244, 351, 329, and 278 bp, respectively) were analyzed by 2% (w/v) agarose gel electrophoresis (see Materials and Methods). The primer pairs for GATA-4, α-MHC, and β-actin were designed from the registered cDNA sequences; NM_008092 (GATA-4), M76601 (α-MHC), and NM_007393 (β-actin), respectively.

the increased expression of Id1 and Id3 likely inhibits GATA-4 transcription and the GATA-4 function, which results in inhibition of expression of cardiac muscle genes and differentiation of P19CL6 cells.

A negative feedback regulatory loop between Ids and cardiac transcription factors such as GATA-4 and Nkx2.5 is proposed since transiently expressed these transcription factors induce Id2 expression in rat and mouse cardiomyocyte precursor cell lines (*28*). Such induction of Id2 was detected in our experiment (Figure 4, left), although increases of Id2 transcripts were detected in the presence of DMSO without GATA-4 expression (Figure 4, middle and right), possibly due to participation of DMSO-inducible factor(s) hitherto unidentified (*26*).

P19-derived cardiomyocytes resemble embryonic cardiomyocytes (*6*). The E-box binding Hey1 and Hey2 bHLH transcription factors (different nomenclature summarized in ref. *33*), which are expressed developmentally in atrial and ventricular compartments (*33*), are repressors of GATA-4 (*34*). Although Id1 could interact with Hey1 (*35*), it is unlikely that Ids cancel repression of the *GATA-4* gene through binding to Hey1 and Hey2 upon DMSO addition since P19CL6 cells do not express Hey1 and Hey2 in the absence of DMSO (Figure S1, *http://www.ddtjournal.com/action/getSupplementalData.php?ID=78*). Actually, the transcript of Hey1 increased starting from 4 days of differentiation (*27*).

Although transcription factors GATA-4, myocyte-specific enhancer factor 2C (Mef2c), Nkx2.5 and Tbx5, which mutually interact (*6*), could stimulate cardiomyocyte differentiation of P19 and P19CL6 cells (*7,36,37*), signaling pathways further govern the expression and function of these transcription factors. Bone morphogenetic protein (BMP) stimulates differentiation of P19CL6 cells through the Smad and TAK1 (a member of the mitogen-activated protein kinase kinase kinase) pathways together with DMSO-inducible factors independent of BMP signaling (*26*). Furthermore, the hedgehog, Wnt and Notch signals may participate in cardiac development (*33,38,39*). BMP-mediated inhibition of Wnt signal stimulated the commitment of cardiac precursor cells to become cardiomyocytes (*39*). Although the BMP signal also induces Ids (*35*), Ids can stimulate cardiomyocyte proliferation (*30,40,41*). The relative contents of Ids and relevant transcription factors would govern the growth and differentiation of cardiac cells since single cell analysis of fate conversion of fibroblasts into cardiomyocytes suggested a strong anti-correlation of *Id* genes with those of *GATA-4*, *Mef2c* and *Tbx5* (*42*).

Ectopic p204 could partially substitute for DMSO in inducing the differentiation of P19 cells and concomitantly stimulate nuclear export of Ids resulting in their degradation by proteasomes (*17,43*). Thus, not only transcription but also cellular localization of Id proteins should be carefully examined. Several modes of regulation by bHLH proteins and Ids have been also postulated (*44*), and their context-dependent regulatory circuits including miRNAs were proposed (*35,45*). Culture conditions might also influence the regulatory circuits since Id expression and cardiac differentiation could be affected by serum (*46*) and the insulin dose (*47*), respectively. Since cardiomyocyte regeneration is clinically important for the repair of a damaged heart (*48*), further study of the molecular mechanisms underlying fine-tuning of such regulatory circuits in which Ids and transcription factors including GATA-4 participate may be helpful for improvement of cardiac cell therapy.

Acknowledgements

This research was supported in part by the JSPS (Grant-in-Aid for Scientific Research (B), 14370744) to M. M.

Funding: None.

Conflict of Interest: The authors have no conflicts of interest to disclose.

References

1. Takaoka K, Hamada H. Cell fate decisions and axis determination in the early mouse embryo. Development. 2012; 139:3-14.
2. Kelly RG, Buckingham ME, Moorman AF. Heart fields and cardiac morphogenesis. Cold Spring Harb Perspect Med. 2014; 4:a015750.
3. Aronson BE, Stapleton KA, Krasinski SD. Role of GATA factors in development, differentiation, and homeostasis of the small intestinal epithelium. Am J Physiol Gastrointest

Liver Physiol. 2014; 306:G474-G490.
4. Heikinheimo M, Scandrett JM, Wilson DB. Localization of transcription factor GATA-4 to regions of the mouse embryo involved in cardiac development. Dev Biol. 1994; 164:361-373.
5. Kodo K, Yamagishi H. Current insight into genetics of congenital heart diseases: GATA and T-box cardiac transcription factors as the hotspot pathogenesis. J Pediatr Cardiol Card Surg. 2017; 1:18-27.
6. van der Heyden MAG, Defize LHK. Twenty-one years of P19 cells: what an embryonal carcinoma cell line taught us about cardiomyocyte differentiation. Cardiovasc Res. 2003; 58:292-302.
7. Grépin C, Robitaille L, Antakly T, Nemer M. Inhibition of transcription factor GATA-4 expression blocks in vitro cardiac muscle differentiation. Mol Cell Biol. 1995; 15:4095-4102.
8. Guittot SM, Bouchard MF, Robert-Grenon J-P, Robert C, Goodyer CG, Silversides DW, Viger RS. Conserved usage of alternative 5' untranslated exons of the *GATA4* gene. PLoS ONE. 2009; 4:e8454.
9. Guittot SM, Prud'homme B, Bouchard MF, Bergeron F, Daems C, Tevosian SG, Viger RS. GATA4 autoregulates its own expression in mouse gonadal cells *via* its distal 1b promoter. Biol Reprod. 2014; 90:1-15.
10. Ishibashi T, Yokura Y, Ohashi K, Yamamoto H, Maeda M. Conserved GC-boxes, E-box and GATA motif are essential for *GATA4* gene expression in P19CL6 cells. Biochem Biophys Res Commun. 2011; 413:171-175.
11. Sab AB, Bouchard M-F, Béland M, Prud'homme B, Souchkova O, Viger RS, Pilon N. An Ebox element in the proximal Gata4 promoter is required for Gata4 expression *in vivo*. PLoS One. 2011; 6:e29038.
12. Srivastava D, Cserjesi P, Olson EN. A subclass of bHLH proteins required for cardiac morphogenesis. Science. 1995; 270:1995-1999.
13. Xu H, Yang C, Wang Y, Tian J, Zhu J. Histone modifications interact with DNA methylation at the GATA4 promoter during differentiation of mesenchymal stem cells into cardiomyocyte-like cells. Cell Prolif. 2016; 49:315-329.
14. Hu W, Xin Y, Hu J, Sun Y, Zhao Y. Inhibitor of DNA binding in heart development and cardiovascular diseases. Cell Commun Signal. 2019; 17:51.
15. Yokota Y, Mori S. Role of Id family proteins in growth control. J Cell Physiol. 2002; 190:21-28.
16. Cunningham TJ, Yu MS, McKeithan WL, *et al.* Id genes are essential for early heart formation. Genes Dev. 2017; 31:1325-1338.
17. Ding B, Liu C-J, Yu J, Kong W, Lengyel P. p204 protein overcomes the inhibition of the differentiation of P19 murine embryonal carcinoma cells to beating cardiac myocytes by Id proteins. J Biol Chem. 2006; 281:14893-14906.
18. Saiki RK, Gelfand DH, Stoffel S, Scharf SJ, Higuchi R, Horn GT, Mullis KB, Erlich HA. Primer-directed enzymatic amplification of DNA with a thermostable DNA polymerase. Science. 1988; 239:487-491.
19. Sanger F, Coulson AR, Barrell BG, Smith AJH, Roe BA. Cloning in single-stranded bacteriophage as an aid to rapid DNA sequencing. J Mol Biol. 1980; 143:161-178.
20. Chiang C-M, Ge H, Wang Z, Hoffman A, Roeder RG. Unique TATA-binding protein-containing complexes and cofactors involved in transcription by RNA polymerases II and III. EMBO J. 1993; 12:2749-2762.
21. Sambrook J, Fritsch EF, Maniatis T. Molecular Cloning: A Laboratory Manual, 2nd ed., Cold Spring Harbor Laboratory, Cold Spring Harbor. 1989.
22. Takeda M, Obayashi K, Kobayashi A, Maeda M. A unique role of an amino terminal 16-residue region of long-type GATA-6. J Biochem. 2004; 135:639-650.
23. Bradford MM. A rapid and sensitive method for the quantitation of microgram quantities of protein utilizing the principle of protein-dye binding. Anal Biochem. 1976; 72:248-254.
24. Laemmli UK. Cleavage of structural proteins during the assembly of the bacteriophage T4. Nature. 1970; 227:680-685.
25. Towbin H, Staehelin T, Gordon J. Electrophoretic transfer of proteins from polyacrylamide gels to nitrocellulose sheets: procedure and some applications. Proc Natl Acad Sci USA. 1979; 76:4350-4354.
26. Monzen K, Hiroi Y, Kudoh S, Akazawa H, Oka T, Takimoto E, Hayashi D, Hosoda T, Kawabata M, Miyazono K, Ishii S, Yazaki Y, Nagai R, Komuro I. Smads, TAK1, and their common target ATF-2 play a critical role in cardiomyocyte differentiation. J Cell Biol. 2001; 153:687-698.
27. Peng C-F, Wei Y, Levsky JM, McDonald TV, Childs G, Kitsis RN. Microarray analysis of global changes in gene expression during cardiac myocyte differentiation. Physiol Genomics. 2002; 9:145-155.
28. Lim JY, Kim WH, Kim J, Park SI. Induction of Id2 expression by cardiac transcription factors GATA4 and Nkx2.5. J Cell Biochem. 2008; 103:182-194.
29. Molkentin JD, Kalvakolanu DV, Markham BE. Transcription factor GATA-4 regulates cardiac muscle-specific expression of the α-myosin heavy-chain gene. Mol Cell Biol. 1994; 14:4947-4957.
30. Meng Q, Jia Z, Wang W, Li B, Ma K, Zhou C. Inhibitor of DNA binding 1 (Id1) induces differentiation and proliferation of mouse embryonic carcinoma P19CL6 cells. Biochem Biophys Res Commun. 2011; 412:253-259.
31. Rojas A, De Val S, Heidt AB, Xu S-M, Bristow J, Black BL. Gata4 expression in lateral mesoderm is downstream of BMP4 and is activated directly by Forkhead and GATA transcription factors through a distal enhancer element. Development. 2005; 132:3405-3417.
32. Simões-Sato AY, Antonioli E, Tambellini R, Campos H. ID1 inhibits USF2 and blocks TGF-β-induced apoptosis in mesangial cells. Am J Physiol Renal Physiol. 2011; 301:F1260-F1269.
33. Fischer A, Leimeister C, Winkler C, Schumacher N, Klamt B, Elmasri H, Steidl C, Maier M, Knobeloch K-P, Amann K, Helosch A, Sendtner M, Gessler M. *Hey* bHLH factors in cardiovascular development. Cold Spring Harb Symp Quant Biol. 2002; 67:63-70.
34. Fischer A, Klattig J, Kneitz B, Diez H, Maier M, Holtmann B, Englert C, Gessler M. Hey basic helix-loop-helix transcription factors are repressors of GATA4 and GATA6 and restrict expression of the GATA target gene ANF in fetal hearts. Mol Cell Biol. 2005; 25:8906-8970.
35. Itoh F, Itoh S, Goumans M-J, Valdimarsdottir G, Iso T, Dotto GP, Hamamori Y, Kedes L, Kato M, ten Dijke P. Synergy and antagonism between Notch and BMP receptor signaling pathways in endothelial cells. EMBO J. 2004; 23:541-551.
36. Skerjanc IS, Petropoulos H, Ridgeway AG, Wilton S. Myocyte enhancer factor 2C and Nkx2-5 up-regulate each

other's expression and initiate cardiomyogenesis in P19 cells. J Biol Chem. 1998; 273:34904-34910.
37. Hiroi Y, Kudoh S, Monzen K, Ikeda Y, Yazaki Y, Nagai R, Komuro I. Tbx5 associates with Nkx2-5 and synergistically promotes cardiomyocyte differentiation. Nat Genet. 2001; 28:276-280.
38. Gianakopoulos PJ, Skerjanc IS. Hedgehog signaling induces cardiomyogenesis in P19 cells. J Biol Chem. 2005; 280:21022-21028.
39. Jain R, Li D, Gupta M, *et al.* Integration of Bmp and Wnt signaling by Hopx specifies commitment of cardiomyoblasts. Science. 2015; 348:aaa6071.
40. Ball AJ, Levine F. Telomere-independent cellular senescence in human fetal cardiomyocytes. Aging Cell. 2005; 4:21-30.
41. Cheng YY, Yan YT, Lundy DJ, Lo AA, Wang YP, Ruan S-C, Lin PJ, Hsieh PC. Reprogramming-derived gene cocktail increases cardiomyocyte proliferation for heart regeneration. EMBO Mol Med. 2017; 9:251-264.
42. Liu Z, Wang L, Welch JD, Ma H, Zhou Y, Vaseghi HR, Yu S, Wall JB, Alimohamadi S, Zheng M, Yin C, Shen W, Prins JF, Liu J, Qian L. Single-cell transcriptomics reconstructs fate conversion from fibroblast to cardiomyocyte. Nature. 2017; 551:100-104.
43. Ding B, Liu C-J, Huang Y, Hickey RP, Yu J, Kong W, Lengyel P. p204 is required for the differentiation of P19 murine embryonal carcinoma cells to beating cardiac myocytes: its expression is activated by the cardiac GATA4, NKX2.5, and TBX5 proteins. J Biol Chem. 2006; 281:14882-14892.
44. Yokota Y. Id and development. Oncogene. 2001; 20:8290-8298.
45. Meier-Stiegen F, Schwanbeck R, Bernoth K, Martini S, Hieronymus T, Ruau D, Zenke M, Just U. Activated Notch1 target genes during embryonic cell differentiation depend on the cellular context and include lineage determinants and inhibitors. PLoS One. 2010; 5:e11481.
46. Springhorn JP, Ellingsen O, Berger H-J, Kelly RA, Smith TW. Transcriptional regulation in cardiac muscle: coordinate expression of Id with a neonatal phenotype during development and following a hypertrophic stimulus in adult rat ventricular myocyte *in vitro*. J Biol Chem. 1992; 267:14360-14365.
47. Li WY, Song YL, Xiong CJ, Lu PQ, Xue LX, Yao CX, Wang WP, Zhang SF, Zhang SF, Wei QX, Zhang YY, Zhao JM, Zang MX. Insulin induces proliferation and cardiac differentiation of P19CL6 cells in a dose-dependent manner. Develop Growth Differ. 2013; 55:676-686.
48. Zhang Y, Mignone J, MacLellan WR. Cardiac regeneration and stem cells. Physiol Rev. 2015; 95:1189-1204.
49. Springhorn JP, Singh K, Kelly RA, Smith TW. Posttranscriptional regulation of Id1 activity in cardiac muscle: alternative splicing of novel Id1 transcript permits homodimerization. J Biol Chem. 1994; 269:5132-5136.

Received July 24, 2021; Revised August 4, 2021; Accepted August 9, 2021.

**Address correspondence to:*
Masatomo Maeda, Graduate School of Pharmaceutical Sciences, Osaka University, Yamada-oka 1-6, Suita, Osaka 565-0871, Japan.
E-mail: qqpe4zr9k@clock.ocn.ne.jp

Released online in J-STAGE as advance publication August 20, 2021.

Brief Report

DOI: 10.5582/ddt.2021.01071

Clarifying the pharmacological mechanisms of action of Shenfu Decoction on cardiovascular diseases using a network pharmacology approach

Qingfeng Zhao[1], Michihisa Tohda[1, 2,*]

[1] Field of Consilienceology for Wakan-yaku, Major of Biological Information System Course, Graduate School of Innovative Life Science, University of Toyama, Toyama, Japan;
[2] Laboratory of Consilienceology for Wakan-yaku, Section of Neuromedical Science, Institute of Natural Medicine, University of Toyama, Toyama, Japan.

SUMMARY Since the molecular mechanisms underlying in the pathogenesis of cardiovascular diseases (CVD) are extremely complex and have not yet been elucidated in detail, CVD remain the leading cause of death worldwide. Traditional Chinese medicine involves the treatment of disease from an overall perspective, and its therapeutic effects on CVD have been demonstrated. However, the mechanisms contributing to the multiscale treatment of cardiovascular diseases at the systematic level remain unclear. Network pharmacology methods and a gene chip data analysis were integrated and applied in the present study, which was conducted to investigate the potential target genes and related pathways of Shenfu Decoction (SFD) for the treatment of myocardial injury. The gene chip analysis was initially performed, followed by network pharmacology to identify differentially expressed genes (DEG) and a functional enrichment analysis. Protein-protein networks were constructed and a module analysis was conducted. A network analysis was used to identify the target genes of SFD. Regarding the results obtained, 1134 DEG were identified using the STRING website. The module analysis revealed that nine hub genes exhibited ubiquitin-protein ligase activity. Therefore, SFD significantly alters the expression of ubiquitination-related genes and, thus, plays an important therapeutic role in the treatment of heart failure. In conclusion, hub genes may provide a more detailed understanding of the molecular mechanisms of action of as well as candidate targets for SFD therapy.

Keywords Cardiovascular diseases, traditional Chinese medicine, Shenfu Decoction, network pharmacology

1. Introduction

Cardiovascular diseases (CVD) are the leading cause of death worldwide (*1*). The application of traditional Chinese medicine (TCM) to the treatment of COVID-19 has been examined and it is now used in clinical settings in China; however, there is currently insufficient evidence for its global expansion (*2*). The use Chinese herbs to prevent various diseases, including CVD, has been investigated (*3*). Bioinformatics has become an important tool in the medical field because it effectively reveals relevant knowledge hidden in big data, thereby promoting the discovery of integrated information (*4*). The core concepts of TCM and network pharmacology are similar (*5*), with multicomponent therapy and network targets as the basis for TCM (*6*) and a molecular network for network pharmacology (*7*). Although many methods may be applied in investigations of the mechanisms of action of TCM in the treatment of CVD, network pharmacology is widely accepted and used because it provides a broad perspective (*8*).

The cardioprotective effects of Shenfu Decoction (SFD) have been demonstrated. It has been shown to inhibit myocardial cell apoptosis in rats with heart failure (*9*) and protect against myocardial ischemia-reperfusion injury (*10*). Metabonomics (*11*) and proteomics also revealed its protective effects against heart failure. Moreover, the chemome (*12*) and serum pharmacochemistry (*13*) of SFD have been characterized.

The rapid development of network pharmacology has contributed to a more detailed understanding of and insights into the mechanisms by which TCM

exerts its effects on complex diseases (*14*). Therefore, in the present study, network pharmacology was used to elucidate the complex molecular mechanisms of action of SFD in the treatment of CVD. We initially treated cells with the corresponding drugs and then subjected samples to a gene chip analysis. Potential targets were mapped to the corresponding database for a bioinformatic analysis, which provides a bridge for clarifying the mechanisms by which SFD exerts its cardiovascular protective effects.

2. Materials and Methods

2.1. Preparation of the SFD extract

Two Chinese herbal medicines, ginseng and aconite, were selected at a ratio of 2:1 to prepare SFD. Forty-five grams of Chinese herbal medicine was added to 900 mL of water to prepare SFD. The hot water extract obtained was then freeze-dried. Tochimoto Tenkai-do (Osaka, Japan) provided Panax ginseng CA Meyer (Lot No. 008607037) and Aconitum carmichaeli Debeaux (Lot No. 032017001) for the present study.

2.2. Cell culture and treatment

The rat cardiac myoblast cell line H9C2 was purchased from the European Collection of Authenticated Cell Cultures (ECACC: Salisbury, England). According to the information provided in the instructions, the medium selected was complete DMEM containing 10% fetal bovine serum and culture conditions were 37°C in a 10% CO_2 humidification box. Three groups were included in the present study: 1) Control group; 2) Model group; 3) SFD treatment group. Doxorubicin (DXR: Sandoz, Yamagata, Japan: Lot No. HY8542)-mediated H9C2 cytotoxicity was induced as previously described (*15*). Following a treatment with SFD or vehicle for 24 hours, cells were incubated with or without DXR (2 μM) for another 24 h to induce cardiotoxicity.

2.3. RNA extraction

Total RNA was extracted from H9C2 cells using TRIsure (Bioline, Luckenwale, Germany), and genomic DNA was removed by DNase I (TaKaRa, Ohtsu, Japan), according to the manufacturers' instructions. The quantity and quality of RNA were assessed using a 2100 biological analyzer (Agilent, CA, USA). High-quality RNA samples ($OD_{260/280}$ = 1.8-2.0 RIN ≥ 7) were used to construct sequencing libraries.

2.4. Microarray data

Three samples each from the Control, Model, and SFD treatment groups were hybridized with an SurePrint G3 Mouse Gene Expression v2 8 × 60K Microarray at 65°C for 14 h to analyze expression levels using microarray methods.

2.5. Identification of differentially expressed genes (DEG)

DEG among Control, Model, and SFD treatment group samples were screened using Venn diagrams. $|\log2FC| \geq 1$ was considered to be significant.

2.6. Protein-protein interaction (PPI) network construction and a module analysis

As a classic PPI network construction tool, the STRING database (*16*) was employed in the present study, and the standard for significance was a combined score > 0.4. In the module analysis after network construction, Cytoscape's plug-in Molecular Complex Detection (MCODE) was selected (*17*). The selection of key hub genes relied on the following three characteristics: "degree", "intermediateness", and "intimacy". The criterion selected in the present study was that these three characteristics were higher than the corresponding median values.

2.7. Enrichment analyses of candidate genes

WebGestalt is a functional enrichment analysis web tool (*18*). The WebGestalt online database, as a popular biological analysis database, facilitates analyses of the functions of DEG. The standard for statistical selection is $p < 0.05$. WebGestalt's over-representation enrichment analysis method is used to identify and analyze potential targets. As a gene annotation tool, a gene ontology analysis involves a functional analysis that includes molecular function, biological pathway, and cell component analyses (*19*). The Kyoto Encyclopedia of Genes and Genomes (KEGG) is a well-known path analysis tool (*20*).

2.8. Co-expression analysis

GeneMANIA is a user friendly and flexible web server that is used to generate hypotheses about gene functions, analyze gene lists, and assess gene priority for a functional analysis (*21*). The database comprises many functions, such as a physical interaction analysis, co-expression predictions, co-localization, and a genetic interaction analysis. These functions were used in the present study to construct the SFD gene network.

3. Results and Discussion

3.1. Identification of DEG

Gene expression datasets were obtained [SET01:

Control group *vs*. Model group, SET02: Model group *vs* SFD treatment group]. After standardizing microarray results, DEG were identified. The overlap between the two data sets contained 1,134 genes, as shown in the Venn diagram (Figure 1).

3.2. Prediction analysis of pharmacological mechanisms based on network pharmacology and module identification

Based on the STRING database, a PPI network was constructed with a combined score > 0.4 (Figure 2A), with 908 nodes and 1822 edges together forming a large biological network (Table S1, *http://www.ddtjournal.com/action/getSupplementalData.php?ID=79*). The network module (cluster or community) is the sub-network that is generally defined. The characteristic of the sub-network is that connections between its nodes are more reliable and firmer than the loose connections in the remainder of the network. In other words, a module is a collection of many nodes with a high degree of correlation. Module identification is important because the amount of crucial information extracted from the network is limited, and it facilitates the discovery of vital information by researchers that may be hidden in the network. Network modules have been utilized in network pharmacology-based TCM studies to reveal the combination rule of TCM herbal formulae (*22*), chemical modules with similar structures (*23*), and proteins with equivalent functions (*24*). Multi-component and multi-objective analyses have always been a difficult and hot issue in TCM research. Network modularity is based on the "Law of Similarity Attraction" analysis method, which is a precise and powerful method to describe the complexity of TCM. Figure 2B shows the PPI network of the 293 nodes and 1083 edges obtained with a degree of between 5 and 42 inclusive. Although the scope of Figure 2B is smaller than that of Figure 2A, it is also difficult to identify target molecules. Therefore, as shown in Figure 2C, we established a novel network to identify target molecules

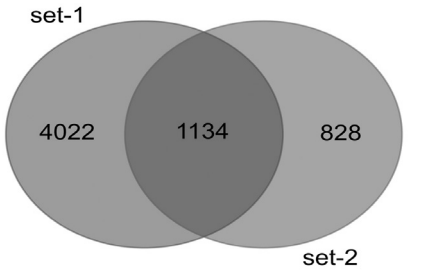

Figure 1. Venn diagram of the number of genes showing treatment-induced changes in expression. Differentially expressed genes with a fold change ≥ 2 in microarray data were selected among mRNA expression profiling set-1 (control vs. DXR) and set-2 (DXR vs. SFD + DXR). The two data sets show the overlap of 1,134 genes.

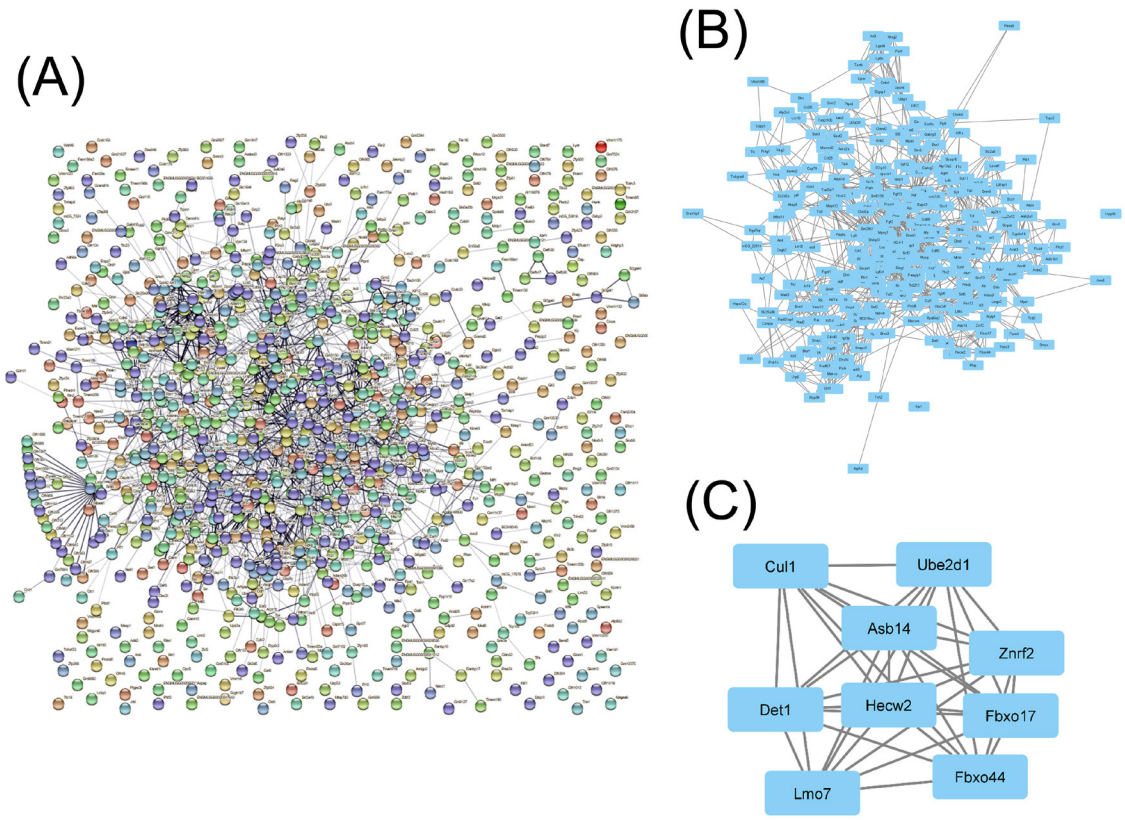

Figure 2. PPI network structure and module identification. (A) PPI network of differentially expressed genes (DEG). **(B)** The PPI network of DEG was constructed using Cytoscape. **(C)** The most significant module with 9 nodes and 36 edges was obtained from the PPI network.

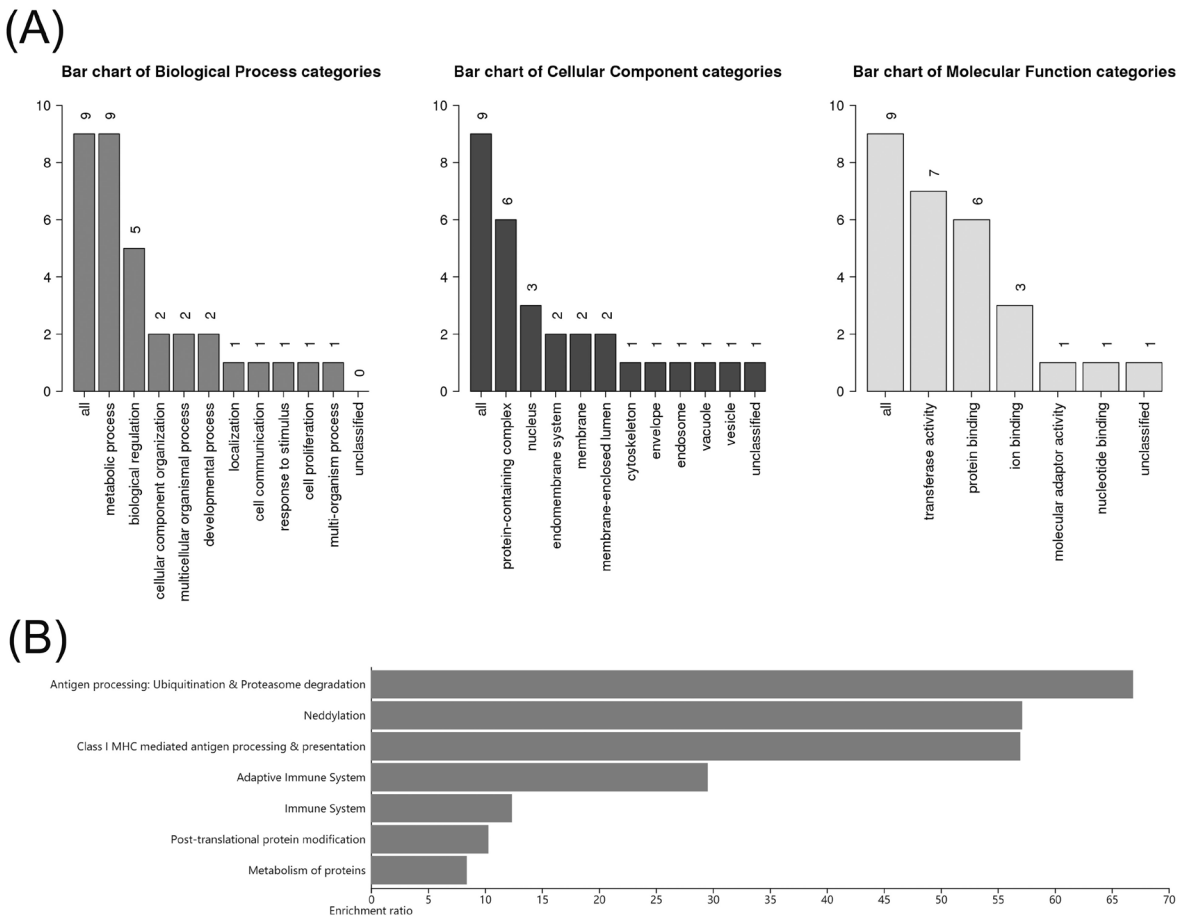

Figure 3. Enrichment analyses of nine hub genes. (A) An enrichment analysis through the WebGestalt database. **(B)** A KEGG pathway analysis of nine hub genes.

more accurately.

Through the plug-in MCODE, the most significant module was obtained from the PPI network with 9 nodes -36 edges. The names, abbreviations, and functions of these hub genes are shown in Table S2 (*http://www.ddtjournal.com/action/getSupplementalData.php?ID=80*). We then calculated three topological features ("degree", "intermediateness", and "compactness") of the candidate molecules. According to the screening criteria described above, three candidate molecules were identified ("degree" > 9, "betweenness" > 0.000111031, and "closeness" > 0.27027027), as shown in Table S3 (*http://www.ddtjournal.com/action/getSupplementalData.php?ID=80*). All 9 genes were associated with the functions of the ubiquitin-proteasome system (UPS), which is important in the etiology of CVD.

UPS plays an essential role in the many mechanisms involved in mediating the degradation of intracellular proteins (*25*). Ubiquitination and proteasome-mediated degradation are the two main steps of UPS-mediated proteolysis. In other words, ubiquitination is a series of enzymatic reactions in cells (*26*). Dysfunctional UPS has been implicated in the development of many CVD (such as atherosclerosis, myocardial ischemia, hypertrophy, and heart failure) (*27*).

One of the main factors restricting the use of anthracycline antibiotics (such as DXR) in clinical settings is cardiotoxicity (*28*). DXR-induced cardiotoxicity may increase the activity of UPS (*29*). Sishi *et al*. also demonstrated that chymotrypsin-like activity in the heart was inhibited by DXR, while the ubiquitination of proteins was simultaneously increased (*30*). Dysfunctions in the ubiquitin-proteasome pathway (UPP) have also been shown to play an important role in CVD (*31*). The overactivation of UPP has been identified as a contributing factor to the development of acute cardiotoxicity as an adverse event of the administration of anthracyclines.

3.3. Enrichment analyses of hub genes

The biological process, cellular composition, molecular function, and pathway of the target protein were analyzed by the WebGestalt database. The results obtained (Figure 3A) indicated that hub genes were significantly involved in a number of biological processes, including metabolic processes,

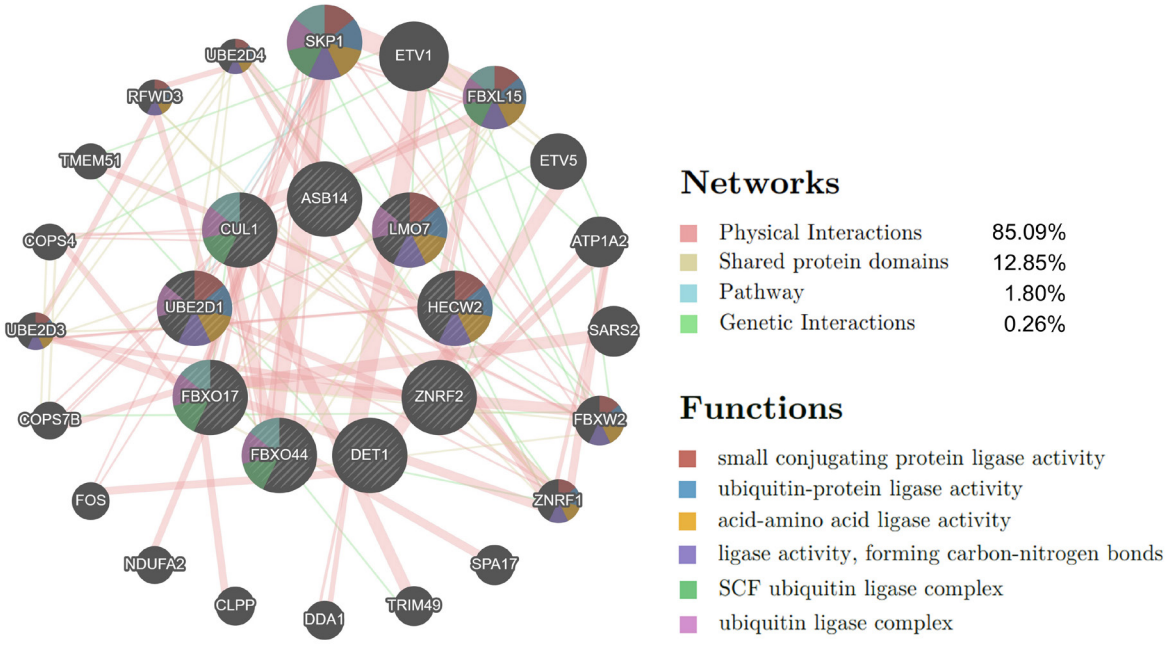

Figure 4. Gene-gene interaction network among hub genes. A gene is represented by a node. The strength of the interaction is expressed by the size of the node. Inter-node connection lines represent the types of gene-gene interactions, while the line color shows the types of interactions. The possible function of each gene is represented by the color of the node.

biological regulation, cellular component organization, multicellular organismal processes, developmental processes, localization, cell communication, responses to stimuli, cell proliferation, and multi-organism processes. According to the classification of cellular components, the protein was located in a protein-containing complex, the nucleus, and endomembrane system. The molecular function of the target protein involved transferase activity and protein binding. To further confirm that the biological processes involved in the treatment of myocardial injury by SFD play a role in the corresponding pathological events in the course of disease progression, we used the KEGG database for a pathway enrichment analysis. Seven important signal pathways were obtained ($p < 0.05$). These results (Figure 3B) indicated that the protective effects of SFD against myocardial injury involve seven signaling pathways. Previous studies demonstrated that SFD exerted cardiotonic effects by regulating the TNF signaling pathway (*32*), apoptosis (*33*), the PI3K-Akt signaling pathway (*34*), TGF-β/Smads signaling pathway (*35*), and Akt/eNOS signaling pathway (*36*). Ubiquitination (*37*) and neddylation (*38*) were also shown to play a role in myocardial injury; however, the relationships between SFD and these pathways need to be confirmed in further studies. Therefore, SFD appears to exert protective effects against myocardial injury by regulating 7 pathways and 10 biological processes. In addition, previous studies demonstrated that SFD may cure heart failure by regulating the TGF-β/Smads signaling pathway, apoptosis, and the PI3K-Akt, Akt/eNOS, and TNF signaling pathways. In summary, regarding myocardial injury, a number of proteins and pathways in the biological network may be regulated by SFD, which ultimately controls the occurrence and development of CVD.

3.4. GeneMANIA analysis

The GeneMANIA database was selected to further analyze the interaction network among hub genes (Figure 4). The 9 central nodes representing hub genes were surrounded by 20 nodes representing genes that strongly correlated with the hub genes in terms of physical interactions (85.09%), shared protein domains (12.85%), pathways (1.8%), and genetic interactions (0.26%). The top five genes displaying the strongest correlations with hub genes included S-phase kinase-associated protein 1 (*SKP1*), ETS variant 1 (*ETV1*), F-box and leucine rich repeat protein 15 (*FBXL15*), *ETV5*, and ATPase Na^+/K^+ transporting subunit alpha 2 (*ATP1A2*), among which SKP1 correlated with cullin 1 (CUL1), ubiquitin-conjugating enzyme E2D 1 (UBE2D1), F-box protein 17 (FBXO17), and FBXO44 in terms of physical interactions. ETV1 correlated with de-etiolated homolog 1 (DET1) in terms of physical interactions and with LIM domain only protein 7 (LMO7) and HECT with C2 and WW domain containing E3 ubiquitin protein ligase 2 (HECW2) in terms of genetic interactions. FBXL15 correlated with CUL1 and HECW2 in terms of physical interactions and with FBXO44 and FBXO17 in terms

of shared protein domains. ETV5 correlated with DET1 in terms of physical interactions and with zinc and ring finger 2 (ZNRF2) and UBE2D1 in terms of genetic interactions. In addition, ATP1A2 correlated with ZNRF2 in terms of physical interactions. Further functional analyses revealed that these proteins showed the strongest correlation with ubiquitin-protein ligase activity (FDR=4.45E–09). Additionally, these proteins correlated with small conjugating protein ligase activity, acid-amino acid ligase activity, ligase activity, the formation of carbon-nitrogen bonds, the Skp, Cullin, F-box containing complex (SCF) ubiquitin ligase complex, ubiquitin ligase complex, and cullin-RING ubiquitin ligase complex.

To simultaneously identify the target genes of SFD for protection against heart failure in the present study, the bioinformatic analysis method, including the identification of DEG, and a functional enrichment analysis were extensively used. A total of 1,134 DEG were identified using the STRING website. A module analysis showed that nine hub genes exhibited ubiquitin-protein ligase activity. In summary, the hub genes and related pathways discovered in the present study will provide a more detailed understanding of the mechanisms by which SFD protects the myocardium, which will lead to novel research concepts for SFD. Since the safety of drug treatments and the importance of communication with patients are increasing (*39*), the preventative and therapeutic effects of SFD on heart failure increase the safety of anticancer drug treatments and will also lead to peace of mind for patients.

Funding: None.

Conflict of Interest: The authors have no conflicts of interest to disclose.

References

1. Lloyd-Jones DM, Leip EP, Larson MG, d'Agostino RB, Beiser A, Wilson PW, Wolf PA, Levy D. Prediction of lifetime risk for cardiovascular disease by risk factor burden at 50 years of age. Circulation. 2006; 113:791-798.
2. Wang J, Qi F. Traditional Chinese medicine to treat COVID-19: the importance of evidence-based research. Drug Discov Ther. 2020; 14:149-150.
3. Kitazawa T, Park CH, Hiratani K, Choi JS, Yokozawa T. Efficacy of Chinese prescription Kangen-karyu for patient with metabolic syndrome. Drug Discov Ther. 2020; 14:54-57.
4. Gu P, Chen H. Modern bioinformatics meets traditional Chinese medicine. Brief Bioinform. 2014; 15:984-1003.
5. Zhao J, Yang J, Tian S, Zhang W. A survey of web resources and tools for the study of TCM network pharmacology. Quant Biol. 2019; 7:17-29.
6. Fang J, Wang L, Wu T, Yang C, Gao L, Cai H, Liu J, Fang S, Chen Y, Tan W, Wang Q. Network pharmacology-based study on the mechanism of action for herbal medicines in Alzheimer treatment. J Ethnopharmacol. 2017; 196:281-292.
7. Zhao J, Jiang P, Zhang W. Molecular networks for the study of TCM pharmacology. Brief Bioinform. 2010; 11:417-430.
8. Li B, Xu X, Wang X, Yu H, Li X, Tao W, Wang Y, Yang L. A systems biology approach to understanding the mechanisms of action of Chinese herbs for treatment of cardiovascular disease. Int J Mol Sci. 2012; 13:13501-13520.
9. Yan X, Wu H, Ren J, Liu Y, Wang S, Yang J, Qin S, Wu D. Shenfu Formula reduces cardiomyocyte apoptosis in heart failure rats by regulating microRNAs. J Ethnopharmacol. 2018; 227:105-112.
10. Zheng SY, Sun J, Zhao X, Xu JG. Protective effect of shen-fu on myocardial ischemia-reperfusion injury in rats. Am J Chin Med. 2004; 32:209-220.
11. Yang D, Wang X, Wu Y, Lu B, Yuan A, Leon C, Guo N. Urinary metabolomic profiling reveals the effect of Shenfu Decoction on chronic heart failure in rats. Molecules. 2015; 20:11915-11929.
12. Chen Y, Yu R, Jiang L, Zhang Q, Li B, Liu H, Xu G. A comprehensive and rapid quality evaluation method of traditional Chinese medicine decoction by integrating UPLC-QTOF-MS and UFLC-QQQ-MS and its application. Molecules. 2019; 24:374.
13. He JL, Zhao JW, Ma ZC, Wang YG, Liang QD, Tan HL, Xiao CR, Tang XL, Gao Y. Serum pharmacochemistry analysis using UPLC-Q-TOF/MS after oral administration to rats of Shenfu Decoction. Evid Based Complement Alternat Med. 2015; 2015:973930.
14. Berger SI, Iyengar R. Network analyses in systems pharmacology. Bioinformatics. 2009; 25:2466-2472.
15. Zhou F, Hao G, Zhang J, Zheng Y, Wu X, Hao K, Niu F, Luo D, Sun Y, Wu L, Ye W, Wang G. Protective effect of 23-hydroxybetulinic acid on doxorubicin-induced cardiotoxicity: a correlation with the inhibition of carbonyl reductase-mediated metabolism. Br J Pharmacol. 2015; 172:5690-5703.
16. Szklarczyk D, Morris JH, Cook H, Kuhn M, Wyder S, Simonovic M, Santos A, Doncheva NT, Roth A, Bork P, Jensen LJ, von Mering C. The STRING database in 2017: quality-controlled protein-protein association networks, made broadly accessible. Nucleic Acids Res. 2017; 45:D362-D368.
17. Bader GD, Hogue CW. An automated method for finding molecular complexes in large protein interaction networks. BMC Bioinformatics. 2003; 4:2.
18. Liao Y, Wang J, Jaehnig EJ, Shi Z, Zhang B. WebGestalt 2019: gene set analysis toolkit with revamped UIs and APIs. Nucleic Acids Res. 2019; 47:W199-W205.
19. The Gene Ontology C. Expansion of the Gene Ontology knowledgebase and resources. Nucleic Acids Res. 2017; 45:D331-D338.
20. Kanehisa M, Furumichi M, Tanabe M, Sato Y, Morishima K. KEGG: new perspectives on genomes, pathways, diseases and drugs. Nucleic Acids Res. 2017; 45:D353-D361.
21. Warde-Farley D, Donaldson SL, Comes O, *et al*. The GeneMANIA prediction server: biological network integration for gene prioritization and predicting gene function. Nucleic Acids Res. 2010; 38:W214-220.
22. Li S, Zhang B, Jiang D, Wei Y, Zhang N. Herb network construction and co-module analysis for uncovering the combination rule of traditional Chinese herbal formulae. BMC Bioinformatics. 2010; 11 (Suppl 11):S6.

23. Ding F, Zhang Q, Ung CO, Wang Y, Han Y, Hu Y, Qi J. An analysis of chemical ingredients network of Chinese herbal formulae for the treatment of coronary heart disease. PLoS One. 2015; 10:e0116441.
24. Guimera R, Nunes Amaral LA. Functional cartography of complex metabolic networks. Nature. 2005; 433:895-900.
25. Wang X, Robbins J. Proteasomal and lysosomal protein degradation and heart disease. J Mol Cell Cardiol. 2014; 71:16-24.
26. Powell SR, Herrmann J, Lerman A, Patterson C, Wang X. The ubiquitin-proteasome system and cardiovascular disease. Prog Mol Biol Transl Sci. 2012; 109:295-346.
27. Li YF, Wang X. The role of the proteasome in heart disease. Biochim Biophys Acta. 2011; 1809:141-149.
28. Minotti G, Menna P, Salvatorelli E, Cairo G, Gianni L. Anthracyclines: molecular advances and pharmacologic developments in antitumor activity and cardiotoxicity. Pharmacol Rev. 2004; 56:185-229.
29. Ranek MJ, Wang X. Activation of the ubiquitin-proteasome system in doxorubicin cardiomyopathy. Curr Hypertens Rep. 2009; 11:389-395.
30. Sishi BJ, Loos B, van Rooyen J, Engelbrecht AM. Doxorubicin induces protein ubiquitination and inhibits proteasome activity during cardiotoxicity. Toxicology. 2013; 309:23-29.
31. Bulteau AL, Lundberg KC, Humphries KM, Sadek HA, Szweda PA, Friguet B, Szweda LI. Oxidative modification and inactivation of the proteasome during coronary occlusion/reperfusion. J Biol Chem. 2001; 276:30057-30063.
32. Yu M, Ye L, Bian J, Ma L, Zheng C, Guo H. Effect of Jiawei Shenfu decoction on tumor necrosis factor-alpha and nuclear factor-kappa B in patients who have chronic heart failure with syndromes of deficiency of heart Yang. J Tradit Chin Med. 2019; 39:418-424.
33. Chen RJ, Rui QL, Wang Q, Tian F, Wu J, Kong XQ. Shenfu injection attenuates lipopolysaccharide-induced myocardial inflammation and apoptosis in rats. Chin J Nat Med. 2020; 18:226-233.
34. Zhu J, Song W, Xu S, Ma Y, Wei B, Wang H, Hua S. Shenfu injection promotes vasodilation by enhancing eNOS activity through the PI3K/Akt signaling pathway *in vitro*. Front Pharmacol. 2020; 11:121.
35. Ni J, Shi Y, Li L, Chen J, Li L, Li M, Zhu J, Zhu Y, Fan G. Cardioprotection against heart failure by Shenfu injection *via* TGF-beta/Smads signaling pathway. Evid Based Complement Alternat Med. 2017; 2017:7083016.
36. Wang YY, Li YY, Li L, Yang DL, Zhou K, Li YH. Protective effects of Shenfu injection against myocardial ischemia-reperfusion injury *via* activation of eNOS in rats. Biol Pharm Bull. 2018; 41:1406-1413.
37. Willis MS, Townley-Tilson WH, Kang EY, Homeister JW, Patterson C. Sent to destroy: the ubiquitin proteasome system regulates cell signaling and protein quality control in cardiovascular development and disease. Circ Res. 2010; 106:463-478.
38. Zou J, Ma W, Li J, Littlejohn R, Zhou H, Kim IM, Fulton DJR, Chen W, Weintraub NL, Zhou J, Su H. Neddylation mediates ventricular chamber maturation through repression of Hippo signaling. Proc Natl Acad Sci U S A. 2018; 115:E4101-E4110.
39. Yaguchi-Saito A, Yamamoto K, Sengoku T, Suka M, Sato T, Hinata M, Nakamura T, Nakayama T, Yamamoto M. Evaluation of rapid drug safety communication materials for patients in Japan. Drug Discov Ther. 2021; 15:101-107.

Received August 3, 2021; Revised August 26, 2021; Accepted August 27, 2021.

**Address correspondence to:*
Michihisa Tohda, Laboratory of Consilienceology for Wakan-yaku, Section of Neuromedical Science, Institute of Natural Medicine, University of Toyama, Sugitani 2630, Toyama 930-0194, Japan.
E-mail: tohdam@inm.u-toyama.ac.jp

Released online in J-STAGE as advance publication August 31, 2021.

Brief Report

DOI: 10.5582/ddt.2021.01010

Frequent expression of a novel cancer testis antigen, protein kinase human monopolar spindle 1 (hMps1/TTK) in human urinary bladder transitional cell carcinoma

Pankaj Kumar Singh[1,2], Madan Lal Brahma Bhatt[2,*], Prabhat Singh[3], Srikanta Kumar Rath[4], Diwakar Dalela[5], Madhu Mati Goel[6]

[1] Department of Biochemistry, All India Institute of Medical Sciences Bibinagar, Telangana, India;
[2] Department of Radiotherapy, King George's Medical University, Lucknow, Uttar Pradesh, India;
[3] Department of Biological Sciences, Indian Institute of Science Education and Research Berhampur, Odisha, India;
[4] Genotoxicity Laboratory, Division of Toxicology, CSIR-Central Drug Research Institute, Lucknow, Uttar Pradesh, India;
[5] Department of Urology, King George's Medical University, Lucknow, Uttar Pradesh, India;
[6] Department of Pathology, King George's Medical University, Lucknow, Uttar Pradesh, India.

SUMMARY Urothelial bladder cancer (UBC) is a frequently occurring malignancy of the urinary tract. The present study was undertaken to evaluate the mRNA and immunohistochemical (IHC) expression of protein kinase human monopolar spindle 1 (hMps1/TTK) gene in transitional cell carcinoma (TCC) of the bladder and correlate its expression with the clinicopathological characteristics of patients. In the present study, quantitative real-time reverse-transcriptase polymerase chain reaction (qRT-PCR) was used to evaluate TTK mRNA expression in TCC. IHC analysis of TTK was also evaluated. Independent Student's *t*, ANOVA and chi-square (χ^2) tests were used to analyze the data statistically. The frequency of TTK mRNA over expression was detected in 50% of UBC (38/76) by qRT-PCR. Relative mean fold expression of TTK mRNA was found significantly ($p < 0.05$) higher in muscle-invasive bladder cancer (MIBC) as compared to non-muscle-invasive bladder cancer (NMIBC) patients (8.96 ± 4.51 vs. 5.64 ± 3.53, $p = 0.03$). Moreover, IHC reveals heterogenous immunostaining pattern of TTK in TCC tissues. The frequency of TTK protein over expression was detected in 56.9% (37 of 65) UBC patients. No significant IHC expression of TTK was detected among adjacent noncancerous tissues (ANCTs) and benign prostatic hyperplasia (BPH) used as control. Collectively our study observations conclude that TTK is a novel cancer/testis antigen (CTA) as a diagnostic marker for early diagnosis of UBC.

Keywords TTK protein kinase, cancer/testis antigen, transitional cell carcinoma, urinary bladder cancer, immunotherapy

1. Introduction

Human urinary bladder cancer (UBC) is the one of the most common malignancies worldwide and occurs at a higher frequency in male individuals (*1*). It is a heterogeneous disease encompassing distinct biologic features that lead to extremely different clinical behaviors (*2*). Approximately 75% of patients with transitional cell carcinoma (TCC) present a disease at a non-invasive stage that involves only the inner lining of the bladder (*3*). Patients with non-muscle-invasive bladder cancer (NMIBC) are usually treated with transurethral resection with or without intravesical chemotherapy and have a favourable prognosis; however, some of these patients suffer from recurrence with grade progression (*4*).The remaining 25% of newly diagnosed UBCs present with muscle invasion and have a higher risk of cancer-specific mortality (*5*) with the need of aggressive radical surgery or radiotherapy, with or without chemotherapy.

The field of cancer vaccine therapy is currently expected to become the fourth option in the treatment of UBC after surgery, chemotherapy and radiation therapy and a large number of clinical and translational investigations are underway at present in this direction (*6*). To date, only few pilot clinical trials have been conducted to evaluate vaccine candidates for UBC (*7*). These trials were conducted on a limited number of study patients and only in the context advanced invasive UBC (*6,8-10*), and metastatic UBC after failure of platinum-based regimens (*7*). Thus, identification of additional

cancer/testis antigen (CTA) in TCC of urinary bladder with increased potential is need of hour. In this quest, we evaluated one of the protein kinase human monopolar spindle 1 (hMps1/TTK) gene (NM_003318) which encodes a dual serine/threonine and tyrosine protein kinase and locates on chromosome 6q13-q21. *TTK* gene also belongs to cancer-testis (CT) gene family that is hardly detected in normal tissue except the testis. TTK is expressed at relatively high levels in testis, thymus tissues and various malignant tumor tissues (*11-22*), but not detected in most other benign tissues. Moreover, TTK has been also identified as novel targets in human UBC using microarray (*6,21*). TTK is over expressed in various malignancies; however, detailed expression pattern of TTK in association with clinicopathological characteristics of TCC remain unclear. Therefore, the objective of the present study was to evaluate mRNA and protein expression in tissue specimens of TCC patients by using quantitative real-time polymerase chain reaction (qRT-PCR) and immunohistochemistry (IHC), and correlate its expression with clinicopathological parameters of patients.

Table 1. Patient clinciopathological parameters

Clinicopathological characteristics	Real-time-PCR Assay (76), *n* (%)	Immunohistochemistry Assay (65), *n* (%)
Age (years, %)		
≤ 45	24 (31.6%)	17 (26.2%)
> 45	52 (68.4%)	48 (73.8%)
Sex		
Male	67 (88.2%)	63 (96.9%)
Female	9 (11.8%)	2 (3.1%)
Grade		
Low	33 (43.4%)	23 (35.4%)
High	43 (56.6%)	42 (64.6%)
Stage		
Ta	3 (3.9%)	6 (9.2%)
T1	33 (43.4%)	23 (35.4%)
T2-T4	40 (52.6%)	36 (55.4%)
Smoking		
No	34 (44.7%)	29 (44.6%)
Yes	42 (55.3%)	36 (55.4%)
Tobacco chewers		
No	36 (47.4%)	33 (50.8%)
Yes	40 (52.6%)	32 (49.2%)

2. Materials and Methods

2.1. Clinical specimens

A total of 76 freshly frozen UBC tissues (male: 67; female: 9) were collected from the TCC of urinary bladder patients for the evaluation of TTK mRNA expression using qRT-PCR. All patients underwent transurethral resection of bladder tumour (TURBT) or radical cystectomy (RC) between March 2006 and April 2012 at Department of Urology, KGMU, Lucknow, India. The mean age of the UBC patients included in qRT-PCR assay was 54.75 ± 11.51 years. In addition to analyse IHC expression of TTK, 65 formalin-fixed, paraffin-embedded (FFPE) bladder tissues, 12 adjacent noncancerous tissue (ANCT) specimens and 10 benign prostatic hyperplasia (BPH) tissues were obtained from the archives of the Pathology Department, KGMU, Lucknow, India. The mean age of the UBC patients included in IHC assay was 53.83 ± 11.47 years whereas mean age of BPH patients was 64.14 ± 11.46 years. The participants gave informed consent before taking part and given consent to use their tissues in the experiments. None of the TCC of urinary bladder patients has received any therapy, including chemotherapy, radiotherapy or other treatment, prior to surgery. Bladder tumours were staged according to the 2002 tumour-lymph node-metastasis (TNM) classification system (*23*). Tumours were graded according to the 2004 World Health Organization (WHO) bladder tumour classification criteria (*24*). Detailed clinicopathological parameters of the UBC patients are given in Table 1. All UBC patients provided signed informed consent and the study design was approved by the research ethics committee of our institution.

All tumours were histologically proven as TCCs and UBC was confirmed via examination of cystoscopic biopsy. All tissue specimens were coded with unique code and the results of qRT-PCR and IHC assays were interpreted blind of the histopathological characteristics of the bladder tumours. Upon surgical resection, all tissue specimens were initially stored in RNAlater® (Ambion Inc., Austin, TX) and immediately frozen at -80°C in liquid nitrogen until further analysis.

2.2. RNA extraction and quantitative reverse transcription-PCR

Total RNA was extracted from tissue specimens using Trizol reagent (Invitrogen, Carlsbad, CA, USA). RNA from different normal tissues was purchased (Clonetech, Palo Alto, CA, USA). First-strand cDNA was synthesized from total RNA using Quantitect® Reverse Transcription Reagent (Qiagen GmbH, Hilden, Germany) as per manufacturer's instructions. In brief, the expression of the housekeeping gene β-actin, as an internal standard, and the gene of interest was evaluated using SYBR® GreenER™ qPCR SuperMix Universal (Invitrogen). Human Bladder Total RNA (Clontech, Palo Alto, CA, USA) was used as a reference for evaluation of TTK mRNA levels in bladder cancerous tissues. Among normal tissues, TTK mRNA levels were expressed as n-fold differences relative to β-actin (internal control) and the levels in the normal testis (calibrator). The primer sequences and PCR conditions were the same as described previously (*25*).

2.3. Immunohistochemistry

IHC assay was performed on FFPE tissue sections

Table 2. Correlation between relative mean fold TTK mRNA expression and clinicopathological parameters of UBC patients

Characteristics Age (years):	Non-muscle-invasive Mean ± SD	*p* value	Muscle-invasive Mean ± SD	*p* value	Total	*p* value
≤ 45	8.00 ± 2.83 (2)	0.320	7.78 ± 3.07 (9)	0.344	7.82 ± 2.89 (11)	0.875
> 45	5.11 ± 3.59 (9)		9.56 ± 5.06 (18)		8.07 ± 5.02 (27)	
Sex:						
Female	6.00 ± 0.00 (1)	0.921	8.00 ± 0.00 (1)	0.833	7.00 ± 1.41 (2)	0.750
Male	5.60 ± 3.72 (10)		9.00 ± 4.60 (26)		8.06 ± 4.59 (36)	
Grade:						
Low	4.29 ± 3.15 (7)	0.093	6.83 ± 5.23 (6)	0.195	5.46 ± 4.26 (13)	0.010
High	8.00 ± 3.16 (4)		9.57 ± 4.23 (21)		9.32 ± 4.06 (25)	
Smoking:						
No	5.60 ± 4.10 (5)	0.977	8.08 ± 4.70 (12)	0.375	7.35 ± 4.55 (17)	0.430
Yes	5.67 ± 3.39 (6)		9.67 ± 4.39 (15)		8.52 ± 4.45 (21)	
Tobacco:						
No	5.50 ± 2.89 (4)	0.929	8.27 ± 5.20 (15)	0.380	7.68 ± 4.88 (19)	0.669
Yes	5.71 ± 4.07 (7)		9.83 ± 3.49 (12)		8.32 ± 4.14 (19)	

Numbers in parenthesis indicate the number of UBC patients.

according to our previously published protocol (*26*). The TTK protein in UBC tissues was detected using a rabbit polyclonal antibody against TTK (C-19; sc-540; 1:100 dilution, Santa Cruz Biotechnology, Santa Cruz, CA) overnight at 4°C. The IHC expression of TTK was evaluated according to the following criteria. The immunostaining patterns were applied into scales on the percentage of cells with positive immunostaining: 0, complete absence or negative stained cells; 1, < 10% positive cells; 2, > 10% positive cells but ≤ 50% and 3, > 50% positive cells. The IHC expression of TTK was scored as being present or not. Heterogenous staining of urothelial and cancer cells were scored negative when tumour biopsies stained less than 10%, while those stained more than 10% was considered as positive on IHC.

2.4. Statistical analysis

Continuous data were defined as Mean ± SD, while categorical in %. Qualitative variables were illustrated as percentages and numbers. Independent Student's *t* test and ANOVA was used to analyse comparison between groups and significance of mean difference was analyzed by Tukey's post hoc test after adjusting the multiple contrasts for significance. Associations between categorical groups (*i.e.*, TTK expression and clinicopathological parameters) were analyzed using the chi-square (χ^2) test and $p < 0.05$ was considered to be statistically significant. All statistical analysis was implemented with the SPSS software (Windows version 18.0).

3. Results and Discussion

3.1. Quantitative expression of TTK mRNA

Quantitative analysis of TTK mRNA expression was analyzed using qRT-PCR in 16 normal tissues and 76 bladder tumour tissues. The frequency of TTK mRNA expression was observed in 30.6% (11 of 36) of NMIBC and 67.5% (27 of 40) MIBC patients. Thus, overall 50.0% (38 of 76) TCC of urinary bladder patients were found to be positive for TTK mRNA expression. TTK mRNA expression was observed in higher number of MIBC patients than NMIBC patients (67.5% *vs*. 30.6%, $p < 0.001$). In the MIBC patients, relative mean fold expression of TTK was significantly higher as compared to NMIBC (8.96 ± 4.51 *vs*. 5.64 ± 3.53, $p = 0.03$). We detected TTK mRNA expression in 39.3% patients with low-grade and 58.1% with high-grade bladder tumours respectively.

TTK mRNA expression was detected only in testis, and thymus using qRT-PCR. However, over expression was detected only in testis and relative mean fold expression level of TTK mRNA in thymus was 112-fold lower than that in the testis.

The relationship between TTK mRNA expression and clinicopathological parameters of the TCC patients is summarized in Table 2. No significant correlation was found between TTK mRNA expression and clinicopathological parameters such as patient's age, gender, grade, disease stage, cigarette smoking and tobacco chewing *etc*. in both NMIBC and MIBC patients. However, high relative mean fold expression of TTK mRNA was detected in older age patients *vs*. younger patients, males *vs*. females, advanced stage *vs*. early stage, high-grade *vs*. low-grade and with cigarette smoking and chewing tobacco habit.

3.2. Expression of TTK protein

IHC revealed heterogenous (TTK protein to be expressed and located to both nuclei and cytoplasm) positive immunostaining in bladder tumour tissues and were interpreted as IHC-positive. Heterogenous

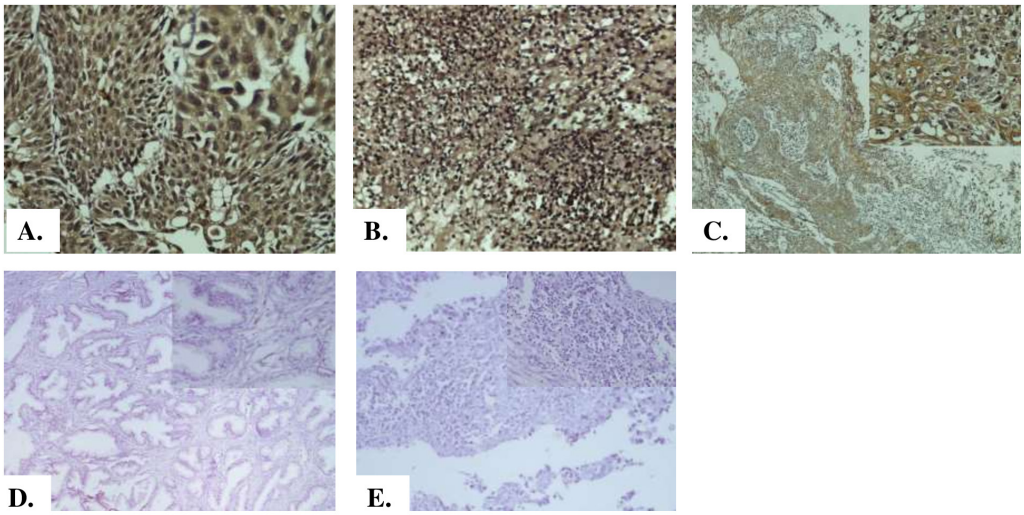

Figure 1. Immunohistochemical analysis of TTK in UBC. UBC tissues were stained with TTK specific rabbit polyclonal antibody. (A) NMIBC tissue showing strong positive expression; **(B)** MIBC showing strong positive expression; **(C)** MIBC showing positive expression; **(D)** BPH tissue showing negative expression; **(E)** NMIBC showing positive expression.

Table 3. Correlation between TTK protein expression and clinicopathological parameters of UBC patients

Characteristics	Non-muscle-invasive (n = 29)			Muscle-invasive (n = 36)			Total (n = 65)		
	Negative n (%)	Positive n (%)	p value	Negative n (%)	Positive n (%)	p value	Negative n (%)	Positive n (%)	p value
Age (years):									
≤ 45	4 (23.5%)	2 (16.7%)	0.653	4 (36.4%)	7 (28.0%)	0.616	8 (28.6%)	9 (24.3%)	0.700
> 45	13 (76.5%)	10 (83.3%)		7 (63.6%)	18 (72.0%)		20 (71.4%)	28 (75.7%)	
Sex:									
Female	0 (0.0%)	0 (0.0%)	NA	1 (9.1%)	1 (4.0%)	0.539	1 (3.6%)	1 (2.7%)	0.841
Male	17 (100%)	12 (100%)		10 (90.9%)	24 (96.0%)		27 (96.4%)	36 (97.3%)	
Grade:									
Low (G1)	12 (70.6%)	5 (41.7%)	0.119	1 (9.1%)	5 (20.0%)	0.418	13 (46.4%)	10 (27.0%)	0.105
High (G2-G3)	5 (29.4%)	7 (58.3%)		10 (90.9%)	20 (80.0%)		15 (53.6%)	27 (73.0%)	
Stage									
Ta	2 (11.8%)	4 (33.3%)	0.158	0 (0.0%)	0 (0.0%)	NA	2 (7.1%)	4 (10.8%)	0.28
T1	15 (88.2%)	8 (66.7%)		0 (0.0%)	0 (0.0%)		15 (53.6%)	8 (21.6%)	
T2 - T4	0 (0.0%)	0 (0.0%)		11 (100%)	25 (100%)	0	11 (39.3%)	25 (67.6%)	
Smoking:									
No	12 (70.6%)	7 (58.3%)	0.494	5 (45.5%)	5 (20.0%)	.116	17 (60.7%)	12 (32.4%)	0.023
Yes	5 (29.4%)	5 (41.7%)		6 (54.5%)	20 (80.0%)		11 (39.3%)	25 (67.6%)	
Tobacco chewing:									
No	8 (47.1%)	8 (66.7%)	0.296	8 (72.7%)	9 (36.0%)	0.042	16 (57.1%)	17 (45.9%)	0.371
Yes	9 (52.9%)	4 (33.3%)		3 (27.3%)	16 (64.0%)		12 (42.9%)	20 (54.1%)	

Numbers in parenthesis indicate the number of UBC patients.

expression of TTK was detected in 41.4% (12 of 29) of NMIBC and 69.4% (25 of 36) MIBC patients (Figure 1). Thus an overall frequency of TTK IHC expression was found to be positive in 56.9% (37 of 65) TCC patients. TTK protein expression was observed in significantly higher number of MIBC patients than NMIBC patients (69.4% *vs*. 41.4%, $p = 0.02$). Furthermore, heterogenous expression of TTK was detected in 43.4% patients with low-grade and 64.2% with high-grade urothelial tumours respectively. No significant expression of TTK protein was observed among ANCTs and BPH tissues. The relationship between TTK protein expression and clinicopathological parameters of the TCC patients is summarized in Table 3. The protein expression of TTK was not found to be significantly associated with the clinicopathological parameters as well as habits of NMIBC and MIBC patients. However, the protein expression of TTK was found to be significantly ($p = 0.042$) associated with the tobacco chewing habit in MIBC patients.

UBC is a heterogeneous disease which is specified by a high recurrence rate that necessitates continuous cystoscopic surveillance. Despite a better understanding of UBC biology and the use of adjuvant therapies, UBC remains one of the most expensive carcinoma to

treat due to its high recurrence rate, risk of progression, chemotherapeutic resistance and requirement of long-term follow-up strategies.

TTK over expression has been reported in many different types of cancers, and significantly correlated with specific clinicopathological tumour features. However, little is known about the expression status and clinical significance in TCC. Thus in the present study, we analyzed the detailed mRNA and protein expression pattern of TTK to evaluate its clinical significance in human TCC. In the present study, we have detected TTK mRNA expression in 50.0% UBC patients using qRT-PCR. Our study findings derived by qRT-PCR are in agreement with previous observations reporting TTK upregulation in a variety of tumours, such as breast, esophageous, lung, prostate, lung, anaplastic thyroid and bladder (*13-21*). Our study findings are also consistent with the previous studies of CTA expression in UBC that MAGE-A8 and MAGE-A9 expression was detected in 56% and 54% of bladder tumours (*27*), whereas NY-ESO-1 expression were observed in 35% and 45.1% tumours (*28,29*).

TTK mRNA expression characteristics were investigated in different tissues to determine whether TTK possess CTA expression characteristics. In present study TTK mRNA expression was detected in testis and thymus normal tissues using qRT-PCR. These findings were consistent with the previous report (*22*). Thus our study results imply that TTK mRNA expression plays an important role in bladder tumorigenesis. Our study further evaluated IHC expression of TTK in FFPE sections of bladder tissues, which affirm heterogenous expression pattern in TCC but no significant expression was observed among ANCTs. These results are consistent with the previous published reports in which high protein expression of TTK was observed in tumour specimens but not in ANCTs (*13*). In the present study, heterogenous immunostaining pattern of TTK was observed in FFPE sections of bladder tissues. These results are consistent with previous report that detected heterogenous expression pattern of various other CTAs in urothelial carcinoma (*30*). In our study no significant association was observed between TTK expression and clinicopathological parameters such as sex, age, stage, and grade of the UBC patients. These results are in accordance with findings from earlier published observations in TCC of bladder (*29*).

The present study had few limitations. The bladder tumor tissues used to evaluate mRNA and protein expression of TTK was obtained from different patient's cohort. In this quest, no association was observed between TTK mRNA expression and protein expression. Moreover, the relatively smaller sample size of TCC of urinary bladder patients did not granted to perform sub analysis.

In conclusion, the present study indicated upregulation of TTK mRNA expression and over expression of IHC staining in most of TCC patients irrespective of stage, grade and other clinicopathological parameters of TCC patients, indicative of its diagnostic potential as a molecular marker. However, it is further warranted to be compared with available gold standard diagnostic methods like biopsy and urine cytology to find out diagnostic efficacy of TTK over expression as a molecular marker in diagnosis of TCC. Our study findings also conclude that TTK might be a potential vaccine candidate for immunotherapy in TCC due to its expression among bladder tumours and restricted expression in normal tissues. However, findings remain to be verified in larger prospective clinical studies to evaluate its potential as a molecular biomarker and immunotherapeutic target for the TCC of urinary bladder.

Acknowledgements

First author (Pankaj Kumar Singh) would like thank to Indian Council of Medial Research (ICMR), New Delhi, India for awarding Senior Research Fellowship (ICMR-SRF) (IRIS ID-2007-04520) under the guidance of corresponding author.

Funding: None.

Conflict of Interest: The authors have no conflicts of interest to disclose.

References

1. Liu X, Yao D, Liu C, Cao Y, Yang Q, Sun Z, Liu D. Overexpression of ABCC3 promotes cell proliferation, drug resistance, and aerobic glycolysis and is associated with poor prognosis in urinary bladder cancer patients. Tumour Biol. 2016; 37:8367-8374.
2. Zhang XY, Yan QX, Guo XY, Chen CR, Chen RQ, Cai ZM, Tang AF. Expression profile of SPACA5/Spaca5 in spermatogenesis and transitional cell carcinoma of the bladder. Oncol Lett. 2016; 12:3731-3738.
3. Brausi M, Witjes JA, Lamm D, Persad R, Palou J, Colombel M, Buckley R, Soloway M, Akaza H, Bohle A. A review of current guidelines and best practice recommendations for the management of nonmuscle invasive bladder cancer by the International Bladder Cancer Group. J Urol. 2011; 186:2158-2167.
4. Okegawa T, Ushio K, Imai M, Morimoto M, Hara T. Orphan nuclear receptor HNF4G promotes bladder cancer growth and invasion through the regulation of the hyaluronan synthase 2 gene. Oncogenesis. 2013; 2:e58.
5. Burger M, Catto JW, Dalbagni G, Grossman HB, Herr H, Karakiewicz P, Kassouf W, Kiemeney LA, La Vecchia C, Shariat S, Lotan Y. Epidemiology and risk factors of urothelial bladder cancer. Eur Urol. 2013; 63:234-241.
6. Obara W, Ohsawa R, Kanehira M, Takata R, Tsunoda T, Yoshida K, Takeda K, Katagiri T, Nakamura Y, Fujioka T. Cancer peptide vaccine therapy developed from oncoantigens identified through genome-wide expression profile analysis for bladder cancer. Jpn J Clin Oncol. 2012;

42:591-600.
7. Noguchi M, Matsumoto K, Uemura H, *et al*. An open-label, randomized phase II trial of personalized peptide vaccination in patients with bladder cancer that progressed after platinum-based chemotherapy. Clin Cancer Res. 2016; 22:54-60.
8. Matsumoto K, Noguchi M, Satoh T, Tabata K, Fujita T, Iwamura M, Yamada A, Komatsu N, Baba S, Itoh K. A phase I study of personalized peptide vaccination for advanced urothelial carcinoma patients who failed treatment with methotrexate, vinblastine, adriamycin and cisplatin. BJU Int. 2011; 108:831-838.
9. Nishiyama T, Tachibana M, Horiguchi Y, Nakamura K, Ikeda Y, Takesako K, Murai M. Immunotherapy of bladder cancer using autologous dendritic cells pulsed with human lymphocyte antigen-A24-specific MAGE-3 peptide. Clin Cancer Res. 2001; 7:23-31.
10. Obara W, Eto M, Mimata H, *et al*. A phase I/II study of cancer peptide vaccine S-288310 in patients with advanced urothelial carcinoma of the bladder. Ann Oncol. 2017; 28:798-803.
11. King JL, Zhang B, Li Y, Li KP, Ni JJ, Saavedra HI, Dong JT. TTK promotes mesenchymal signaling via multiple mechanisms in triple negative breast cancer. Oncogenesis. 2018; 7:69.
12. Chen X, Yu C, Gao J, Zhu H, Cui B, Zhang T, Zhou Y, Liu Q, He H, Xiao R, Huang R, Xie H, Gao D, Zhou H. A novel USP9X substrate TTK contributes to tumorigenesis in non-small-cell lung cancer. Theranostics. 2018; 8:2348-2360.
13. Chen F, Wu P, Hu H, Tian D, Jiang N, Wu C. Protein kinase TTK promotes proliferation and migration and mediates epithelial-mesenchymal transition in human bladder cancer cells. Int J Clin Exp Pathol. 2018; 11:4854-4861.
14. Maire V, Baldeyron C, Richardson M, *et al*. TTK/hMPS1 is an attractive therapeutic target for triple-negative breast cancer. PloS One. 2013; 8:e63712.
15. Shiraishi T, Terada N, Zeng Y, Suyama T, Luo J, Trock B, Kulkarni P, Getzenberg RH. Cancer/Testis Antigens as potential predictors of biochemical recurrence of prostate cancer following radical prostatectomy. J Transl Med. 2011; 9:153.
16. Finetti P, Cervera N, Charafe-Jauffret E, Chabannon C, Charpin C, Chaffanet M, Jacquemier J, Viens P, Birnbaum D, Bertucci F. Sixteen-kinase gene expression identifies luminal breast cancers with poor prognosis. Cancer Res. 2008; 68:767-776.
17. Landi MT, Dracheva T, Rotunno M, *et al*. Gene expression signature of cigarette smoking and its role in lung adenocarcinoma development and survival. PloS One. 2008; 3:e1651.
18. Mizukami Y, Kono K, Daigo Y, Takano A, Tsunoda T, Kawaguchi Y, Nakamura Y, Fujii H. Detection of novel cancer-testis antigen-specific T-cell responses in TIL, regional lymph nodes, and PBL in patients with esophageal squamous cell carcinoma. Cancer Sci. 2008; 99:1448-1454.
19. Salvatore G, Nappi TC, Salerno P, Jiang Y, Garbi C, Ugolini C, Miccoli P, Basolo F, Castellone MD, Cirafici AM, Melillo RM, Fusco A, Bittner ML, Santoro M. A cell proliferation and chromosomal instability signature in anaplastic thyroid carcinoma. Cancer Res. 2007; 67:10148-10158.
20. Yuan B, Xu Y, Woo JH, Wang Y, Bae YK, Yoon DS, Wersto RP, Tully E, Wilsbach K, Gabrielson E. Increased expression of mitotic checkpoint genes in breast cancer cells with chromosomal instability. Clin Cancer Res. 2006; 12:405-410.
21. Thykjaer T, Workman C, Kruhoffer M, Demtroder K, Wolf H, Andersen LD, Frederiksen CM, Knudsen S, Orntoft TF. Identification of gene expression patterns in superficial and invasive human bladder cancer. Cancer Res. 2001; 61:2492-2499.
22. Mills GB, Schmandt R, McGill M, Amendola A, Hill M, Jacobs K, May C, Rodricks AM, Campbell S, Hogg D. Expression of TTK, a novel human protein kinase, is associated with cell proliferation. J Biol Chem. 1992; 267:16000-16006.
23. Greene FL, Page DL, FIeming ID, Fritz A, Balch CM, Haller DG, Morrow M. AJCC Cancer Staging Manual. Spriner-Verlag, New York, 2002.
24. Eble JN, Sauter G, Epstein JI, Sesterhenn IA (eds.). Pathology and Genetics of Tumours of the Urinary System and Male Genital Organs. IARC Press, Lyon, France, 2004.
25. Chiaretti S, Li X, Gentleman R, Vitale A, Vignetti M, Mandelli F, Ritz J, Foa R. Gene expression profile of adult T-cell acute lymphocytic leukemia identifies distinct subsets of patients with different response to therapy and survival. Blood. 2004; 103:2771-2778.
26. Singh PK, Srivastava AK, Dalela D, Rath SK, Goel MM, Bhatt ML. Frequent expression of zinc-finger protein ZNF165 in human urinary bladder transitional cell carcinoma. Immunobiology. 2015; 220:68-73.
27. Picard V, Bergeron A, Larue H, Fradet Y. MAGE-A9 mRNA and protein expression in bladder cancer. Int J Cancer. 2007; 120:2170-2177.
28. Dyrskjot L, Zieger K, Kissow Lildal T, Reinert T, Gruselle O, Coche T, Borre M, Orntoft TF. Expression of MAGE-A3, NY-ESO-1, LAGE-1 and PRAME in urothelial carcinoma. Br J Cancer. 2012; 107:116-122.
29. Yin B, Liu G, Wang XS, Zhang H, Song YS, Wu B. Expression profile of cancer-testis genes in transitional cell carcinoma of the bladder. Urol Oncol. 2012; 30:886-892.
30. Sharma P, Shen Y, Wen S, Bajorin DF, Reuter VE, Old LJ, Jungbluth AA. Cancer-testis antigens: expression and correlation with survival in human urothelial carcinoma. Clin Cancer Res. 2006; 12:5442-5447.

Received January 31, 2021; Revised August 25, 2021; Accepted August 26, 2021

**Address correspondence to:*
Madan Lal Brahma Bhatt, Department of Radiotherapy, King George's Medical University, Lucknow, Uttar Pradesh, India 226003.
E-mail: mlbbhatt@yahoo.in

Released online in J-STAGE as advance publication August 28, 2021.

Brief Report

DOI: 10.5582/ddt.2021.01066

Analysis of onset and clinical characteristics in Japanese patients with infantile hemangioma

Aya Hashimoto[1], Kayo Kunimoto[1,*], Ami Kawaguchi[1], Yutaka Inaba[1], Chikako Kaminaka[1], Yuki Yamamoto[1], Nobuyuki Kakimoto[2], Tomohiro Suenaga[2], Takashi Takeuchi[2], Hiroyuki Suzuki[2], Masatoshi Jinnin[1]

[1] Department of Dermatology, Wakayama Medical University, Wakayama, Japan;
[2] Department of Pediatrics, Wakayama Medical University, Wakayama, Japan.

SUMMARY Infantile hemangioma (IH) is a common benign tumor during infancy, although the detailed mechanism behind it has not been fully elucidated. Based on previous studies, we hypothesized that formation of hemangioma might be triggered by secondary physiological events (perinatal hypoxia or mechanical stress during delivery) in patients carrying germline risk mutations. We aimed to clarify the mechanism by evaluating whether head and neck lesions were more frequent in patients in who IH appeared after birth compared with those in who it was present at birth. Clinical data of 62 lesions in 51 patients with IH were collected. All patients were analyzed for correlation of onset with gender, localization, family histories, gestational age, birth weight, and clinical subtypes. Distribution of lesions on the head and neck was slightly more frequent in the after-birth IH group, compared with those with IH present at birth, but without significant difference (47.6% *vs.* 40.0%, $p = 0.32$). On the other hand, the ratio of superficial and deep type IH at birth was significantly altered compared with that in IH after birth (19:0 *vs.* 26:7, $p = 0.039$). In addition, IHs appearing after birth tended to more commonly have multiple lesions than those with IH present at birth, with statistically significant difference (25.8% *vs.* 0%, $p = 0.0164$). There may therefore be different triggers for IHs at birth and IH after birth. Further studies with greater number of patients are necessary to validate these findings.

Keywords Distribution, infantile hemangioma, onset

1. Introduction

Infantile hemangioma (IH) is one of the most common benign tumors during infancy. It occurs in an estimated 3-10% infants, with a recent increase in prevalence (*1*). IH typically appears at approximately 2 weeks of age and rapidly proliferates within 6-10 months followed by spontaneous involution over 7-10 years (*1*). Most IHs become apparent after birth, but a portion of the patients have precursor lesions at birth (*2*). Risk factors of IH include low birth weight, multiple gestation, preterm birth, progesterone therapy, and family history (*1*).

Detailed mechanisms have not been fully elucidated, but there are several hypotheses seeking to explain its specific clinical manifestation. One hypothesis is emboli of placental cells. Gene expression patterns of cellular markers differ from those of endothelial cells in the surrounding skin, but resemble those of endothelial cells lining fetal microvessels in the human placenta (*2*). A second hypothesis is related to hypoxia. The intrauterine hypoxia associated with glucose transporter (GLUT)-1 and indoleamine 2,3-dioxygenase may have a role in pathogenesis (*1*). A third hypothesis is related to endothelial progenitor cells or stem cells. Endothelial progenitor cell generated IH-like lesions in immunologically-deficient mice (*3*).

Meanwhile, we previously identified germline mutations in genes encoding tumor endothelial marker 8 (TEM8) and vascular endothelial growth factor receptor (VEGFR)-2, resulting in VEGFR-1 down-regulation and endothelial proliferation, survival, adhesion and migration by activating VEGF signaling through VEGFR2 (*4*). Considering the emergence after birth and age-dependent involution of IH, we hypothesize that formation of hemangioma is triggered in patients carrying the germline risk mutations by secondary physiological events, for example perinatal hypoxia or mechanical stress during delivery (*2*). Consistently, when the distribution of 104 lesions in 100 patients with IH was analyzed, lesions in the jaw or chin area were significantly less frequent than in other areas (*5*). Mechanical stress to the jaw or chin areas may be less

than in other areas in normal cephalic delivery.

If mechanical stress during delivery is really one of the causes of IH, in this retrospective study, we tried to prove the hypothesis that head and neck lesions would be more frequent in the IH group with patients in who IH appeared after birth compared with those with IH present at birth.

2. Materials and Method

2.1. Clinical assessment and patient material

We conducted a retrospective study of 51 Japanese patients with IH who visited Wakayama Medical University Hospital between August 2019 and March 2020. All patients were diagnosed based on clinical manifestation and/or image findings.

The following variables, obtained from medical records and clinical pictures, were collected for the analysis: date of onset, gender, number of lesions, localization (head and neck, limbs, or trunk), family histories, gestational age, birth weight, and clinical subtype.

Clinical subtypes were defined according to the depth of soft tissue involvement. Superficial-type IHs involve the superficial dermis and manifest with a raised, lobulated and bright red appearance (*2*). Deep-type IHs arise from the reticular dermis and/or the subcutis layer, and appear as a bluish-hued subcutaneous nodule or tumor. Mixed-type IHs have features of both subtypes.

2.2. Statistical analysis

Statistical analysis was carried out with the Fisher's exact test for comparison of frequency. $P < 0.05$ was considered statistically significant.

3. Result and Discussion

3.1. Clinical characteristics of patients with IH in our study

We collected the clinical data of 62 lesions in 51 patients with IH (32 girls, 19 boys). Distribution of the 62 lesions was 28 lesions on the head or neck (45%), 19 on limbs (31%), and 15 on trunk (24%). No patients had segmental IH. The clinical subtypes of the 62 lesions were 45 superficial (73%), 7 deep (11%), and 10 mixed (16%). Eight cases (13%) had multiple lesions. In 51 patients with IH, only one patient had notable family history. Information on gestational age was available for 26 cases, four of whom were born earlier than 37 weeks. Birth weight was available for 25 patients, four of whom were born at low birth weight (< 2,500 g).

Reportedly, girls are more likely than boys to have IH (*2*). For example, in the recent investigation by Anderson *et al.* there were 644 females and 355 males, and approximately 44% of lesions were located in the head and neck (*6*). The majority of IHs occur as solitary lesions, but approximately 20% of patients have multiple lesions (*7*). Superficial IH are thought to be the main clinical subtype (*8*). Furthermore, formation of hemangioma is believed to be primarily sporadic, whereas, although rare, there are some cases of familial IH (*2*). Accordingly, the characteristics of the 51 patients in our study, such as gender, localization, number of lesions, clinical subtype, and family histories, are consistent with previous reports.

On the other hand, Katelyn *et al.* reported average gestational age at birth (38.7 weeks) and birth weight (3.28 kg) of infants diagnosed with IH between 1976 and 2010 (*6*). In the present study, the mean birth weight of six infants with IH present at birth was 2.82 kg and that of the 19 infants with IH appearing after birth was 2.92 kg (Table 1). These birth weights were lower than the previous result, perhaps due to racial differences.

3.2. Correlation of onset with clinical characteristics in infants with IH

Next, we classified 51 patients with IH into two groups according to the timing of onset; those with IH present at birth (n = 20) and those whose IH appeared after birth (n = 31: average 18 days after birth). All patients were analyzed for correlation of onset with gender, localization, family history, gestational age, birth weight, and clinical subtypes (Table 1).

Table 1. Clinical characteristics in infants with infantile hemangioma

Items	Number of cases	
	At birth (n = 20)	After birth (n = 31)
Gender		
Female	14	18
Male	6	13
Localization		
Head and neck	8	20
Limbs	8	11
Trunk	4	11
(Multiple)	(0)	(8)
Clinical type		
Superficial	19	26
Deep	0	7
Mixed	1	9
Family histories		
+	1	0
–	19	30
Unknown	0	1
Gestational age		
1 < 37 week	1	3
≥ 37 week	6	16
Unknown	13	12
Birth weight		
Mean weight (kg)	2.82	2.92
Low birth weight	1	3

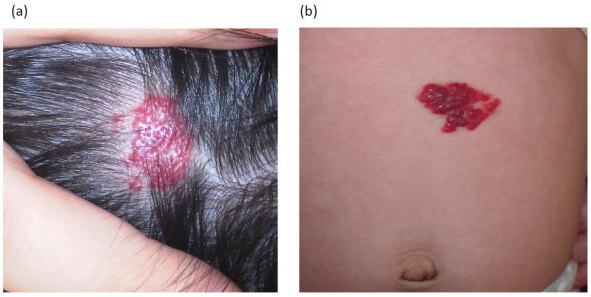

Figure 1. Representative clinical manifestation of multiple infantile hemangioma appeared 11 days after birth: head (a) and upper abdomen (b).

Table 2. Correlation of onset with number of lesions

Items	at birth	after birth	all
single	20	23	43
multiple	0	8	8
all	20	31	51

Table 3. Correlation of onset with clinical subtypes

Items	at birth	after birth	all
superficial	19	26	45
deep	0	7	7
all	19	33	52

There was no statistically significant correlation between timing of onset and the gender ratio (girl:boy = 14:6 *vs.* 18:13, $p = 0.55$). The most frequent location of the 20 cases of IH present at birth was the head and neck ($n = 8$), and limbs ($n = 8$) followed by the trunk ($n = 4$). In contrast, among infants with IH that appeared after birth, 8 cases had multiple lesions. Of the 23 cases of single IH, the most common site was the head and neck ($n = 13$), followed by the limbs ($n = 5$) and the trunk ($n = 5$). Of the 19 lesions on the 8 infants with multiple IH, 7 were on the head and neck, 6 were on the trunk, and 6 were on the limbs. Clinical images of representative patients with multiple lesions of IHs are shown in Figure 1. The distribution of lesions on the head and neck was slightly more common in the group with IH that appeared after birth, compared with those with IH present at birth, but without significant difference (47.6% *vs.* 40.0%, $p = 0.32$).

As described in the Introduction, we hypothesized that the expansion of endothelial cells within the lesion might be triggered by physiological factors, such as mechanical stress during delivery. As a limitation of this study, medical records on delivery (*e.g.*, vaginal delivery or cesarean section) were not available. Direct evidence could not therefore be shown, but we tried to clarify the mechanism by evaluating whether head and neck lesions were more frequent in the group in which IH appeared after birth compared with the patients in which it was present at birth. As a result, there was such a tendency, but the difference was not statistically significant.

On the other hand, we unexpectedly found IH that appeared after birth tended to have multiple lesions more commonly than those with IH present at birth, with statistically significant difference (25.8% *vs.* 0%, $p = 0.0164$) (Table 2). Given that recognition of multiple lesions will be easier and earlier than solitary lesions, our result may indicate that there may be different triggers between IHs present at birth and those appearing after birth. In other words, IH present at birth are likely caused by a local trigger, while IH appearing after birth may be induced by systemic factors in addition to local triggers, such as cytokines related to systemic neovascularization or sensory nerve growth after birth.

In addition, clinical subtypes of IHs at birth were as follows: 19 superficial and one mixed. On the other hand, clinical subtype of IHs after birth was 26 superficial, 7 deep, and 9 mixed. The ratio of superficial and deep IH present at birth was significantly different to that in IH after birth (19:0 *vs.* 26:7, $p = 0.039$) (Table 3). Thus, deep type IH was significantly more common in infants with IH appearing after birth than those with IH present at birth. The reason may be simply because of the difficulty and time taken to recognize deep type IHs due to the depth of the lesions and normal skin coloration.

Among four patients with IH born at < 37 weeks, one had IH present at birth and three had IH after birth. Among the four patients with IH with low birth weight, one had IH at birth and three developed IH after birth. There was no statistically significant correlation between onset and these parameters.

In conclusion, IHs appearing after birth tended to more commonly have multiple lesions than those with IH present at birth, with statistically significant difference. Our result suggests that there may be different triggers between IHs present at birth and those appearing after birth. Further studies with a greater number of patients are necessary to validate these findings.

Acknowledgements

We acknowledge proofreading and editing by Benjamin Phillis at the Clinical Study Support Center, Wakayama Medical University.

Funding: None.

Conflict of Interest: The authors have no conflicts of interest to disclose.

References

1. Ding Y, Zhang JZ, Yu SR, Xiang F, Kang XJ. Risk factors for infantile hemangioma: a meta-analysis. World

J Pediatr. 2020; 16:377-384.
2. Jinnin M, Ishihara T, Boye E, Olsen BR. Recent progress in studies of infantile hemangioma. J. Dermatol. 2010; 37:283-298.
3. Khan ZA, Boscolo E, Picard A, Psutka S, Melero-Martin JM, Bartch TC, Mulliken JB, Bischoff J. Multipotential stem cells recapitulate human infantile hemangioma in immunodeficient mice. J Clin Invest. 2008; 118:2592-2599.
4. Jinnin M, Medici D, Park L, Limaye N, Liu Y, Boscolo E, Bischoff J, Vikkula M, Boye E, Olsen BR. Suppressed NFAT-dependent VEGFR1 expression and constitutive VEGFR2 signaling in infantile hemangioma. Nat Med. 2008; 14:1236-1246.
5. Kawaguchi A, Kunimoto K, Inaba Y, Mikita N, Kaminaka C, Kanazawa N, Yamamoto Y, Kakimoto N, Suenaga T, Takeuchi T, Suzuki H, Baba N, Jinnin M. Distribution analysis of infantile hemangioma or capillary malformation on the head and face in Japanese patients. J Dermatol. 2019; 46:849-852.
6. Anderson KR, Schoch JJ, Lohse CM, Hand JL, Davis DM, Tollefson MM. Increasing incidence of infantile hemangiomas (IH) over the past 35 years: Correlation with decreasing gestational age at birth and birth weight. J Am Acad Dermatol. 2016; 74:120-126.
7. Mulliken JB, Fishman SJ, Burrows PE. Vascular anomalies. Curr Probl Surg. 2000; 37:517-584.
8. Chang LC, Haggstrom AN, Drolet BA, Baselga E, Chamlin SL, Garzon MC, Horii KA, Lucky AW, Mancini AJ, Metry DW, Nopper AJ, Frieden IJ, Group HI. Growth characteristics of infantile hemangiomas: implications for management. Pediatrics. 2008; 122:360-367.

Received July 9, 2021; Revised August 4, 2021; Accepted August 13, 2021

Address correspondence to:
Kayo Kunimoto, Department of Dermatology, Wakayama Medical University, 811-1 Kimiidera, Wakayama-shi, Wakayama 641-0012, Japan.
E-mail: k-jigen@wakayama-med.ac.jp

Released online in J-STAGE as advance publication August 26, 2021.

Case Report

DOI: 10.5582/ddt.2021.01063

An unusual case of acute motor axonal neuropathy (AMAN) complicating dengue fever

Swasthi S Kumar[1], Upendra Baitha[1,*], Surabhi Vyas[2]

[1] Department of Medicine, All India Institute of Medical Sciences, New Delhi, India;
[2] Department of Radiodiagnosis, All India Institute of Medical Sciences, New Delhi, India.

SUMMARY Neurological complications are increasingly being reported in dengue fever, and the dengue virus is now recognized as a neurotrophic virus. The damage caused by inflammatory cytokines in the febrile phase and molecular mimicry in the recovery phase is responsible for these neurological manifestations. We report such an unusual neurological complication occurring in a 27-year-old female in the recovery phase of dengue fever, who developed an acute onset of ascending symmetric weakness of all four limbs without any sensory, autonomic, cerebellar, or cranial nerve involvement. She was diagnosed as having an acute motor axonal neuropathy (AMAN) variant of Guillain-Barre syndrome (GBS) based on a nerve conduction study (NCS) showing axonal neuropathy and contrast-enhanced magnetic resonance imaging (CE-MRI) showing root enhancement at the region of the cauda equina. She was treated with intravenous immunoglobulin (IVIG) and showed full recovery from symptoms with treatment. Our case highlights the importance of being aware of such rare neurological complications in dengue fever. Early detection and rapid initiation of treatment can lead to the complete reversal of neurological deficits.

Keywords Guillain-Barre syndrome, intravenous immunoglobulin, demyelination, dengue fever, nerve conduction study

1. Introduction

Dengue virus is now known to be a neurotropic virus, and neurological complications are being increasingly reported in dengue fever. The damage caused by inflammatory cytokines in the febrile phase and molecular mimicry in the recovery phase are responsible for these neurological manifestations. Encephalitis, myelitis, myositis, Guillain-Barre syndrome (GBS), hypokalemic periodic paralysis have been reported in dengue fever. We report an unusual case of a 27-year-old female, in the recovery phase of dengue fever, who presented with acute onset of ascending symmetric weakness of all four limbs, diagnosed as acute motor axonal neuropathy (AMAN) variant of GBS based on nerve conduction study (NCS) showing axonal neuropathy and contrast-enhanced magnetic resonance imaging (CE-MRI) showing root enhancement at the region of cauda equina. She was treated with intravenous immunoglobulin (IVIG) and showed full recovery from symptoms with treatment.

2. Case Report

A 27-year-old female with no comorbidities presented with acute onset weakness of all four limbs. Weakness started in the lower limbs and progressed to the upper limbs after 24 hours. Weakness in the lower limbs involved the distal muscles in the form of difficulty in wearing footwear and proximal muscles in the form of difficulty in walking, standing up from a sitting position, and climbing stairs. Upper limb weakness was more distal in the form of difficulty holding a pen, weak handgrip and difficulty in braiding hair. There was no history suggestive of any cranial nerve involvement like drooping of eyelids, diplopia, deviation of tongue or angle of mouth. There were no associated sensory symptoms like numbness or paraesthesia. There was no associated headache, memory loss, behavioural abnormalities, abnormal movements or vomiting. There was no associated bowel or bladder involvement. There was no associated shortness of breath suggestive of diaphragmatic weakness. There was no history of recent

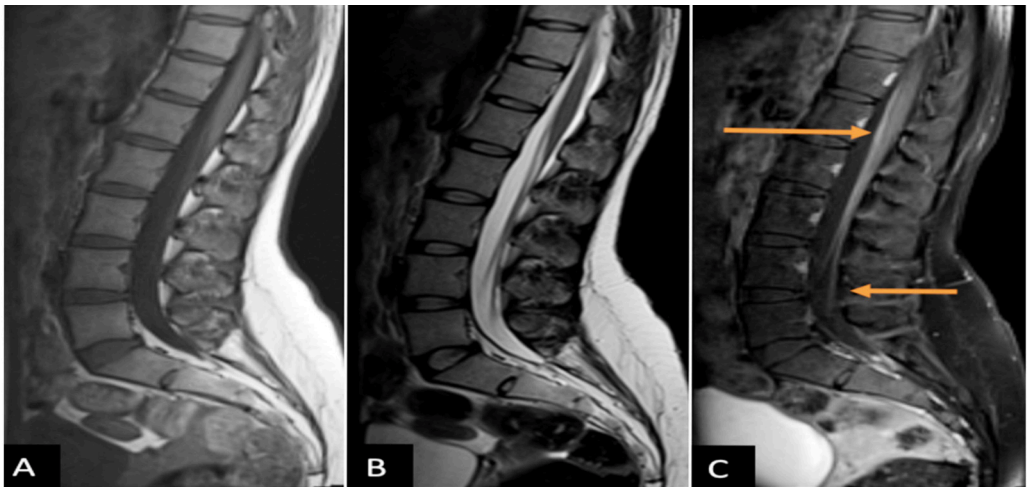

Figure 1. Arachnoiditis. Sagittal MRI images of the lumbar spine, T1w (A), T2w (B), Post-contrast (C) show thickening and enhancement of the thecal sac and the Cauda equina nerve roots (arrow).

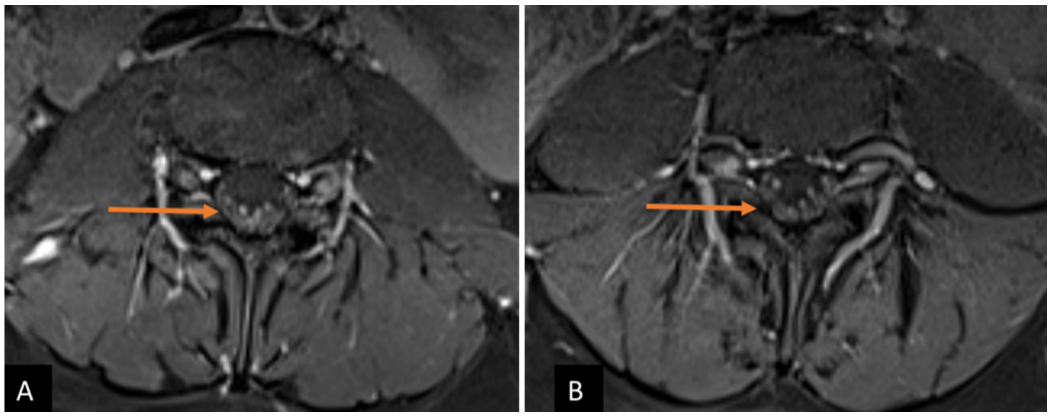

Figure 2. Arachnoiditis. Axial post contrast MRI images (A, B) of the lumbar spine, show posterior layering with thickening and enhancement of the lumbar nerve roots (arrow).

vaccination before the onset of weakness. There was no history of recent diarrhoeal or respiratory disease.

A week before the onset of weakness, she had a high-grade fever for 2 days associated with calf muscle pain and blanching rashes over arms and neck. She tested positive for NS1 antigen and was diagnosed as having dengue fever without warning signs.

At presentation, she was conscious, oriented to time, place, person and cooperative. Her pulse rate was 78 bpm and blood pressure was within normal limits. She was not tachypneic, had room air saturation of 98% and single breath count of 36. Examination of the nervous system revealed symmetric lower motor neuron type of weakness involving all four limbs. She had a power of 4+/5 at shoulder joint; 4-/5 at the elbow, wrist; 4-/5 at the hip, knee; 3/5 at the ankle joint, with normal bulk and generalised hypotonia. All deep tendon reflexes were preserved and Babinski response was negative.

Given the acute onset of ascending, symmetric lower motor type of weakness involving all limbs, a provisional diagnosis of GBS was made. Other possible differentials kept were acute porphyria and lead intoxication.

Routine blood investigations showed a normal leukocyte count of 5,110 cells/uL with 63.2% neutrophils, mild anaemia (haemoglobin 10.8 g/dL) secondary to folate deficiency and normal platelet counts. Hepatic and renal functions were within normal limits. Creatine phosphokinase (CPK) and lactate dehydrogenase (LDH) levels were within normal limits. NCS showed reduced compound muscle action potential (CMAP) in bilateral median and ulnar, left tibial and right peroneal nerves; unrecordable CMAPs in the right tibial and left peroneal nerves and normal F waves. CE-MRI of brain and spine showed nerve root enhancement in the cauda equina. Lumbar puncture was deferred as the patient was in the initial week of illness.

A diagnosis of AMAN variant of GBS was made and the patient was started on IVIG 2 g/kg given over 5 days. By day 3 of treatment, the patient reported modest improvement in symptoms and she was discharged after the course of IVIG. At the time of discharge, power was 5/5 in all joints of upper and lower limbs, except the ankle joint where the power was 4-/5. The patient was closely followed up on OPD basis and gradually power at the ankle joint also returned to normal.

3. Discussion

Sanguansermsri in 1976 first reported neurological complications in dengue fever (DF) (*1*). Initially believed to be a non-neurotrophic virus, today there is enough evidence to suggest that dengue virus is neurovirulent. Viral proteins, RNA and antibodies directed against dengue virus have been detected in cerebral-spinal fluid (CSF). Dengue virus 2 and 3 are more likely to cause neurological complications (*2*).

Hendarto *et al*. reported the incidence of neurological complications in dengue fever as 0.5-6% (*3*). In dengue endemic countries like Brazil, neurological complications have been reported in as high as 21% of dengue cases (*4*). Koshy *et al*. conducted a prospective study in north west India to identify the prevalence of neurological manifestations in dengue fever. 799 dengue patients during the epidemic of 2010 were screened for neurological manifestations and it was present in 21 patients (2.63%) (*5*). Neurologic manifestations are so prevalent in some endemic areas such that in patients presenting with acute flaccid paralysis, dengue viral infection must be ruled out as a cause. World Health Organisation (WHO), in the 2009 classification of DF, has categorised the presence of neurological complications as severe dengue (*6*).

Nervous system involvement has been reported in both the febrile phase as well as in the convalescence phase. Damage caused by pro-inflammatory cytokines like tumour necrosis factor (TNF), interleukins, complements and molecular mimicry in the form of the immune response to the dengue virus antigens that have been misdirected against the host nerve tissue are believed to be the plausible cause in the febrile phase and recovery phase respectively. Higher body temperatures, presence of severe thrombocytopenia, transaminitis and rashes, hemoconcentration are risk factors for neurological complications (*7*).

Verma *et al*. and Murthy, Marzia and colleagues classified neurological complications of dengue fever into (a) neurotrophic complications like encephalitis, myelitis, myositis; (b) systemic complications like hypokalemic periodic paralysis; and (c) post-infectious immune mediated complications like GBS, acute disseminated encephalomyelitis (ADEM), opsoclonus myoclonus syndrome, neuromyelitis optica (NMO) (*8-10*). Solbrig *et al*. proposed a different classification system: (a) involvement of central nervous system and eyes, (b) peripheral nervous system and (c) post dengue immune mediated syndromes (*11*). Peripheral nervous system manifestations contribute to 5% of neurological manifestations of DF (*12*).

GBS affecting dengue patients is being increasingly reported now. Tan *et al*. in 2019 published a study evaluating 95 patients admitted with GBS between 2010 and 2018 at a tertiary care centre in Kaula Lampur. Sera of these patients were tested for IgM antibodies against cytomegalovirus (CMV), Ebstein Barr virus (EBV), dengue, mycoplasma pneumoniae and IgG antibodies against *Clostridium jejuni*. Twenty percent of the patients were positive for dengue IgM antibodies and this was statistically significant (p value = 0.034) and dengue related GBS was more likely to have diarrhoea, facial palsy and more severe neurological deficit (*13*). GBS is more likely to occur early in the course of dengue fever. Average time between onset of fever and neurological deficit was 2 days (*14*).

Our patient presented with symptoms suggestive of AMAN in the recovery phase of dengue fever. She was treated with IVIG 2 g/kg given over five days and started showing improvement in weakness by day 3 of IVIG. Treatment response with both IVIG and plasmapheresis are equivalent and there is no extra benefit from combining the two modalities of treatment (*15*). When the patient was followed up a month after discharge, she had recovered completely from the neurological deficit.

Funding: None.

Conflict of Interest: The authors have no conflicts of interest to disclose.

References

1. Sanguansermsri T, Poneprasert B, Phornphutkul B, Kulapongs P, Tantachamrun T. Acute encephalopathy associated with dengue infection. Bangkok: Seameo Tropmed. 1976:10-11.
2. Puccioni-Sohler M, Orsini M, Soares CN. Dengue: A new challenge for neurology. Neurol Int. 2012; 4:e15.
3. Hendarto SK, Hadinegoro SR. Dengue encephalopathy. Acta Paediatr Jpn. 1992; 34:350-357.
4. Carod-Artal FJ, Wichmann O, Farrar J, Gascon J. Neurological complications of dengue virus infection. Lancet Neurol. 2013; 12:906-919.
5. Koshy JM, Joseph DM, John M, Mani A, Malhotra N, Abraham GM, Pandian J. Spectrum of neurological manifestations in dengue virus infection in Northwest India. Trop Doct. 2012; 42:191-194.
6. World Health Organization. Dengue: Guidelines for Diagnosis, Treatment, Prevention and Control 2009. *https://www.who.int/tdr/publications/documents/dengue-diagnosis.pdf* (accessed August 27, 2021).
7. Miagostovich MP, Ramos RG, Nicol AF, Nogueira RM, Cuzzi-Maya T, Oliveira AV, Marchevsky RS, Mesquita RP, Schatzmayr HG. Retrospective study on dengue fatal cases. Clin Neuropathol. 1997; 16:204-208.
8. Sahu R, Verma R, Jain A, Garg RK, Singh MK, Malhotra HS, Sharma PK, Parihar A. Neurologic complications in dengue virus infection: a prospective cohort study. Neurology. 2014; 83:1601-1609.
9. Murthy JMK. Neurological complication of dengue infection. Neurol India. 2010; 58:581-584.
10. Puccioni-Sohler M, Rosadas C, Cabral-Castro MJ. Neurological complications in dengue infection: a review for clinical practice. Arq Neuropsiquiatr. 2013; 71:667-671.
11. Solbrig MV, Perng GC. Current neurological observations

and complications of Dengue virus infection. Curr Neurol Neurosci Rep. 2015; 15:29.
12. Oehler E, Le Henaff O, Ghawche F. Neurological manifestations of dengue. Presse Med. 2012; 41:e547-552.
13. Tan CY, Razali SNO, Goh KJ, Sam IC, Shahrizaila N. Association of dengue infection and Guillain-Barré syndrome in Malaysia. J Neurol Neurosurg Psychiatry. 2019; 90:1298-1300.
14. Simon O, Billot S, Guyon D, Daures M, Descloux E, Gourinat AC, Molko N, Dupont-Rouzeyrol M. Early Guillain-Barré Syndrome associated with acute dengue fever. J Clin Virol. 2016; 77:29-31.
15. Hughes RA, Wijdicks EF, Barohn R, Benson E, Cornblath DR, Hahn AF, Meythaler JM, Miller RG, Sladky JT, Stevens JC; Quality Standards Subcommittee of the American Academy of Neurology. Practice parameter: immunotherapy for Guillain-Barré syndrome: report of the Quality Standards Subcommittee of the American Academy of Neurology. Neurology. 2003; 61:736-740.

Received July 2, 2021; Revised August 27, 2021; Accepted August 28, 2021.

Address correspondence to:
Upendra Baitha, Department of Medicine, All India Institute of Medical Sciences, FTA-504, Ayur Vigyan Nagar, New Delhi 110049, India.
E-mail: drupendraraj14@gmail.com

Released online in J-STAGE as advance publication August 31, 2021.

Case Report

DOI: 10.5582/ddt.2021.01006

Nivolumab induced hypophysitis in a patient with recurrent non-small cell lung cancer

Smile Kajal[1], Pooja Gupta[2,*], Anam Ahmed[3], Anurag Gupta[4]

[1] Department of Otolaryngology, All India Institute of Medical Sciences (AIIMS), New Delhi, India;
[2] Department of Pharmacology, All India Institute of Medical Sciences (AIIMS), New Delhi, India;
[3] Department of Anatomy, All India Institute of Medical Sciences (AIIMS), New Delhi, India;
[4] Department of Pathology, University College of Medical Sciences, New Delhi, India.

SUMMARY Nivolumab is a programmed death receptor-1 blocking monoclonal antibody which has been approved by United States Food and Drug Administration for patients with metastatic non-squamous non-small cell lung cancer. Endocrinopathies like thyroid dysfunction and adrenal insufficiency are its known immune related adverse effects. Hypophysitis is very rare and usually presents with minimal symptoms. We report development of hypophysitis in an 84-year-old female patient who developed a range of symptoms (fatigue, headache, nausea) as well as laboratory confirmation of both central hypothyroidism and central adrenal deficiency which is unusual in cases of nivolumab induced hypophysitis. The patient had well differentiated adenocarcinoma of the left upper lobe of the lung. She underwent wedge resection followed by chemotherapy and was started on nivolumab due to recurrence. After 14 cycles of nivolumab, she started complaining of intense fatigue. She was found to have central thyroid deficiency and was started on levothyroxine. But her symptoms did not improve. Then she underwent adrenocorticotropic hormone stimulation test which showed central adrenal deficiency, but her brain magnetic resonance imaging did not reveal any pituitary or sellar changes. A diagnosis of nivolumab induced hypophysitis was made, based on clinical grounds and hormonal profile and she was started on oral steroids. She responded dramatically to this steroidal therapy within four weeks of its initiation and her immunotherapy with nivolumab was restarted.

Keywords Nivolumab, hypophysitis, non-small cell lung cancer, hypopituitarism

1. Introduction

Nivolumab is a monoclonal antibody of immunoglobulin G4 type which targets the programmed death-1 (PD-1) receptor. It was approved by United States Food and Drug Administration (FDA) in October 2015 for patients with metastatic non-squamous non-small cell lung cancer (NSCLC) based on the CheckMate 057 trial that showed improvement in overall survival as compared to docetaxel in patients who progressed on or after platinum-based chemotherapy. It has also been approved for the treatment of advanced melanoma, malignant pleural mesothelioma, advanced renal cell carcinoma, classical Hodgkin's lymphoma, advanced squamous cell carcinoma of head and neck, urothelial carcinoma, metastatic colorectal cancer, hepatocellular carcinoma, and advanced esophageal squamous cell carcinoma (*1,2*). The main immune-related adverse events (irAEs) associated with nivolumab include diarrhea, colitis, hepatitis, skin toxicities and endocrinopathies such as hypophysitis and thyroid dysfunction (*3*). Although thyroid dysfunction is a common adverse effect of nivolumab, hypophysitis is rare with an incidence of less than 1% and only a handful cases of nivolumab induced hypophysitis in patients with NSCLC have been described in literature (*4-6*). Usually, such cases present with less symptoms and radiological features as compared to other immunotherapy related hypophysitis (*5,6*). We present a novel case of an elderly patient with recurrent NSCLC who was diagnosed with nivolumab induced hypophysitis based on clinical suspicion due to her hormonal profile and a range of symptoms which she developed during nivolumab immunotherapy.

2. Case Report

An 84-year-old Caucasian female, who was first diagnosed with well differentiated adenocarcinoma of the left upper lobe of lung in 2009, underwent left

Table 1. Result of Adrenocorticotropic hormone (ACTH) stimulation test done in patient

Hormone	Reference Range	Baseline levels (10:15 am)	30 mins after ACTH stimulation	60 mins after ACTH stimulation
ACTH (pg/mL)	10 - 48	8	–	–
Cortisol (mcg/dL)	6.0 - 18.4 (7 - 10 am) 2.7 - 10.5 (3 - 6 pm)	9.7	24.7	29.8
Aldosterone (ng/dL)	0.0 - 30.0	< 1.0	4.8	5.8

upper lobe wedge resection and mesh brachytherapy in November 2009. She did not have history of smoking and had hypertension controlled with oral medications. She was put on systemic chemotherapy with pemetrexed, and carboplatin and the treatment response was monitored with Computed Tomography (CT) imaging of chest, abdomen, and pelvis. In January 2012, her CT scan images showed disease recurrence at the wedge resection site, thereby increasing the size of the right upper lobe, and left upper lobe nodules. The tumor was EGFR (epidermal growth factor receptor) and EML 4/ALK (echinoderm microtubule-associated protein-like 4/anaplastic lymphoma kinase) mutation negative. She then completed her systemic chemotherapy with pemetrexed and carboplatin in March 2012 which was followed by oral erlotinib for four years. Erlotinib had to be discontinued in January 2016 due to continued adverse effects. Later, in March 2016 she was started on nivolumab immunotherapy which was well tolerated till October 2016 (11 cycles) when she complained of intense fatigue occasionally which led to prolonged sleeping. Occasional headaches were also an added complaint accompanied with dryness of mouth and eyes. Her thyroid profile showed low thyroid stimulating hormone (TSH) and low thyroid hormone (T4). However, no thyroid autoantibodies were found in blood, and she was started on oral thyroxine. By November 2016 she had completed 14 cycles of nivolumab immunotherapy and still had similar complaints of fatigue, increased sleepiness, and headaches during her office visits in December 2016. The patient received one more treatment with nivolumab in mid-December 2016 post which a 2-month break from the treatment was approved. On continuing with the same treatment in February 2017, she complained of frequent episodes of lightheadedness and nausea. Her fatigue and headache had still not improved but she did not have any visual symptoms. Adrenocorticotropic hormone (ACTH) stimulation test confirmed central adrenal deficiency (Table 1). Her brain magnetic resonance imaging (MRI) did not show any significant abnormality. A diagnosis of depressed anterior pituitary function was made owing to her earlier decreased TSH and now central adrenal deficiency. The patient was started on oral glucocorticoids (Tablet prednisolone 1 mg/kg for a week and then tapering dose over a month). The patient's symptoms subsided within four weeks. Nivolumab immunotherapy was restarted and the low dose prednisolone along with same dose levothyroxine was continued till the end of therapy.

3. Discussion

Hypophysitis is an acute or chronic inflammation of pituitary gland. It is a rare condition in the general population and its incidence has not yet been quantified. However, less than 1% of surgically treated pituitary lesions demonstrate histological features of hypophysitis (*7*). Autoimmune hypophysitis, which is a subtype, has a prevalence of about 5 per million and an annual incidence of 1 in 7 to 9 million (*8*). Immunotherapy-associated hypophysitis is commonly associated with headache and anterior hypopituitarism. Anterior hypopituitarism presents with a characteristic but atypical pattern of deficiency of ACTH followed by TSH, gonadotrophins and prolactin deficiency or hyperprolactinemia (*9*). The degree of pituitary enlargement is generally mild which goes undetected on MRI or is completely absent, and compression of the optic apparatus is extremely rare (*5,6,9*).

Prior to the nivolumab, hypophysitis was relatively common in patients treated with ipilimumab, a human monoclonal antibody against the cytotoxic T-Lymphocyte antigen 4 (CTLA-4 Ab), which was approved by the FDA in 2011 for the treatment of advanced melanoma (*10-15*). It has been seen that as compared to ipilimumab associated hypophysitis, nivolumab induced hypophysitis is still rare, is diagnosed late (median of 25 weeks) and is less commonly associated with any symptoms like headache or any pituitary changes detected on MRI (*5,6*). However, our patient presented with a range of symptoms (fatigue, headache, nausea) as well as laboratory confirmation of both central hypothyroidism and central adrenal deficiency which is unusual in cases of nivolumab induced hypophysitis. A review of the trial data of immune checkpoint-induced hypophysitis showed that the incidence of hypophysitis for ipilimumab was 0-17% (*6,16,17*) while the incidence was less for nivolumab (< 1%) (*7,18*) and pembrolizumab (< 1%) (*7, 19*).

In a retrospective analysis of 83 patients treated with immunotherapy to observe the immune checkpoint inhibitor related hypophysitis (irH), the irH was defined as (*i*) ACTH or TSH deficiency plus MRI changes or (*ii*) ACTH and TSH deficiencies plus headache/ fatigue in the absence of MRI findings. As per this

definition, 62 patients had irH at initial evaluation and the most common symptom was fatigue (66%) followed by headache (60%). Central hypothyroidism and central adrenal insufficiency were seen in 94% and 69% patients, respectively and 77% of the irH patients had MRI changes like stalk thickening, suprasellar convexity, and heterogeneous enhancement of the pituitary gland. 48 out of 62 (77%) patients were on ipilimumab, 2/62 (3%) on tremelimumab, 3/62 (5%) on nivolumab, and 9/62 (15%) on a combination of both nivolumab and ipilimumab. When compared to therapies without ipilimumab, those with ipilimumab had a statistically significant association with irH ($p < 0.01$) and the median time interval from initiation of immunotherapy to development of irH was less for ipilimumab (9-12 weeks) as compared to nivolumab (30.4-37.7 weeks) (*20*).

Patients with irH have been treated with physiologic to high-dose glucocorticoids resulting in improvement of symptoms and pituitary function. In most patients, the steroids and other hormone replacements, like for thyroid, need to be continued till the end of immunotherapy or even after the end of immunotherapy as the recovery rate is variable. The chance of recovery of thyroidal axis is more than the adrenal or gonadal axis (*5,6,9,20*).

Our patient developed central hypothyroidism followed by central adrenal deficiency as evident by ACTH stimulation test. Her brain MRI did not show any significant finding, but she had history of episodes of headache, prolonged sleepiness, and nausea. Her presentation was novel for nivolumab induced hypophysitis and a diagnosis was made, based on clinical grounds and hormonal profile. She was started on glucocorticoids to which she responded well symptomatically which further supported our diagnosis. In almost all cases of immune mediated hypophysitis, the histopathological diagnosis of hypophysitis by biopsy of pituitary gland is never indicated due to increased risk-to-benefit ratio. Hence, a high degree of clinical suspicion is required for its timely diagnosis.

4. Conclusion

Immunotherapy induced hypophysitis is a rare condition and has frequently been described with Anti-CTLA4 agents like ipilimumab, but it is rare with Anti-PD1 agents like nivolumab and usually presents with less symptoms. A normal MRI of the brain does not exclude hypophysitis. Therefore, a high degree of clinical suspicion and multidisciplinary team involving medical oncologists, clinical pharmacologists, endocrinologists, and radiologists is required to diagnose such cases.

Acknowledgements

We would like to thank Dr Moses Raj (Associate Professor, Temple University, Allegheny Health Network Cancer Institute, Pittsburgh, United States) for his expert opinion on this case.

Funding: None.

Conflict of Interest: The authors have no conflicts of interest to disclose.

References

1. Keating GM. Nivolumab: A review in advanced non squamous non-small cell lung cancer. Drugs. 2016; 76:969-978.
2. Kazandjian D, Suzman DL, Blumenthal G, Mushti S, He K, Libeg M, Keegan P, Pazdur R. FDA approval summary: Nivolumab for the treatment of metastatic non-small cell lung cancer with progression on or after platinum-based chemotherapy. Oncologist. 2016; 21:634-642.
3. Spain L, Diem S, Larkin J. Management of toxicities of immune checkpoint inhibitors. Cancer Treat Rev. 2016; 44:51-60.
4. Ishikawa M, Oashi K. Case of hypophysitis caused by nivolumab. J Dermatol. 2017; 44:109-110.
5. Garon-Czmil J, Petitpain N, Rouby F, Sassier M, Babai S, Yéléhé-Okouma M, Weryha G, Klein M, Gillet P. Immune check point inhibitors-induced hypophysitis: a retrospective analysis of the French pharmacovigilance database. Sci Rep. 2019; 9:19419.
6. Faje A, Reynolds K, Zubiri L, Lawrence D, Cohen JV, Sullivan RJ, Nachtigall L, Tritos N. Hypophysitis secondary to nivolumab and pembrolizumab is a clinical entity distinct from ipilimumab-associated hypophysitis. Eur J Endocrinol. 2019; 181:211-219.
7. Joshi MN, Whitelaw BC, Palomar MT, Wu Y, Carroll PV. Immune checkpoint inhibitor-related hypophysitis and endocrine dysfunction: Clinical review. Clin Endocrinol. 2016; 85:331-339.
8. Howlett TA, Levy MJ, Robertson IJ. How reliably can autoimmune hypophysitis be diagnosed without pituitary biopsy. Clin Endocrinol (Oxf). 2010; 73:18-21.
9. Faje A. Hypophysitis: Evaluation and management. Clin Diabetes Endocrinol. 2016; 2:15.
10. Faje A. Immunotherapy and hypophysitis: clinical presentation, treatment, and biologic insights. Pituitary. 2016; 19:82-92.
11. Faje AT, Sullivan R, Lawrence D, Tritos NA, Fadden R, Klibanski A, Nachtigall L. Ipilimumab induced hypophysitis: a detailed longitudinal analysis in a large cohort of patients with metastatic melanoma. J Clin Endocrinol Metab. 2014; 99:4078-4085.
12. Chodakiewitz Y, Brown S, Boxerman JL, Brody JM, Rogg JM. Ipilimumab treatment associated pituitary hypophysitis: clinical presentation and imaging diagnosis. Clin Neurol Neurosurg. 2014; 125:125-130.
13. Lam T, Chan MM, Sweeting AN, De Sousa SM, Clements A, Carlino MS, Long GV, Tonks K, Chua E, Kefford RF, Chipps DR. Ipilimumab-induced hypophysitis in melanoma patients: an Australian case series. Intern Med J. 2015; 45:1066-1073.
14. Ryder M, Callahan M, Postow MA, Wolchok J, Fagin JA. Endocrine-related adverse events following

ipilimumab in patients with advanced melanoma: a comprehensive retrospective review from a single institution. Endocr Relat Cancer. 2014; 21:371-381.
15. Gambale E, Tinari C, Carella C, Paolo AD, Tursi MD. Immunotherapy and hypophysitis in the clinical practice: A case report. J Clin Case Rep. 2016; 6:861.
16. Corsello SM, Barnabei A, Marchetti P, De Vecchis L, Salvatori R, Torino F. Endocrine side effects induced by immune checkpoint inhibitors. J Clin Endocrinol Metabol. 2013; 98:1361-1375.
17. Torino F, Barnabei A, Paragliola RM, Marchetti P, Salvatori R, Corsello SM. Endocrine side-effects of anti-cancer drugs: mAbs and pituitary dysfunction: clinical evidence and pathogenic hypotheses. European J Endocrinol. 2013; 169:R153-R164.
18. Topalian SL, Sznol M, McDermott DF, *et al*. Survival, durable tumor remission, and long-term safety in patients with advanced melanoma receiving nivolumab. J Clin Oncol. 2014; 32:1020-1030.
19. Robert C, Ribas A, Wolchok JD, *et al*. Anti-programmed-death-receptor-1 treatment with pembrolizumab in ipilimumab-refractory advanced melanoma: a randomized dose comparison cohort of a phase 1 trial. Lancet. 2014; 384:1109-1117.
20. Nguyen H, Shah K, Waguespack SG, *et al*. Immune checkpoint inhibitor related hypophysitis: diagnostic criteria and recovery patterns. Endocr Relat Cancer. 2021; 28:419-431.

Received January 19, 2021; Revised August 22, 2021; Accepted August 27, 2021

**Address correspondence to:*
Pooja Gupta, Department of Pharmacology, Room 5004, Convergence block, All India Institute of Medical Sciences (AIIMS), New Delhi, India.
E-mail: drgupta.pooja@gmail.com

Released online in J-STAGE as advance publication August 29, 2021.

Communication

DOI: 10.5582/ddt.2021.01064

Emergency use of COVID-19 vaccines recommended by the World Health Organization (WHO) as of June 2021

Xiaoni Cui[1], Pengxiang Wang[1], Zhun Wei[2,*]

[1] Sino-Cell Biomed Co., Ltd., Qingdao, Shandong, China;
[2] Institute of Innovative Drugs and Department of Pharmacology, School of Pharmacy, Qingdao University, Qingdao, Shandong, China.

SUMMARY In December 2019, the novel severe acute respiratory syndrome coronavirus 2 (SARS-CoV-2) caused the outbreak of coronavirus disease 2019 (COVID-19), and the resulting pandemic has caused widespread health problems and social and economic disruption. Thus far in 2021, more than 4 million people worldwide have died from COVID-19, so safe and efficacious vaccines are urgently needed to restore normal economic and social activities. According to the official guidance documents of the World Health Organization (WHO), vaccines based on four major strategies including mRNA, adenoviral vectors, inactivated viruses, and recombinant proteins have entered the stage of emergency use authorization and pre-certification evaluation. The current review summarizes these vaccines and it looks ahead to the development of additional COVID-19 vaccines in the future.

Keywords COVID-19, vaccine research, mRNA, adenoviral vectors, inactivated viruses, recombinant proteins

On March 11, 2020, the World Health Organization (WHO) declared novel coronavirus disease 2019 (COVID-19) a global pandemic (*1*). Severe acute respiratory syndrome coronavirus 2 (SARS-CoV-2), the virus that causes COVID-19, has now infected more than 200 million people and caused more than 4 million deaths. A promising avenue for human beings to overcome epidemics, the research and development of vaccines has been compressed from the usual 10-15 years to 1-2 years as a result of joint efforts worldwide; these efforts are encouraging and fruitful (*2*). Earlier documents from the WHO described seven platforms or strategies for COVID-19 vaccine development (*3*). As of June 2021, there are four major categories of vaccines including mRNA vaccines, adenovirus-vectored vaccines, inactivated virus vaccines, and recombinant protein vaccines. Vaccines have been produced by 23 businesses and research institutions in 8 countries, leading to the 19 vaccines in the 'emergency use listing/pre-qualification evaluation process' as shown in Table 1 (*4*).

mRNA vaccines An mRNA vaccine encapsulates the mRNA that encodes the SARS-CoV-2 spike protein (S protein) into lipid nanoparticles, and these nanoparticles are then injected into the human body. After the nanoparticles enter cells, antigen information will be presented on the surface of the cell membrane and an immune response will be induced. Examples of mRNA vaccines are BNT162b2 (produced by Pfizer & BioNTech) and mRNA-1273 (produced by Modena). An mRNA vaccine has many advantages such as being noninfectious, being easy to production, and being easy to standardize (*5,6*). BNT162b2 was granted emergency use authorization by the WHO on December 31, 2020. It is the first mRNA vaccine that was approved for human use. In Israel, more than 6.5 million people over the age of 16 have been vaccinated once BNT162b2 was authorized for emergency use. Its efficacy is as high as 95.3% within 7 days of 2 rounds of vaccination (*7*). A study of nearly 4,000 frontline healthcare workers at eight locations in the United States from December 2020 to March 2021 indicated that the rate of infection dropped sharply after 2 rounds of vaccination within 14 days, and vaccine efficacy was 90% according to the Centers for Disease Control and Prevention (CDC) (*8*). Another study indicated that neutralizing antibodies and memory B cells remain stable over a period of 6-12 months after BNT162b2 is injected twice. These findings indicate that mRNA vaccines can confer long-lasting protection (*9*) and still remain efficacious against mutants (*10*).

Adenovirus-vectored vaccines When the S protein gene of SARS-CoV-2 is injected into a nonpathogenic adenovirus, it will express the antigen once it enters the human body, thereby inducing both humoral immunity and cellular immunity. An adenovirus-vectored vaccine should be transported and stored at low temperatures (2-8°C) (*11*). Examples of adenovirus-vectored vaccines

Table 1. Emergency use/pre-certification list of COVID-19 vaccines according to the WHO as of June 2021

Platform	Name of Vaccine	Manufacturer	Country
mRNA vaccine	BNT162b2/COMIRNATY Tozinameran (INN)	Pfizer & BioNTech	USA, Germany
	mRNA-1273	Moderna	USA
	CVnCoV/CV07050101	CureVac	Germany
Adenovirus-vectored vaccine	AZD1222	AstraZeneca & University of Oxford	UK
	Covishield (ChAdOx1_nCoV-19)	Serum Institute of India Pvt. Ltd.	India
	Ad26.COV2.S	Janssen (Johnson & Johnson)	USA
	Sputnik V	The Gamaleya National Center	Russia
	Ad5-nCoV	CanSinoBIO	China
Inactivated vaccine	SARS-CoV-2 Vaccine (Vero Cell), Inactivated (lnCoV)	Sinopharm/BIBP	China (Beijing)
	CoronaVac	Sinovac	China
	Inactivated SARS-CoV-2 Vaccine (Vero Cell)	Sinopharm/WIBP	China (Wuhan)
	COVAXIN	Bharat Biotech	India
	SARS-CoV-2 Vaccine, Inactivated (Vero Cell)	IMBCAMS	China
Recombinant protein vaccine	NVX-CoV2373/Covovax	NOVAVAX	USA
	CoV2 preS dTM-AS03 vaccine	Sanofi Pasteur	France
	EpiVacCorona	SRC VB VECTOR	Russia
	Recombinant Novel Coronavirus Vaccine (CHO Cell)	Zhifei Longcom	China
	SCB-2019	Clover Biopharmaceuticals	China
	Soberana 01, Soberana 02, Soberana Plus, Abdala	BioCubaFarma	Cuba

are AZD1222 (developed by the Jenner Institute of Oxford & AstraZeneca), Ad26.COV2.S (produced by Johnson & Johnson), and Ad5-nCoV (produced by CanSinoBIO). Numerous studies involving hundreds of thousands of people in Great Britain have indicated that AZD1222 and BNT162b2 are both effective at preventing infection and severe symptoms of COVID-19 (*12-14*). A phase 3 trial randomized double-blind study involving tens of thousands of people has indicated that Ad26.COV2.S was equally effective at preventing infection and at treating severe-critical disease (including hospitalization and death) (*15*). Data from a phase 3 trial on Sputnik V (developed by the Gamaleya National Center of Epidemiology and Microbiology) will be released later (*16,17*).

Inactivated vaccines An advantage of an inactivated vaccine is that it retains immunogenicity while lacking the infectivity of a virus. Vaccination with an inactivated virus can stimulate the body to generate a humoral immune response to defend against SARS-CoV-2 (*18*). The main manufacturers of inactivated vaccines against COVID-19 are Sinopharm/BIBP, Sinovac, and Sinopharm/WIBP. Clinical data indicate that the vaccine produced by Sinopharm/BIBP has an efficacy of 79% (*19*). In one study, 13,459 individuals received an initial injection with a vaccine by Sinopharm/WIBP, and 13,066 individuals received the second injection (*20*). High titers of antibodies developed within 14 days of the second injection, resulting in effective protection, positivity for neutralizing antibodies higher than 99%, and a protective efficacy of 72.8%. The vaccine produced by Sinovac was the second Chinese vaccine approved by the WHO. Although it had an initial efficacy of only 51%, its efficacy at preventing severe illness and mortality was 100% (*19*). Inactivated vaccines from Bharat Biotech and the Institute of Medical Biology, Chinese Academy of Medical Sciences (IMBCAMS) have also entered phase III clinical trials or are in development.

Recombinant protein vaccines A target gene (like that encoding a SARS-CoV-2 antigen) is expressed *in vitro*, transfected into bacteria, yeast, mammal, or insect cells using specific protein vectors, and then the expression of large amounts of antigenic protein is induced under certain conditions. Once the protein is collected and purified, a recombinant protein vaccine can be prepared. There are currently two strategies to prepare recombinant protein vaccines against COVID-19: expression of the S protein and expression of virus-like particles (VLPs). The former ultimately uses purified S protein. An example is NVX-CoV2373/Covovax (produced by NOVAVAX), which was used to vaccinate more than 2,000 volunteers in a phase III clinical trial. Results indicated that the vaccine was 100% efficacious at preventing moderate to severe disease and that it had an overall efficacy of up to 90.4% (*21*). The latter is still being developed and is in the early clinical stage. An example is AS03 (Medicago Inc.), which contains VLPs self-assembled from capsid proteins of SARS-CoV-2 within a heterologous system. VLPs are similar to SARS-CoV-2 since they have its outer shell, but VLPs are hollow since they do not contain the virus' genetic material, so they have no infectivity or replicative capacity. However, VLPs can effectively trigger cellular immunity and humoral immunity (*22,23*).

In addition to the four main types of vaccines described thus far, several novel manufacturing approaches are being developed. As an example, the diversity and spread of coronaviruses spurred a research team at the Duke University School of Medicine to recently develop several 'mixed' mRNA vaccines with multiple immunogenicity (*24*). Results from animal trials indicated that these vaccines can target 2-3 different

coronaviruses at the same time

There are nearly 300 COVID-19 vaccine projects in the research and development stage worldwide, and more than 100 have entered the clinical trial stage (*25*). More vaccines will appear, and global vaccine production is continually expanding. The resulting vaccines will be able to cover more countries and regions and provide safety and effective protection from this global pandemic.

Funding: None.

Conflict of Interest: The authors have no conflicts of interest to disclose.

References

1. WHO Director-General's opening remarks at the media briefing on COVID-19 - 11 March 2020. *https://www.who.int/director-general/speeches/detail/who-director-general-s-opening-remarks-at-the-media-briefing-on-covid-19---11-march-2020* (accessed March 11, 2021).
2. Huang Q, Yan J. SARS-CoV-2 virus: Vaccines in development. Fundam Res. 2021; 1:131-138.
3. Dai L, Gao GF. Viral targets for vaccines against COVID-19. Nat Rev Immunol. 2021; 21:73-82.
4. Status of COVID-19 Vaccines within WHO EUL/PQ evaluation process. *WHO. https://extranet.who.int/pqweb/sites/default/files/documents/Status_COVID_VAX_16June2021.pdf* (accessed June 16, 2021).
5. mRNA vaccines to address the COVID-19 pandemic. *https://biontech.de/covid-19-portal/mrna-vaccines* (accessed June 16, 2021).
6. Pardi N, Hogan MJ, Porter FW, Weissman D. mRNA vaccines a new era in vaccinology. Nat Rev Drug Discov. 2018; 17:261-279.
7. Haas EJ, Angulo FJ, McLaughlin JM, Anis E, Singer SR, Khan F, Brooks N, Smaja M, Mircus G, Pan K, Southern J, Swerdlow DL, Jodar L, Levy Y, Alroy-Preis S. Impact and effectiveness of mRNA BNT162b2 vaccine against SARS-CoV-2 infections and COVID-19 cases, hospitalisations, and deaths following a nationwide vaccination campaign in Israel: an observational study using national surveillance data. Lancet. 2021; 397:1819-1829.
8. Thompson MG, Burgess JL, Naleway AL, *et al*. Interim estimates of vaccine effectiveness of BNT162b2 and mRNA-1273 COVID-19 vaccines in preventing SARS-CoV-2 infection among health care personnel, first responders, and other essential and frontline workers - Eight U.S. locations, December 2020-March 2021. MMWR. 2021; 70:495-500.
9. Wang Z, Muecksch F, Schaefer-Babajew D, *et al*. Naturally enhanced neutralizing breadth against SARS-CoV-2 one year after infection. Nature. 2021; 595:426-431.
10. Liu J, Liu Y, Xia H, Zou J, Weaver SC, Swanson KA, Cai H, Cutler M, Cooper D, Muik A, Jansen KU, Sahin U, Xie X, Dormitzer PR, Shi PY. BNT162b2-elicited neutralization of B.1.617 and other SARS-CoV-2 variants. Nature. 2021; doi: 10.1038/s41586-021-03693-y.
11. Aboul Fotouh K, Cui Z, Williams RO. Next-generation COVID-19 vaccines should take efficiency of distribution into consideration. AAPS PharmSciTech. 2021; 22:126.
12. Bernal JL, Andrews N, Gower C, Robertson C, Stowe J, Tessier E, Simmons R, Cottrell S, Roberts R, O'Doherty M, Brown K, Cameron C, Stockton D, McMenamin J, Ramsay M. Effectiveness of the Pfizer-BioNTech and Oxford-AstraZeneca vaccines on covid-19 related symptoms, hospital admissions, and mortality in older adults in England: test negative case-control study. BMJ. 2021; 373:n1088.
13. Vasileiou E, Simpson CR, Shi T, *et al*. Interim findings from first-dose mass COVID-19 vaccination roll-out and COVID-19 hospital admissions in Scotland: a national prospective cohort study. Lancet. 2021; 397:1646-1657.
14. Pritchard E, Matthews PC, Stoesser N, *et al*. Impact of vaccination on new SARS-CoV-2 infections in the United Kingdom. Nat Med. 2021; doi: 10.1038/s41591-021-01410-w.
15. Sadoff J, Gray G, Vandebosch A, *et al*. Safety and efficacy of single-dose Ad26.COV2.S vaccine against Covid-19. N Engl J Med. 2021; 384:2187-2201.
16. Kifle ZD, Enyew EF, Mekuria AB. A recent achievement in the discovery and development of vaccines and therapeutic agents in the race for COVID-19 protection and treatment. J Evid Based Integr Med. 2021; 26:1-10.
17. Mishra SK, Tripathi T. One year update on the COVID-19 pandemic: Where are we now? Acta Trop. 2021; 214:105778.
18. Kandeil A, Mostafa A, Hegazy RR, *et al*. Immunogenicity and safety of an inactivated SARS-CoV-2 vaccine: Preclinical studies. Vaccines (Basel). 2021; 9:214.
19. Mallapaty S. WHO approval of Chinese CoronaVac COVID vaccine will be crucial to curbing pandemic. Nature. 2021; 594:161-162.
20. Al Kaabi N, Zhang Y, Xia S, *et al*. Effect of 2 inactivated SARS-CoV-2 vaccines on symptomatic COVID-19 infection in adults: A randomized clinical trial. JAMA. 2021; 326:35-45.
21. Shinde V, Bhikha S, Hoosain Z, *et al*. Efficacy of the NVX-CoV2373 Covid-19 vaccine against the B.1.351 variant. N Engl J Med. 2021; 384:1899-1909.
22. Brisse M, Vrba SM, Kirk N, Liang Y, Ly H. Emerging concepts and technologies in vaccine development. Front Immunol. 2020; 11:583077.
23. LiY, Tenchov R, Smoot J, Liu C, Watkins S, Zhou Q. A comprehensive review of the global efforts on COVID-19 vaccine development. ACS Cent Sci. 2021; 7:512-533.
24. Martinez DR, Schäfer A, Leist SR, *et al*. Chimeric spike mRNA vaccines protect against sarbecovirus challenge in mice. bioRxiv. 2021; doi: https://doi.org/10.1101/2021.03.11.434872
25. COVID-19 - Landscape of novel coronavirus candidate vaccine development worldwide. *https://www.who.int/publications/m/item/draft-landscape-of-covid-19-candidate-vaccines* (accessed June22, 2021).

Received July 4, 2021; Revised July 14, 2021; Accepted July 16, 2021.

**Address correspondence to:*
Zhun Wei, Institute of Innovative Drugs and Department of Pharmacology, School of Pharmacy, Qingdao University, Qingdao 266003, Shandong, China.
E-mail: biowei@163.com

Released online in J-STAGE as advance publication July 19, 2021.

Letter

DOI: 10.5582/ddt.2021.01068

Less is more: A novel single-tablet regimen with two-drugs, dolutegravir/lamivudine

Jianjun Sun, Hongzhou Lu*

Department of Infection and Immunity, Shanghai Public Health Clinical Center, Shanghai, China.

SUMMARY Combined antiretroviral therapy (cART) has significantly reduced human immunodeficiency virus (HIV) associated morbidity and mortality and turned HIV infection into a manageable chronic condition. However, lifelong cART is still required. Two-drug regimens could reduce the number of HIV agents and lower the adverse events caused by lifelong medication. A new two-drug regimen, Dovato, consisting of dolutegravir and lamivudine has durable efficacy, is well-tolerated, and has a high barrier to viral resistance, which is why it is recommended as a new first-line treatment option for people living with HIV infection.

Keywords HIV infection, two-drug regimen, dolutegravir/lamivudine

Combined antiretroviral therapy (cART) has significantly reduced human immunodeficiency virus (HIV) associated morbidity and mortality and today HIV infection has largely become a manageable chronic disease. Without timely cART, however, HIV infection can still progress to acquired immune deficiency syndrome (AIDS) and result in death. People with HIV infection can be treated with cART, which can suppress the level of HIV in the body, control the spread of the virus, and encourage the immune system response to other pathogens.

Based on the achievements of anti-HIV treatments, AIDS-related deaths have been reduced by 64% since a peak in 2004 and by 47% since 2010 (1). At the same time, there were 27.5 million people receiving cART in 2020 (*1*). Along with the aforementioned success of HIV treatments, cART is lifelong and a high level of adherence is required. A particular regimen for a patient with HIV requires consideration of virologic efficacy, toxicity, pill burden, dose frequency, drug-drug interaction potential, HIV resistance test results, comorbidity status, accessibility of medication, and cost. Consequently, the strategy of antiretroviral therapy still needs to be optimized.

As is well known, a classic cART regimen for HIV patients generally consists of two nucleoside/nucleotide reverse transcriptase inhibitors (NRTIs) in combination with a third core antiretroviral drug from one of three drug classes: a non-nucleoside reverse transcriptase inhibitor (NNRTI), a protease inhibitor (PI), or an integrase strand transfer inhibitor (INSTI). In the early days of cART, the available antiretroviral drugs were associated with substantial short-term and long-term adverse events and were not well tolerated (*2*). Patients were further encumbered by a heavy pill burden. This led to the exploration of an NRTI-sparing treatment strategy: a one- or two-drug regimen that does not include antiretroviral drugs from the NRTI drug class (*3,4*).

Two-drug regimens (2DRs) have been investigated as an approach to reduce the number of antiretroviral agents taken by individuals receiving lifelong cART (*5,6*). Previous findings from studies of 2DRs have indicated the efficacy of regimens consisting of lamivudine (3TC) and a core agent with a high barrier to HIV resistance. Dolutegravir (DTG) has demonstrated a high barrier to resistance both in clinical trials and in the real world. DTG and 3TC provide a dual target blockade of the HIV life cycle and have complementary pharmacokinetic (PK) profiles, with matched 24-hour PK and PK tails (intracellular 3TC metabolism). The PADDLE study (*7*) indicated that 3TC in combination with DTG had a high potency and efficacy. Two clinical studies, GEMINI-1 and GEMINI-2 (ClinicalTrials.gov identifiers NCT02831673 and NCT02831764, respectively), were identically designed randomized, double-blind, parallel-group, multi-center, phase III, non-inferiority studies. Participants with HIV RNA ≤ 500,000 c/mL at screening were randomized in a 1:1 ratio (stratified by plasma HIV RNA and CD4+ cell count) to once-daily treatment with DTG + 3TC or DTG + tenofovir/emtricitabine (TDF/FTC). The primary endpoint was the proportion of participants with plasma HIV RNA < 50 c/mL at week 48 (*8*). In the primary analysis of the GEMINI-1 and

GEMINI-2 studies at week 48, the 2DR regimen DTG + 3TC was non-inferior to the 3-drug regimen DTG + TDF/FTC in the treatment of cART-naive adults with HIV (*8*). The DTG + 3TC regimen maintained non-inferior efficacy over 96 weeks *vs*. DTG + TDF/FTC in cART-naive adults, with low rates of confirmed virologic withdrawal (CVW) and no development of resistance in either treatment group (*9*). DTG + 3TC maintained non-inferior efficacy *vs*. DTG + TDF/FTC in ART-naive adults and demonstrated a high barrier to resistance, with low rates of CVW through week 144 (*10*). Moreover, overall safety and tolerability were comparable between the two groups. There was a lower risk of drug-related adverse effects with DTG + 3TC than with DTG + TDF/FTC. Changes in renal and bone biomarkers generally favored DTG + 3TC. These results confirmed the durable efficacy, tolerability, and high barrier to resistance of DTG + 3TC, further substantiating the regimen of DTG + 3TC as a first-line treatment option for people living with HIV infection (PLWH).

In the guidelines for HIV prevention and treatment in both the US and Europe, DTG + 3TC is now recommended as an initial regimen for most PLWH, with exceptions for individuals with HIV RNA > 500,000 c/mL, co-infection with hepatitis B virus (HBV), or in whom therapy is started before the results of HIV genotypic resistance testing for reverse transcriptase or HBV testing are available (*11,12*).

In addition, the regimen of DTG/3TC is cost-effective and would offer significant cost savings (*13,14*). In addition to the confirmed durable efficacy and tolerability, the lower cost of DTG/3TC would make it a reasonable, and possibly preferred, treatment option for patients who are either treatment-naive or who need a different regimen. Conceivably, the number of HIV patients who could benefit from the DTG/3TC regimen could be substantial.

Funding: The work was supported by the Shanghai Project to Establish Key Clinical Specialties (grant no. shslczdzk01102).

Conflict of Interest: The authors have no conflicts of interest to disclose.

References

1. UNAIDS. Global HIV & AIDS statistics-Fact sheet. *https://www.unaids.org/en/resources/fact-sheet* (accessed July 20, 2021).
2. Nolan D, Mallal S. Complications associated with NRTI therapy: Update on clinical features and possible pathogenic mechanisms. Antivir Ther. 2004; 9:849-863.
3. Canadian Agency for Drugs and Technologies in Health. Clinical Review Report: Dolutegravir/Lamivudine (Dovato): (ViiV Healthcare ULC): Indication: As a complete regimen for the treatment of human immunodeficiency virus type 1 (HIV-1) infection in adults and adolescents 12 years of age and older and weighing at least 40 kg. *https://pubmed.ncbi.nlm.nih.gov/31877000/* (accessed July 20, 2021).
4. Riddler SA, Haubrich R, DiRienzo AG, *et al*. Class-sparing regimens for initial treatment of HIV-1 infection. N Engl J Med. 2008; 358:2095-2106.
5. Back D. 2-Drug regimens in HIV treatment: Pharmacological considerations. Germs. 2017; 7:113-114.
6. Kelly SG, Nyaku AN, Taiwo BO. Two-drug treatment approaches in HIV: Finally getting somewhere? Drugs. 2016; 76:523-531.
7. Fida M, Rizza SA, Temesgen Z. Dolutegravir plus lamivudine dual therapy - A new option for initial antiretroviral therapy. Drugs Today (Barc). 2019; 55:297-304.
8. Cahn P, Madero JS, Arribas JR, *et al*. Dolutegravir plus lamivudine versus dolutegravir plus tenofovir disoproxil fumarate and emtricitabine in antiretroviral-naive adults with HIV-1 infection (GEMINI-1 and GEMINI-2): Week 48 results from two multicentre, double-blind, randomised, non-inferiority, phase 3 trials. Lancet. 2019; 10167:143-155.
9. Cahn P, Madero JS, Arribas JR, *et al*. Durable efficacy of dolutegravir plus lamivudine in antiretroviral treatment-naive adults with HIV-1 infection: 96-week results from the GEMINI-1 and GEMINI-2 randomized clinical trials. J Acquir Immune Defic Syndr. 2020; 83:310-318.
10. Cahn P, Madero JS, Arribas JR, *et al*. Durable efficacy of dolutegravir (DTG) plus lamivudine (3TC) in antiretroviral treatment-naïve adults with HIV-1 infection: 3-year results from the GEMINI studies. J Int AIDS Soc. 2020 (Suppl. 7). *https://onlinelibrary.wiley.com/doi/epdf/10.1002/jia2.25616* (accessed July 25, 2021).
11. Panel on Antiretroviral Guidelines for Adults and Adolescents. Guidelines for the Use of Antiretroviral Agents in Adults and Adolescents with HIV. Department of Health and Human Services. *https://clinicalinfo.hiv.gov/sites/default/files/guidelines/documents/AdultandAdolescentGL.pdf* (accessed July 20, 2021).
12. European AIDS Clinical Society. EACS Guidelines 2020. *https://www.eacsociety.org/guidelines/eacs-guidelines/* (accessed July 20, 2021).
13. Butler K, Anderson SJ, Hayward O, Jacob I, Punekar YS, Evitt LA, Oglesby A. Cost-effectiveness and budget impact of dolutegravir/lamivudine for treatment of human immunodeficiency virus (HIV-1) infection in the United States. J Manag Care Spec Pharm. 2021; 27:891-903.
14. Girouard MP, Sax PE, Parker RA, Taiwo B, Freedberg KA, Gulick RM, Weinstein MC, Paltiel AD, Walensky RP. The cost-effectiveness and budget impact of 2-drug dolutegravir-lamivudine regimens for the treatment of HIV infection in the United States. Clin Infect Dis. 2016; 62:784-791.

Received July 22, 2021; Revised July 26, 2021; Accepted July 30, 2021.

**Address correspondence to:*
Hongzhou Lu, Department of Infection and Immunity, Shanghai Public Health Clinical Center, Shanghai, China.
E-mail: luhongzhou@fudan.edu.cn

Released online in J-STAGE as advance publication August 1, 2021.

DD&T
Drug Discoveries & Therapeutics

Guide for Authors

1. Scope of Articles

Drug Discoveries & Therapeutics (Print ISSN 1881-7831, Online ISSN 1881-784X) welcomes contributions in all fields of pharmaceutical and therapeutic research such as medicinal chemistry, pharmacology, pharmaceutical analysis, pharmaceutics, pharmaceutical administration, and experimental and clinical studies of effects, mechanisms, or uses of various treatments. Studies in drug-related fields such as biology, biochemistry, physiology, microbiology, and immunology are also within the scope of this journal.

2. Submission Types

Original Articles should be well-documented, novel, and significant to the field as a whole. An Original Article should be arranged into the following sections: Title page, Abstract, Introduction, Materials and Methods, Results, Discussion, Acknowledgments, and References. Original articles should not exceed 5,000 words in length (excluding references) and should be limited to a maximum of 50 references. Articles may contain a maximum of 10 figures and/or tables. Supplementary Data are permitted but should be limited to information that is not essential to the general understanding of the research presented in the main text, such as unaltered blots and source data as well as other file types.

Brief Reports definitively documenting either experimental results or informative clinical observations will be considered for publication in this category. Brief Reports are not intended for publication of incomplete or preliminary findings. Brief Reports should not exceed 3,000 words in length (excluding references) and should be limited to a maximum of 4 figures and/or tables and 30 references. A Brief Report contains the same sections as an Original Article, but the Results and Discussion sections should be combined.

Reviews should present a full and up-to-date account of recent developments within an area of research. Normally, reviews should not exceed 8,000 words in length (excluding references) and should be limited to a maximum of 10 figures and/or tables and 100 references. Mini reviews are also accepted, which should not exceed 4,000 words in length (excluding references) and should be limited to a maximum of 5 figures and/or tables and 50 references.

Policy Forum articles discuss research and policy issues in areas related to life science such as public health, the medical care system, and social science and may address governmental issues at district, national, and international levels of discourse. Policy Forum articles should not exceed 3,000 words in length (excluding references) and should be limited to a maximum of 5 figures and/or tables and 30 references.

Case Reports should be detailed reports of the symptoms, signs, diagnosis, treatment, and follow-up of an individual patient. Case reports may contain a demographic profile of the patient but usually describe an unusual or novel occurrence. Unreported or unusual side effects or adverse interactions involving medications will also be considered. Case Reports should not exceed 3,000 words in length (excluding references).

Communications are short, timely pieces that spotlight new research findings or policy issues of interest to the field of global health and medical practice that are of immediate importance. Depending on their content, Communications will be published as "Comments" or "Correspondence". Communications should not exceed 1,500 words in length (excluding references) and should be limited to a maximum of 2 figures and/or tables and 20 references.

Editorials are short, invited opinion pieces that discuss an issue of immediate importance to the fields of global health, medical practice, and basic science oriented for clinical application. Editorials should not exceed 1,000 words in length (excluding references) and should be limited to a maximum of 10 references. Editorials may contain one figure or table.

News articles should report the latest events in health sciences and medical research from around the world. News should not exceed 500 words in length.

Letters should present considered opinions in response to articles published in *Drug Discoveries & Therapeutics* in the last 6 months or issues of general interest. Letters should not exceed 800 words in length and may contain a maximum of 10 references. Letters may contain one figure or table.

3. Editorial Policies

For publishing and ethical standards, *Drug Discoveries & Therapeutics* follows the Recommendations for the Conduct, Reporting, Editing, and Publication of Scholarly Work in Medical Journals (*http://www.icmje.org/recommendations*) issued by the International Committee of Medical Journal Editors (ICMJE), and the Principles of Transparency and Best Practice in Scholarly Publishing (*https://doaj.org/bestpractice*) jointly issued by the Committee on Publication Ethics (COPE), the Directory of Open Access Journals (DOAJ), the Open Access Scholarly Publishers Association (OASPA), and the World Association of Medical Editors (WAME).

Drug Discoveries & Therapeutics will perform an especially prompt review to encourage innovative work. All original research will be subjected to a rigorous standard of peer review and will be edited by experienced copy editors to the highest standards.

Ethics: *Drug Discoveries & Therapeutics* requires that authors of reports of investigations in humans or animals indicate that those studies were formally approved by a relevant ethics committee or review board. For research involving human experiments, a statement that the participants gave informed consent before taking part (or a statement that it was not required and why) should be indicated. Authors should also state that the study conformed to the provisions of the Declaration of Helsinki (as revised in 2013). When reporting experiments on animals, authors should indicate whether the institutional and national guide for the care and use of laboratory animals was followed.

Conflict of Interest: All authors are required to disclose any actual or potential conflict of interest including financial

interests or relationships with other people or organizations that might raise questions of bias in the work reported. If no conflict of interest exists for each author, please state "There is no conflict of interest to disclose".

Submission Declaration: When a manuscript is considered for submission to *Drug Discoveries & Therapeutics*, the authors should confirm that 1) no part of this manuscript is currently under consideration for publication elsewhere; 2) this manuscript does not contain the same information in whole or in part as manuscripts that have been published, accepted, or are under review elsewhere, except in the form of an abstract, a letter to the editor, or part of a published lecture or academic thesis; 3) authorization for publication has been obtained from the authors' employer or institution; and 4) all contributing authors have agreed to submit this manuscript.

Cover Letter: The manuscript must be accompanied by a cover letter prepared by the corresponding author on behalf of all authors. The letter should indicate the basic findings of the work and their significance. The letter should also include a statement affirming that all authors concur with the submission and that the material submitted for publication has not been published previously or is not under consideration for publication elsewhere. The cover letter should be submitted in PDF format. For example of Cover Letter, please visit: Download Centre (*https://www.ddtjournal.com/downcentre)*.

Copyright: When a manuscript is accepted for publication in *Drug Discoveries & Therapeutics*, the transfer of copyright is necessary. A JOURNAL PUBLISHING AGREEMENT (JPA) form will be e-mailed to the authors by the Editorial Office and must be returned by the authors as a scan. Only forms with a hand-written signature are accepted. This copyright will ensure the widest possible dissemination of information. Please note that your manuscript will not proceed to the next step in publication until the JPA form is received. In addition, if excerpts from other copyrighted works are included, the author(s) must obtain written permission from the copyright owners and credit the source(s) in the article.

Peer Review: *Drug Discoveries & Therapeutics* uses single-blind peer review, which means that reviewers know the names of the authors, but the authors do not know who reviewed their manuscript. The external peer review is performed for research articles by at least two reviewers, and sometimes the opinions of more reviewers are sought. Manuscripts sent out for peer review are evaluated by independent reviewers. Peer reviewers are selected based on their expertise and ability to provide high quality, constructive, and fair reviews. For research manuscripts, the editors may, in addition, seek the opinion of a statistical reviewer. Consideration for publication is based on the article's originality, novelty, and scientific soundness, and the appropriateness of its analysis.

Suggested Reviewers: A list of up to 3 reviewers who are qualified to assess the scientific merit of the study is welcomed. Reviewer information including names, affiliations, addresses, and e-mail should be provided at the same time the manuscript is submitted online. Please do not suggest reviewers with known conflicts of interest, including participants or anyone with a stake in the proposed research; anyone from the same institution; former students, advisors, or research collaborators (within the last three years); or close personal contacts. Please note that the Editor-in-Chief may accept one or more of the proposed reviewers or may request a review by other qualified persons.

Language Editing: Manuscripts prepared by authors whose native language is not English should have their work proofread by a native English speaker before submission. If not, this might delay the publication of your manuscript in *Drug Discoveries & Therapeutics*.

The Editing Support Organization can provide English proofreading, Japanese-English translation, and Chinese-English translation services to authors who want to publish in *Drug Discoveries & Therapeutics* and need assistance before submitting a manuscript. Authors can visit this organization directly at *http://www.iacmhr.com/iac-eso/support.php?lang=en.* IAC-ESO was established to facilitate manuscript preparation by researchers whose native language is not English and to help edit works intended for international academic journals.

4. Manuscript Preparation

Manuscripts are suggested to be prepared in accordance with the "Recommendations for the Conduct, Reporting, Editing, and Publication of Scholarly Work in Medical Journals", as presented at *http://www.ICMJE.org*.

Manuscripts should be written in clear, grammatically correct English and submitted as a Microsoft Word file in a single-column format. Manuscripts must be paginated and typed in 12-point Times New Roman font with 24-point line spacing. Please do not embed figures in the text. Abbreviations should be used as little as possible and should be explained at first mention unless the term is a well-known abbreviation (*e.g.* DNA). Single words should not be abbreviated.

Title page: The title page must include 1) the title of the paper (Please note the title should be short, informative, and contain the major key words); 2) full name(s) and affiliation(s) of the author(s), 3) abbreviated names of the author(s), 4) full name, mailing address, telephone/fax numbers, and e-mail address of the corresponding author; and 5) conflicts of interest (if you have an actual or potential conflict of interest to disclose, it must be included as a footnote on the title page of the manuscript; if no conflict of interest exists for each author, please state "There is no conflict of interest to disclose"). Please visit Download Centre and refer to the title page of the manuscript sample.

Abstract: The abstract should briefly state the purpose of the study, methods, main findings, and conclusions. For article types including Original Article, Brief Report, Review, Policy Forum, and Case Report, a one-paragraph abstract consisting of no more than 250 words must be included in the manuscript. For Communications, Editorials, News, or Letters, a brief summary of main content in 150 words or fewer should be included in the manuscript. Abbreviations must be kept to a minimum and non-standard abbreviations explained in brackets at first mention. References should be avoided in the abstract. Three to six key words or phrases that do not occur in the title should be included in the Abstract page.

Introduction: The introduction should be a concise statement of the basis for the study and its scientific context.

Materials and Methods: The description should be brief but with sufficient detail to enable others to reproduce the experiments. Procedures that have been published previously should not be described in detail but appropriate references should simply be cited. Only new and significant modifications of previously published procedures require complete description. Names of products and manufacturers with their locations (city and state/country) should be given and sources of animals and cell lines should always be indicated. All clinical investigations must have been conducted in accordance with Declaration of Helsinki principles. All human and animal studies must have been approved by the appropriate institutional review board(s) and a specific declaration of approval must be made within this section.

Results: The description of the experimental results should be succinct but in sufficient detail to allow the experiments to be analyzed and interpreted by an independent reader. If necessary, subheadings may be used for an orderly presentation. All figures and tables must be referred to in the text.

Discussion: The data should be interpreted concisely without repeating material already presented in the Results section. Speculation is permissible, but it must be well-founded, and discussion of the wider implications of the findings is encouraged. Conclusions derived from the study should be included in this section.

Acknowledgments: All funding sources should be credited in the Acknowledgments section. In addition, people who contributed to the work but who do not meet the criteria for authors should be listed along with their contributions.

References: References should be numbered in the order in which they appear in the text. Citing of unpublished results, personal communications, conference abstracts, and theses in the reference list is not recommended but these sources may be mentioned in the text. In the reference list, cite the names of all authors when there are fifteen or fewer authors; if there are sixteen or more authors, list the first three followed by *et al*. Names of journals should be abbreviated in the style used in PubMed. Authors are responsible for the accuracy of the references. The EndNote Style of *Drug Discoveries & Therapeutics* could be downloaded at **EndNote** (*https://www.ddtjournal.com/examples/Drug_Discoveries_Therapeutics.ens*).

Examples are given below:

Example 1 (Sample journal reference):

Nakata M, Tang W. Japan-China Joint Medical Workshop on Drug Discoveries and Therapeutics 2008: The need of Asian pharmaceutical researchers' cooperation. Drug Discov Ther. 2008; 2:262-263.

Example 2 (Sample journal reference with more than 15 authors):

Darby S, Hill D, Auvinen A, *et al*. Radon in homes and risk of lung cancer: Collaborative analysis of individual data from 13 European case-control studies. BMJ. 2005; 330:223.

Example 3 (Sample book reference):

Shalev AY. Post-traumatic stress disorder: Diagnosis, history and life course. In: Post-traumatic Stress Disorder, Diagnosis, Management and Treatment (Nutt DJ, Davidson JR, Zohar J, eds.). Martin Dunitz, London, UK, 2000; pp. 1-15.

Example 4 (Sample web page reference):

World Health Organization. The World Health Report 2008 – primary health care: Now more than ever. *http://www.who.int/whr/2008/whr08_en.pdf* (accessed September 23, 2010).

Tables: All tables should be prepared in Microsoft Word or Excel and should be arranged at the end of the manuscript after the References section. Please note that tables should not in image format. All tables should have a concise title and should be numbered consecutively with Arabic numerals. If necessary, additional information should be given below the table.

Figure Legend: The figure legend should be typed on a separate page of the main manuscript and should include a short title and explanation. The legend should be concise but comprehensive and should be understood without referring to the text. Symbols used in figures must be explained. Any individually labeled figure parts or panels (A, B, *etc*.) should be specifically described by part name within the legend.

Figure Preparation: All figures should be clear and cited in numerical order in the text. Figures must fit a one- or two-column format on the journal page: 8.3 cm (3.3 in.) wide for a single column, 17.3 cm (6.8 in.) wide for a double column; maximum height: 24.0 cm (9.5 in.). Please make sure that artwork files are in an acceptable format (TIFF or JPEG) at minimum resolution (600 dpi for illustrations, graphs, and annotated artwork, and 300 dpi for micrographs and photographs). Please provide all figures as separate files. Please note that low-resolution images are one of the leading causes of article resubmission and schedule delays.

Units and Symbols: Units and symbols conforming to the International System of Units (SI) should be used for physicochemical quantities. Solidus notation (*e.g*. mg/kg, mg/mL, mol/mm^2/min) should be used. Please refer to the SI Guide *www.bipm.org/en/si/* for standard units.

Supplemental data: Supplemental data might be useful for supporting and enhancing your scientific research and *Drug Discoveries & Therapeutics* accepts the submission of these materials which will be only published online alongside the electronic version of your article. Supplemental files (figures, tables, and other text materials) should be prepared according to the above guidelines, numbered in Arabic numerals (*e.g*., Figure S1, Figure S2, and Table S1, Table S2) and referred to in the text. All figures and tables should have titles and legends. All figure legends, tables and supplemental text materials should be placed at the end of the paper. Please note all of these supplemental data should be provided at the time of initial submission and note that the editors reserve the right to limit the size and length of Supplemental Data.

5. Submission Checklist

The Submission Checklist will be useful during the final checking of a manuscript prior to sending it to *Drug Discoveries & Therapeutics* for review. Please visit Download Centre and download the Submission Checklist file.

6. Online Submission

Manuscripts should be submitted to *Drug Discoveries & Therapeutics* online at *https://www.ddtjournal.com*. The manuscript file should be smaller than 5 MB in size. If for any reason you are unable to submit a file online, please contact the Editorial Office by e-mail at *office@ddtjournal.com*.

7. Accepted Manuscripts

Proofs: Galley proofs in PDF format will be sent to the corresponding author *via* e-mail. Corrections must be returned to the editor (*proof-editing@ddtjournal.com*) within 3 working days.

Offprints: Authors will be provided with electronic offprints of their article. Paper offprints can be ordered at prices quoted on the order form that accompanies the proofs.

Page Charge: Page charges will be levied on all manuscripts accepted for publication in *Drug Discoveries & Therapeutics* ($140 per page for black white pages; $340 per page for color pages). Under exceptional circumstances, the author(s) may apply to the editorial office for a waiver of the publication charges at the time of submission.

Misconduct: *Drug Discoveries & Therapeutics* takes seriously all allegations of potential misconduct and adhere to the ICMJE Guideline (*http://www.icmje.org/recommendations*) and COPE Guideline (*http://publicationethics.org/files/Code_of_conduct_for_journal_editors.pdf*). In cases of suspected research or publication misconduct, it may be necessary for the Editor or Publisher to contact and share submission details with third parties including authors' institutions and ethics committees. The corrections, retractions, or editorial expressions of concern will be performed in line with above guidelines.

(As of June 2020)

Drug Discoveries & Therapeutics
Editorial and Head Office
Pearl City Koishikawa 603,
2-4-5 Kasuga, Bunkyo-ku,
Tokyo 112-0003, Japan.
E-mail: office@ddtjournal.com